

**Mitochondrial localization of two brain proteins,
p42^{IP4}/centaurin- α 1/ADAP1 and CNP, and their
involvement in regulation of mitochondrial Ca²⁺**

Dissertation

zur Erlangung des akademischen Grades

**doctor rerum naturalium
(Dr. rer. nat.)**

genehmigt durch die Fakultät für Naturwissenschaften
der Otto-von-Guericke-Universität Magdeburg

von M. Sc. Anastasia Galvita

geb. am 11.05.1973 in Novosibirsk, Russia

Gutachter: **Prof. Dr. Georg Reiser**

Prof. Dr. Carsten Culmsee

eingereicht am: 15 Januar, 2010

verteidigt am: 28 Juni 2010

ACKNOWLEDGEMENTS

I am very grateful to those who gave me all kinds of help and support during this work at the Institute of Neurobiochemistry, Otto-von-Guericke University Magdeburg.

First of all, I would like to sincerely thank my supervisor, Prof. Dr. Georg Reiser, for providing me an opportunity to join his lab to complete my Ph.D. work. His invaluable knowledge, constructive discussion, professional guidance and constant support enabled me to achieve my goals efficiently and easily, and to be of great benefit to my scientific career throughout my life. I am happy to be a member of the Graduate School directed by Prof. Reiser, and the wonderful lectures, seminars and practical courses he organized opened my scientific ken and stimulated my idea. Of course, many thanks also to our Graduate School secretary Frau Manuela Dullin-Viehweg, who assisted the nice organization of the scientific and social activities.

I am greatly indebted to the group of Dr. Tamara Azarashvili from Institute of Theoretical and Experimental Biophysics RAS, Pushchino, Russia: Dr. Dmitry Grachev, Dr. Olga Krestinina and Yulia Baburina. During their visits in Magdeburg they were introducing and helping me with mitochondrial techniques. My special appreciation goes to Dr. Dmitry Grachev who performed the measurement of mitochondrial parameters in chamber in the frame of our cooperative project. The data of these measurements are presented in the following Figures: 3.3.1; 3.3.2; 3.3.3; 3.3.4; 3.3.6; 3.3.7; 3.6.3; 3.6.4; 3.6.5; 3.6.6.

I am thankful to Dr. Roland Hartig from Institute of Immunology, Otto-von-Guericke University Magdeburg. He performed flow cytometry analysis.

I am grateful to Dr. Rolf Stricker for valuable scientific suggestions and discussions. His long-standing research experience and in-depth knowledge in the field of protein chemistry was important for channelling the direction of my study. He helped me in the critical analysis of the data obtained, which was crucial to the completion of my work.

I am thankful to Dr. Fariba Sedehizade and Dr. Theodor Hanck who helped me in my work involving the molecular biology aspect, in the establishment of stable cell lines and in the introduction of the GST pull-down assays.

I am also thankful to Dr. Mohan E. Tulapurkar for helping me with the techniques of confocal laser scanning microscopy

I also appreciate Dr. Abidat Schneider, Frau Evelyn Busse, Frau Ilka Kramer, Frau Petra Grüneberg, for their excellent technical assistance, as well as other colleagues in the lab, Dr. Andrea Haase, Frau Anke Imrich, Frau Annette Jürgen, Frau Claudia Borrmann, Dr. Denise Ecke, Frau Dorothe Terhardt, Dr. Elena Sokolova, Dr. Ewa Ostrowska, Dr. Gregor

Zündorf, Dr. Marina Sergeeva, Dr. Mikhail L. Strokin, Dr. Rainer Schäfer, Herr Rongyu Li, Frau Sabine Hein, Dr. Stefan Kahlert, Dr. Stepan Aleshin, Dr. Tanuja Rohatgi, Dr. Victoria Bunik, Dr. Weibo Luo and Dr. Ying Fei Wang for their cooperation and support, and Frau Ines Klaes, Herr Peter Ehrbarth for their kind support, during the course of this work.

Finally, I would express my special gratitude to my husband Dr. Vladimir Galvita for his advises, encouragement and love, and to my parents for their support and understanding.

Contents

| | |
|--|-----------|
| 1. Introduction | 7 |
| 1.1 Mitochondria in cellular Ca²⁺ signalling and cell death. | 7 |
| 1.1.1 Permeability transition pore (PTP) | 7 |
| 1.1.2 Re-evaluation of the classical model of PTP | 9 |
| 1.1.3 Role of PTP in cell death | 11 |
| 1.2 p42^{IP4}/centaurin-α1/ADAP1 | 13 |
| 1.2.1 p42 ^{IP4} /centaurin- α 1 domain structure | 13 |
| 1.2.2 Localization of p42 ^{IP4} in brain | 14 |
| 1.2.3 Interaction partners of p42 ^{IP4} | 15 |
| 1.2.4 Known functions of p42 ^{IP4} | 16 |
| 1.2.5 The ligands of p42 ^{IP4} | 18 |
| 1.3 2,3'-Cyclic nucleotide-3'-phosphodiesterase (CNP) | 20 |
| 1.3.1 Two isoforms of CNP | 20 |
| 1.3.2 Motifs in primary structure and modifications of CNP | 20 |
| 1.3.3 Mitochondrial localization of CNP | 22 |
| 1.3.4 Enzymatic characteristics of CNP | 22 |
| 1.3.5 Three-dimensional structural features of CNP and link to RNA metabolism | 23 |
| 1.3.6 Interaction partners of CNP | 24 |
| 1.3.7 Functions of CNP | 25 |
| 1.4 Aims of this study | 28 |
| 1.4.1 Motivation | 28 |
| 1.4.2 Main aims and goals of study | 28 |
| 1.4.3 Strategy | 29 |
| 2. Materials and Methods | 30 |
| 2.1 Materials | 30 |
| 2.1.1 Chemicals and Reagents | 30 |
| 2.1.2 Antibodies | 31 |
| 2.1.3 Cells, medium and related reagents | 32 |
| 2.1.4 Animals | 33 |
| 2.1.5 Plasmid vectors: | 33 |
| 2.1.6 Small interfering RNAs (siRNAs) | 34 |
| 2.1.7 Enzymes | 34 |
| 2.1.8. Molecular weight markers | 34 |
| 2.1.9 Kits | 35 |
| 2.1.10 Laboratory instruments | 35 |
| 2.1.11 Buffers and solvents | 37 |
| 2.1.12. Oligonucleotides for PCR and sequencing | 38 |
| 2.2 Methods | 39 |
| 2.2.1 RT-PCR | 39 |
| 2.2.2 Plasmid constructs | 39 |
| 2.2.3 Agarose gel electrophoresis of DNA | 40 |

| | |
|---|-----------|
| 2.2.4 Transformation of E. coli with plasmid DNA by heat-shock method (CaCl ₂ based) | 40 |
| 2.2.5 Expression and purification of glutathione S-transferase (GST) and GST-p42 ^{IP4} constructs from E. coli | 41 |
| 2.2.6 Cell culture and transfection | 42 |
| 2.2.7 Confocal microscopy | 42 |
| 2.2.8 Subcellular fractionation by differential centrifugation | 43 |
| 2.2.9 Preparation of mitochondrial lysate and cytosolic fraction from rat brain | 43 |
| 2.2.10 Isolation of mitochondria from cultured cells | 44 |
| 2.2.11 Subfractionation of mitochondria | 44 |
| 2.2.12 Electrophoresis and immunoblotting | 45 |
| 2.2.13 GST-pull-down assay | 45 |
| 2.2.14 Immunoprecipitation and co-immunoprecipitation | 46 |
| 2.2.15 Isolation of rat brain mitochondria for functional study | 46 |
| 2.2.16 Evaluation of mitochondrial functions | 47 |
| 2.2.17 Detection of CNP activity in isolated mitochondria | 47 |
| 2.2.18 Small interfering RNA (siRNA) | 48 |
| 2.2.19 Apoptosis detection | 48 |
| 2.3 Statistical analysis | 49 |
| 3. Results | 50 |
| 3.1. Possible role of p42^{IP4} in cell protection or cell death | 50 |
| 3.1.1 Influence of p42 ^{IP4} overexpression on apoptosis induced in N2a cells. | 50 |
| 3.1.2 Influence of p42 ^{IP4} overexpression on cell cycle in N2a cells. | 52 |
| 3.2. Novel localization of p42^{IP4}: mitochondrial localization | 54 |
| 3.2.1 p42 ^{IP4} is localized in mitochondria, isolated from transfected CHO cells | 54 |
| 3.2.2 p42 ^{IP4} is localized in inner mitochondrial compartments of transfected CHO cells. | 55 |
| 3.2.3 p42 ^{IP4} is localized in mitochondria, isolated from transfected N2a cells | 57 |
| 3.3 p42^{IP4} is involved in regulation of mitochondrial Ca²⁺ | 60 |
| 3.3.1 p42 ^{IP4} accelerates Ca ²⁺ -induced PTP opening in mitochondria from N2a cells | 60 |
| 3.3.2 Effects of p42 ^{IP4} ligands, phosphatidylinositol(3,4,5)trisphosphate (PIP ₃) and inositol(1,3,4,5)tetrakisphosphate (IP ₄), on mitochondrial functions | 69 |
| 3.4. Interaction of p42^{IP4} with CNP and α-tubulin in rat brain mitochondria | 70 |
| 3.4.1 Localization of p42 ^{IP4} , CNP and α -tubulin in rat brain mitochondria | 71 |
| 3.4.2 p42 ^{IP4} interacts with CNP and α -tubulin <i>in vitro</i> | 71 |
| 3.4.3 p42 ^{IP4} interacts with CNP and α -tubulin <i>in vivo</i> | 72 |
| 3.4.4 CNP interacts with α -tubulin <i>in vivo</i> | 73 |
| 3.5. Mitochondrial localization of CNP | 74 |
| 3.5.1 CNP localization in sub-mitochondrial fractions of RBM | 74 |
| 3.5.2 CNP interaction with ANT and VDAC | 75 |
| 3.6. CNP is involved in regulation of mitochondrial Ca²⁺ | 76 |
| 3.6.1 Influence of Ca ²⁺ -induced PTP on CNP activity in RBM | 76 |
| 3.6.2 Effect of CNP knock-down on Ca ²⁺ -induced PTP | 77 |
| 3.6.3 Effects of CNP substrates, 2',3'-cAMP, 2',3'-cNADP, on mitochondrial functions | 82 |
| 4. Discussion | 89 |

| | |
|---|-----|
| 4.1 The mechanism of mitochondrial Ca ²⁺ -induced PTP opening remains unknown . | 89 |
| 4.2 Known functions of p42 ^{IP4} | 89 |
| 4.3 Novel localization and function of p42 ^{IP4} . Involvement of p42 ^{IP4} and its ligands in regulation of mitochondrial Ca ²⁺ -induced PTP opening..... | 90 |
| 4.4 Known functions of CNP | 92 |
| 4.5 Novel function of CNP. Involvement of CNP and its substrates in regulation of mitochondrial Ca ²⁺ -induced PTP opening..... | 93 |
| 4.6 Hypothesis for functional importance of interaction between p42 ^{IP4} , CNP and α-tubulin in mitochondria..... | 95 |
| 4.7 Conclusions. Novel regulators of Ca ²⁺ -induced PTP opening. | 100 |
| 5. Abstract..... | 101 |
| 6. Zusammenfassung..... | 102 |
| 7. References | 105 |
| 8. Abbreviations..... | 119 |
| 9. Appendix | 121 |
| Curriculum vitae..... | 121 |
| Publications and presentations | 122 |
| Conferences and symposiums | 123 |

1. Introduction

1.1 Mitochondria in cellular Ca²⁺ signalling and cell death.

A basic notion of cell biology is that calcium, in its ionic form (Ca²⁺), is a ubiquitous second messenger of eukaryotic cells, participating in numerous signal transduction pathways. Cellular Ca²⁺ signals are crucial in the control of most physiological processes, cell injury and programmed cell death. Mitochondria, in addition to their function as cellular power plants, have been recognized to play a central role in Ca²⁺ homeostasis and cellular Ca²⁺ signalling (Duszynski et al., 2006).

It has been known for several decades that sequestration of vast amounts of Ca²⁺ in the mitochondria occurs under various pathophysiological conditions and contributes to the demise of the cells (Krieger and Duchen, 2002). In these paradigms, the loss of the balance between plasma membrane Ca²⁺ influx and Ca²⁺ export leads to a sustained elevation in cytosolic Ca²⁺ from 100 nM to $\geq 1 \mu\text{M}$, inducing a progressive increase in mitochondrial Ca²⁺ uptake. Mitochondria dampen changes in cytosolic Ca²⁺ loads and sustain cellular Ca²⁺ homeostasis that is required for normal function of cells. However, mitochondria take up a limited amount of calcium up to a certain threshold. Accumulation of Ca²⁺ over-load leads to increased permeability of the inner mitochondrial membrane due to formation of an unselective pore at the contact site between outer and inner membranes (Smaili et al., 2000; Sullivan et al., 2005). This permeability transition pore (PTP) forms the major Ca²⁺ efflux pathway from mitochondria. Since mitochondria both accumulate and release Ca²⁺, these organelles play various roles within cells (Giacomello et al., 2007).

Opening of the PTP by Ca²⁺ is effectively modulated by several factors, including reactive oxygen species (ROS), pH, mitochondrial membrane potential ($\Delta\psi_m$), the level of which is affected by a variety of metabolic intermediates, signalling molecules and drugs (Bernardi, 1999). Although Ca²⁺-dependent mitochondrial membrane permeabilization has been implicated in a broad range of cell death and tissue injury, the exact mechanism of the PTP opening remains elusive (Hajnoczky et al., 2006). Therefore study and search for new proteins and molecules involved in control of Ca²⁺-induced PTP opening will provide additional insight into pathways that are critical for cell survival and cell death.

1.1.1 Permeability transition pore (PTP)

The mitochondrial permeability transition is defined as the sudden nonselective increase in the permeability of the inner mitochondrial membrane (IMM) to solutes of molecular mass less than $\sim 1500 \text{ Da}$, and results in loss of mitochondrial membrane potential,

mitochondrial swelling, and rupture of the outer mitochondrial membrane (OMM). More than 30 years ago, it was first reported that the mitochondrial permeability transition is a consequence of Ca^{2+} -induced increased permeability of the IMM that is characterized by simultaneous stimulation of ATPase, uncoupling of oxidative phosphorylation, and loss of respiratory control (Hunter et al., 1976).

Later it was suggested that the mitochondrial permeability transition is not a consequence of non-specific mitochondrial membrane damage; it is, instead, the result of the opening of an authentic pore or megachannel. The last 25 years of study dealing with the mitochondrial permeability transition have been characterized by an intensive search for the identity of the components of the mitochondrial permeability transition megachannel.

The permeability transition pore (PTP) is a multi-component protein aggregate in mitochondria that comprises factors in the inner as well as in the outer mitochondrial membrane. The scheme of the classical view of PTP complex is described in Fig.1.1. The pore frame was thought to be formed by the voltage-dependent anion channel (VDAC), known also as porin – adenine nucleotide translocase (ANT) – cyclophilin D (CyP-D) complex, which is located at the contact sites between IMM and OMM. It was found also that the peripheral benzodiazepine receptor (PBR) is a mitochondrial outer membrane protein associated with PTP (Szabo and Zoratti, 1993). Cytosolic hexokinase and mitochondrial creatine kinase also were shown to be involved in mitochondrial permeability transition regulation (Beutner et al., 1998).

It was suspected for a long time that the PTP might play an important role in both apoptotic and necrotic cell death. Therefore, it came as no surprise when PTP was found under the direct control of anti-apoptotic members of the Bcl-2 family (Marzo et al., 1998a). Further, Bax was found to co-purify with known PTP components (Marzo et al., 1998b). Consequently, the Bcl-2 family members were integrated into the PTP model as regulatory components.

The proposed architecture of PTP complex was based on these data. This model has become widely accepted and until now has been recognized by investigators in the field of mitochondrial research.

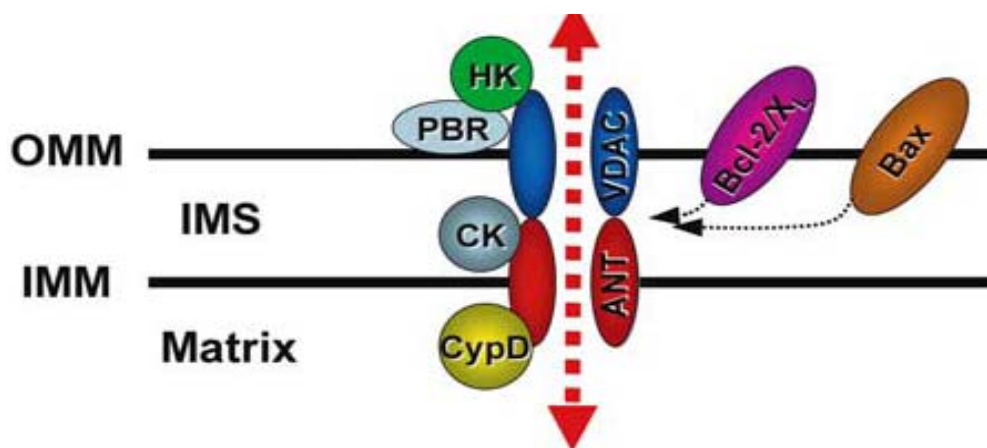


Fig. 1.1. Classical view of proposed PTP complex architecture. The pore structure is formed by the VDAC–ANT–Cyp-D complex, which is located at the contact sites between IMM and OMM. Hexokinase (HK) II and mitochondrial creatine kinase (CK) are regulatory kinases. Peripheral benzodiazepine receptor (PBR) and Bcl-2-family members (Bcl-2, Bcl-xL, and Bax) are included as putative regulatory components (from (Juhaszova et al., 2008)).

1.1.2 Re-evaluation of the classical model of PTP

While not everyone in the mitochondria research community adhered to the model above, there did seem a consensus that as a minimum the PTP contains porin, ANT and Cyp-D. However, recent genetic evidence (based on genetic knockout of individual pore components) has overturned long-standing models.

In particular, in 2004 strong evidence was provided that ANT is not essential for the PTP (Kokoszka et al., 2004). To investigate the role of ANTs in the PTP formation, the two ANT isoform genes, heart-muscle (*Ant1*) and the systemic (*Ant2*), were genetically inactivated in mouse liver. It was demonstrated that the PTP opening could still be induced in mitochondria lacking ANT. However, more Ca^{2+} than usual was required to activate the PTP, and the pore could no longer be regulated by ANT ligands, including adenine nucleotides. Nevertheless, the suggestion arises that a less abundant member of the carrier family than ANT with less sensitivity to Ca^{2+} or oxidative stress can replace ANT in the pore when this protein is absent, i.e. a compensation mechanism comes in (Halestrap, 2004).

Three mammalian VDAC isoforms (*Vdac1*, *Vdac2*, *Vdac3*) have been described, and it has been suggested that they may each have a distinct physiological function. The generation of isoform-specific, *Vdac*-deficient mice allowed the assessment of the role of individual VDAC isoforms in PTP structure. Mice missing *Vdac1* and *Vdac3* were viable but exhibited distinct phenotypes; elimination of *Vdac2* resulted in embryonic lethality. PTP properties in

mitochondria from *Vdac1*-null mice were indistinguishable from those of wild type mice (Krauskopf et al., 2006).

In subsequent work it was found that mitochondria from *Vdac 1*, *Vdac 3*-, and *Vdac 1/Vdac 3*-null mice exhibited Ca^{2+} and oxidative stress-induced opening of PTPs that were indistinguishable from wild type mitochondria (Baines et al., 2007). Furthermore, mouse embryonic fibroblasts lacking VDAC (*Vdac1*, *Vdac2*, *Vdac3*, various combinations of two, or all three VDAC isoforms), showed similar patterns of PTP induction compared to control cells. In addition, the existence of a VDAC-independent model of Bcl-2 family member-mediated cell killing was confirmed. Wild type and *Vdac*-deficient mitochondria and cells responded to activation or over expression of Bax and Bid by equivalent cytochrome c release, caspase cleavage, and cell death. These results make a strong argument against any indispensable role of VDACs in both PTP-mediated and Bax-Bak-mediated cell death. The experiments with *Vdac*-deficient cells and mitochondria strongly cast doubt on the validity of the classical model of PTP formation, which assumes that the pore contains VDAC and is formed at the contact sites between mitochondrial membranes.

While VDAC and ANT had been excluded as essential pore components, it is possible, that these proteins serve some regulatory function. The function of hexokinase II as a regulator of the pore, however, is yet unresolved. Only the role of the CyP-D has been clearly established. Recently, genetic studies from four independent groups on CyP-D knockout mice (*Ppif*^{-/-} mice) confirmed the critical role of CyP-D in regulation of the PTP machinery and provided new insights into the role of PTP in cell death (Baines et al., 2005; Basso et al., 2005; Nakagawa et al., 2005; Schinzel et al., 2005). Fig. 1.2. shows the proposed PTP complex architecture based on re-evaluation of the classical model.

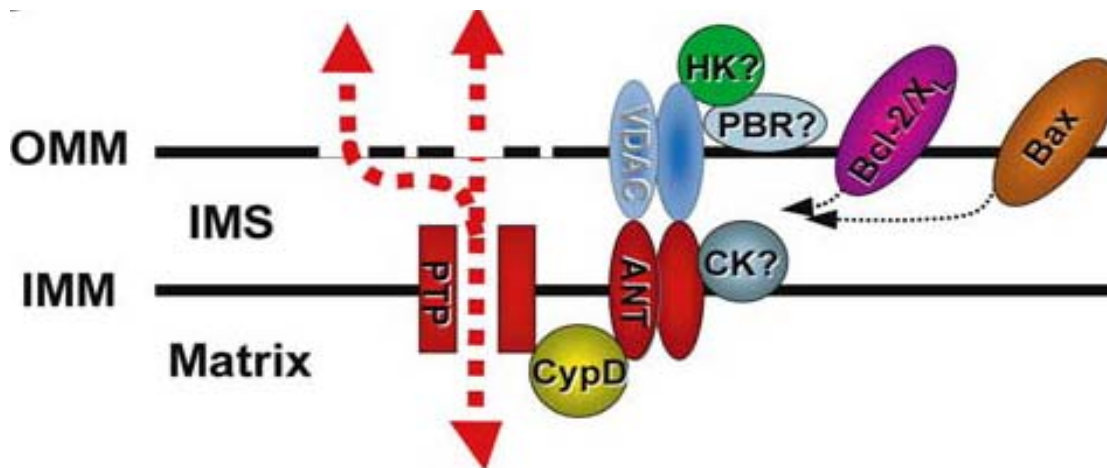


Fig. 1.2 Current view of proposed PTP complex architecture, based on reappraisal of the classical model. The elements comprising the pore itself (denoted “PTP” for permeability transition pore) are presently unidentified, but are probably regulated by the adjacent elements as indicated. Note that VDAC, portrayed as a “shadow,” is no longer seen as an essential pore component based on recent genetic evidence. Question mark symbols signify, where open questions remain (from (Juhaszova et al., 2008)).

Even now, despite major efforts, the molecular nature of the PTP remains enigmatic (Juhaszova et al., 2008). Very recently, it was suggested that the protein fulfilling the role of the transmembrane pore component is the mitochondrial phosphate carrier (PiC) (Leung and Halestrap, 2008). Moreover, these studies implicate the PiC in PTP formation and are consistent with a calcium-triggered conformational change of the PiC, facilitated by CyP-D, inducing pore opening (Leung et al., 2008). It was proposed that this is enhanced by an association of the PiC with the "c" conformation of the ANT, as agents that modulate pore opening may act on either or both of the two proteins, PiC and ANT (Halestrap, 2009).

1.1.3 Role of PTP in cell death

It has been known, and accepted by most investigators for the last 10 years, that cells can undergo a sudden increase in mitochondrial inner membrane permeability to ions and solutes. This disequilibrium causes a dissipation of the membrane potential, loss of ion homeostasis, and impairment of ATP synthesis, which results in passive swelling of the organelle, release of cytochrome c and cellular apoptosis, or necrotic cell death.

Recent genetic experiments provided critical new insights into fundamental mechanisms of cell death (Baines et al., 2005; Basso et al., 2005; Nakagawa et al., 2005; Schinzel et al., 2005). In particular, CyP-D-deficient cells also responded to various apoptotic stimuli in a similar manner as the wild type cells but showed considerable resistance to necrotic cell death, suggesting that CyP-D is not a central component of the apoptotic death pathway. These conclusions lead to a revision of the current dogma and support the idea that

the PTP is not a major participant in apoptotic cell death, but rather plays an important role in necrotic cell death. This seems to be the case at least in cardiac myocytes, neurons, and fibroblasts. These ideas represent a significant contribution to the understanding of the role, which mitochondria play in cell death.

Recently, a model for the activation of the PTP for cell death was proposed (Grimm and Brdiczka, 2007). It was suggested that the PTP alters its composition during apoptosis, that anti-apoptotic factors are released and pro-apoptotic subunits recruited for apoptosis induction (Grimm and Brdiczka, 2007). The best evidence for this is that hexokinase inhibits cytochrome c (Cyt c) release. The structural change of VDAC achieved by interaction with ANT is recognized at the mitochondrial surface and leads to higher affinity of hexokinase. Recent observations suggest that this contact site structure is the preferred target of Bax molecules. It was found that hexokinase and Bax compete for the same binding site of VDAC (Pastorino et al., 2002). Moreover, VDAC and ANT were immuno-precipitated with Bax from extracts of cardiomyocytes (Capano and Crompton, 2002). The binding of hexokinase to the contact sites is induced by protein kinase B (Akt) (Gottlob et al., 2001). Activated protein kinase B can suppress apoptosis. The activity of mitochondrial bound hexokinase was found to be important for protein kinase B-linked suppression of Cyt c release and apoptosis (Majewski et al., 2004).

Hexokinase was furthermore used as a tool to isolate the contact site forming complex of outer membrane VDAC and inner membrane ANT. Cyt c remained attached to the hexokinase VDAC-ANT complexes that were reconstituted in phospholipid vesicles. The vesicles were loaded with malate and treated with Bax in increasing concentrations. Bax liberated the endogenous Cyt c but did not release the internal malate. The Bax dependent liberation of endogenous Cyt c was abolished when the VDAC-ANT complex was dissociated by bongkrekate or by stabilizing the hexokinase binding through addition of glucose. The internal malate could be released through opening the PTP by addition of Ca^{2+} . This suggested that Bax did not form unspecific pores for malate but released the Cyt c dependently on the actual structure of the VDAC-ANT complex (Vyssokikh et al., 2002; Vyssokikh et al., 2004). Thus, the permeability transition in cell death is brought about by dynamic protein complexes that have the physiological function to regulate energy metabolism. These protein complexes change according to the needs of the cell and respond to different external and internal stimuli. During cell death the associations are altered in a way that causes the permeability transition in mitochondria (Grimm and Brdiczka, 2007).

It was also shown that conventionally defined “pro-apoptotic” and “anti-apoptotic” members of the Bcl-2 family are critical mediators of protection signalling downstream of GSK-3 β , where they regulate the susceptibility of the PTP to oxidant stress. Moreover, in the context of limiting PTP induction, the actions of the Bcl-2 family are effecting changes in cell survival and death via necrosis rather than apoptosis-related pathways (Juhaszova et al., 2008).

1.2 p42^{IP4}/centaurin- α 1/ADAP1

1.2.1 p42^{IP4}/centaurin- α 1 domain structure

p42^{IP4} is a brain-specific protein that is also called centaurin- α 1 and phosphatidylinositoltrisphosphate binding protein, PIP₃ BP (Hammonds-Odie et al., 1996; Stricker et al., 1997). This protein specifically recognizes two second messengers, the membrane lipid phosphatidylinositol(3,4,5)trisphosphate (PIP₃) and the soluble inositol(1,3,4,5)tetrakisphosphate (IP₄) (Hanck et al., 1999).

Previously, a receptor protein with high affinity for IP₄ was solubilized from pig cerebellar membranes and purified (Donie and Reiser, 1991). The protein was identified in SDS-PAGE after photoaffinity labelling as a 42 kDa protein band, p42^{IP4} (Reiser et al., 1991).

Later, cloning of pig p42^{IP4} (Stricker et al., 1997) had revealed that this protein is homologous to centaurin- α , the PIP₃ binding protein cloned from a rat brain (Hammonds-Odie et al., 1996). The protein PIP₃ BP, virtually identical to pig p42^{IP4}, was cloned from bovine brain and characterized as a PIP₃ binding protein (Tanaka et al., 1997). In addition, the existence of rat p42^{IP4} was established (Aggensteiner et al., 1998).

p42^{IP4} contains an ADP ribosylation factor (Arf) GTPase activating protein (GAP) homology domain, including N-terminal zinc finger motif, followed by two pleckstrin homology (PH) domains (Fig.1).

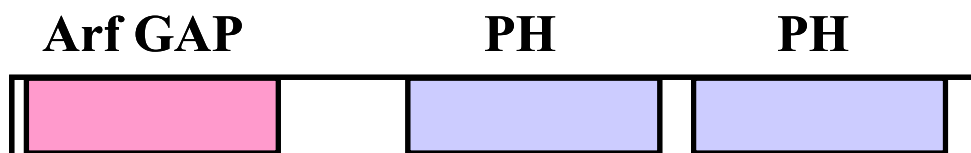


Fig.1. Domain organization of p42^{IP4}. Arf GAP homology and PH domains are depicted.

PH domains contain approximately 120 amino acids and are found in many proteins, such as protein kinase B, Bruton’s tyrosine kinase, phosphoinositide-dependent kinase-1 and phospholipase C- γ 1 (Shepherd et al., 1998; Vanhaesebroeck et al., 2001). They occur in members of the cytohesin family [cytohesin-1, Arf nucleotide-binding-site opener (cytohesin-

2), general receptor for phosphoinositides-1 (cytohesin-3)] (Jackson et al., 2000), RasGTPase activating proteins (GAP1m and GAP1IP4BP) (Cozier et al., 2000) and members of the centaurin- α family (p42^{IP4}/centaurin- α 1; PIP₃BP, and centaurin- α 2) (Tanaka et al., 1997; Stricker et al., 1999; Venkateswarlu et al., 1999; Hanck et al., 2004). For these proteins specific in vitro binding to PIP₃ and IP₄ has been reported (Jackson et al., 2000; Lemmon and Ferguson, 2000). Most of the PH domain-containing proteins have a single PH domain, which is required for ligand binding. In contrast, the centaurin family proteins contain two PH domains in tandem orientation. Both PH domains of p42^{IP4} within the protein are required for full in vitro PIP₃ binding activity (Tanaka et al., 1997). PH domains are also required for phosphoinositide 3-kinase-dependent translocation to the plasma membrane (Hammonds-Odie et al., 1996; Tanaka et al., 1997; Tanaka et al., 1999; Venkateswarlu et al., 1999; Sedehizade et al., 2002).

The **ARF GAP** domain was originally identified in members of a distinct family of ARF1 GAPs (Cukierman et al., 1995; Poon et al., 1996). It contains a characteristic C₄ - type zinc finger motif and a conserved arginine that is required for activity, within a particular spacing (CX₂CX₁₆CX₂CX₄R) (Kahn et al., 2008). It was demonstrated that p42^{IP4} is functionally homologous to Gcs1, a yeast ARF GAP, but it was not possible to detect any ARF GAP activity for p42^{IP4} in this time period (Venkateswarlu et al., 1999; Jackson et al., 2000). Only recently the in vivo Arf GAP activity of p42^{IP4} towards Arf6 has been described (Venkateswarlu et al., 2004). Therefore, p42^{IP4} was renamed systematically ADAP1 (A Dual PH domain ARF GAP) to stress the relationships within the ARF GAP superfamily (Kahn et al., 2008).

1.2.2 Localization of p42^{IP4} in brain

p42^{IP4} is rather exclusively expressed in brain (Stricker et al., 2003). The respective cDNA has been cloned from pig (Stricker et al., 1997), rat (Hammonds-Odie et al., 1996); (Aggensteiner et al., 1998), bovine (Tanaka et al., 1997) and human brain (Venkateswarlu et al., 1999; Sedehizade et al., 2002). Expression of p42^{IP4} was described to be neurone-specific (Kreutz et al., 1997; Tanaka et al., 1999; Sedehizade et al., 2002). p42^{IP4} protein is localized in a majority of neuronal cells of human brain sections. In the hypothalamus a subpopulation of paraventricular and infundibular nucleus neurons were strongly immunoreactive for p42^{IP4}. In cortical areas, the protein was predominantly found in large pyramidal cells. Some immunoreactivity for p42^{IP4} was also observed in the pyramidal cells of the hippocampal formation. Thus, p42^{IP4} is expressed mainly in the neurons of hippocampus, cortex, cerebellum and hypothalamus (Sedehizade et al., 2002).

1.2.3 Interaction partners of p42^{IP4}

In an attempt to delineate the functions of this protein, several protein interaction partners of p42^{IP4} have been determined. The first protein partner identified for p42^{IP4} was casein kinases I (CKI) α (Dubois et al., 2001). Mammalian CKI belong to a family of serine/threonine protein kinases involved in diverse cellular processes including cell cycle progression, membrane trafficking, circadian rhythms, and wingless int (Wnt) signalling. It was shown that CKI α co-purifies with p42^{IP4} in brain and that both proteins interact in vitro and form a complex in cells. In addition, it was shown that p42^{IP4} associates in vitro with all mammalian CKI isoforms. However, p42^{IP4} is not a substrate for CKI α and has no effect on CKI α activity.

Later, interaction of p42^{IP4} with protein kinase C (PKC) was demonstrated (Zemlickova et al., 2003). PKCs comprise a family of serine/threonine kinases classified into different groups according to activation parameters: conventional PKCs (PKC α , β I, β II, and γ), novel PKCs (PKC δ , ϵ , η , and θ), atypical PKCs (PKC ζ and ι/λ), and PKD/PKC μ . Among many other functions, PKC isoforms are involved in nuclear functions, such as cell proliferation, differentiation, and apoptosis. PKC isoforms are also involved in the regulation of cytoskeletal organisation. Members of the PKC family are regulated by several lipid second messengers, such as PIP₃. Binding of p42^{IP4} to all members of the PKC family and its phosphorylation by isoforms from all PKC classes was shown. The sites of phosphorylation by PKC α on p42^{IP4} were identified as S87 (peptide ARFESK) and T276 (peptide WFTMDDRR) (Zemlickova et al., 2003).

Nucleolin has been identified as p42^{IP4} interacting protein (Dubois et al., 2003). Nucleolin, the major protein expressed in the nucleolus, is involved in ribosome biogenesis (Ginisty et al., 1999). It was shown that nucleolin and p42^{IP4} associated both in vitro and in vivo, and that the interaction is abolished by treatment with RNase, indicating the presence of a complex composed of nucleolin, p42^{IP4}, and RNA.

It was demonstrated that in vitro, p42^{IP4} binds F-actin directly, with actin binding activity localized to the PIP₃-binding PH domain (Thacker et al., 2004). It was shown that p42^{IP4} binds Arfs in vitro and colocalizes with Arf6 and Arf5 in vivo (Thacker et al., 2004). Arfs are a family of GTPases that function in vesicular trafficking and cytoskeletal organization. In addition to its characterized roles in trafficking, Arf6 has been implicated in neuronal differentiation. Arfs are regulated by GTP-exchange factors, which facilitate GTP binding, and by Arf GAPs, which stimulate GTP hydrolysis. It was reported that p42^{IP4}

expression diminishes cortical actin and decreases Arf6GTP levels consistent with it functioning as an Arf6 GAP in vivo (Venkateswarlu et al., 2004).

More recently, the kinesin motor protein KIF13B/ guanylate kinase-associated kinesin GAKIN was identified as a $p42^{IP4}$ binding partner (Venkateswarlu et al., 2005). The KIFs are a superfamily of microtubule-associated motor proteins that mediate intracellular vesicle and organelle transport, and cell division. These motor proteins utilize the energy generated from ATP hydrolysis to transport intracellular vesicles and organelles along microtubules (MT). It was demonstrated that direct binding between $p42^{IP4}$ and KIF13B could concentrate $p42^{IP4}$ at the leading edges of the cell periphery and suppress the ARF6 GAP activity of $p42^{IP4}$ in intact cells. Identification of interaction between $p42^{IP4}$ and KIF13B suggests that KIF13B may transport ARF6 and/or PIP_3 using $p42^{IP4}$ as its receptor (Venkateswarlu, 2005).

The peptidase nardilysin, a member of the M16 family of zinc metalloendopeptidases, was found to bind specifically to $p42^{IP4}$ (Stricker et al., 2006). Furthermore, this interaction is controlled by the cognate cellular ligands of $p42^{IP4}$ (Stricker et al., 2006). Nardilysin is a metalloendopeptidase that was identified based on its ability to cleave peptides at the N-terminus of arginine and lysine residues in dibasic moieties (Chesneau et al., 1994). Recently it was shown that nardilysin is involved in the metabolism of amyloid precursor protein. Nardilysin enhances the α -secretase activity of a disintegrin and metalloprotease, which results in a decrease in the amount of amyloid- β peptide generated (Hiraoka et al., 2007).

Our laboratory has also established that a protein that is called Ran binding protein in microtubule-organizing center (RanBPM) interacts with $p42^{IP4}$ (Haase et al., 2008). RanBPM is a scaffold protein found in the nervous and immune system. IP_4 , a specific ligand for $p42^{IP4}$, is a concentration-dependent and stereoselective inhibitor of this interaction. It was hypothesized that RanBPM could act as a modulator together with $p42^{IP4}$ in synaptic plasticity. More recently, RanBPM was implicated also as a novel and potent regulator of amyloid precursor protein processing. It was found that RanBPM strongly increased β -secretase cleavage of amyloid precursor protein and amyloid- β generation (Lakshmana et al., 2009).

1.2.4 Known functions of $p42^{IP4}$

Various functions have been proposed for $p42^{IP4}$. This protein contributes to the activation of extracellular regulated kinase in growth factor signalling, linking the pathway of phosphoinositide 3-kinase (PI 3-K) to the pathway of extracellular regulated kinase mitogen-

activated protein kinase. This occurs through its ability to interact with PIP₃ (Hayashi et al., 2006). There are reports, which showed the involvement of this protein in the activation cascade of the transcription factor activator protein-1 (Chanda et al., 2003). Thrombin-dependent trafficking of p42^{IP4} between cytosol and plasma membrane was demonstrated *in vivo* in cells. All three protein domains of p42^{IP4} are important for the epidermal growth factor-mediated intracellular trafficking (Sedehizade et al., 2005).

p42^{IP4}, containing an ARF GAP domain, specifically inhibits *in vivo* GTP loading of ARF6 and redistribution of ARF6 from the endosomal compartment to the plasma membrane, which is indicative of its activation. p42^{IP4} also inhibits cortical actin formation in a PIP₃-dependent manner. Therefore, p42^{IP4} negatively regulates ARF6 activity by functioning as an *in vivo* PIP₃-dependent ARF6 GAP (Venkateswarlu et al., 2004). Later, it was shown that by acting as an ARF6 GAP, p42^{IP4} is able to switch off ARF6 and so inhibit its ability to mediate β 2-adrenoceptor internalization (Lawrence et al., 2005).

p42^{IP4} expression produces dramatic effects on the actin cytoskeleton, decreasing stress fibers, diminishing cortical actin, and enhancing membrane ruffles and filopodia. Thus, it was suggested that p42^{IP4} may be a component of the neuronal PI 3-K cascade that leads to regulation of the neuronal actin cytoskeleton (Thacker et al., 2004). Moreover, p42^{IP4} regulates the actin cytoskeleton via both ARF GAP-dependent and ARF GAP-independent mechanisms (Thacker et al., 2004).

It was shown that KIF13B directly interacts with p42^{IP4}, and mediates the transport of PIP₃-containing vesicles (Horiguchi et al., 2006). Recombinant KIF13B and p42^{IP4} form a complex on synthetic liposomes containing PIP₃ and support the motility of the liposomes along MT *in vitro*. Finally it was suggest that, in neurons, the KIF13B - p42^{IP4} complex transports PIP₃ to the neurite ends and regulates neuronal polarity formation (Horiguchi et al., 2006).

In cultured dissociated hippocampal neurons, p42^{IP4} localizes to dendrites, dendritic spines and the postsynaptic region (Moore et al., 2007). Both filopodia and lamellipodia have been implicated in dendritic branching and spine formation. Following synaptogenesis in cultured neurons, wild-type p42^{IP4} expression increases dendritic filopodia and spine-like protrusions. Moreover, p42^{IP4} was found to function through GAP-dependent Arf regulation of dendritic branching and spines. Thus, p42^{IP4} was demonstrated as developmentally expressed Arf GAP, which is required for dendritic differentiation in developing neurons. (Moore et al., 2007).

p42^{IP4} has already been linked to short-term regulation of behavioural responses in rat brain (Reiser and Bernstein, 2004). Down-regulation of the mRNA and protein levels within 2 h in amygdala, hypothalamus and cingulate/retrosplenial cortex following acoustic and electric stimulation have been shown. This is the first indication that p42^{IP4} may play an important role in the signal transduction pathways regulating plasticity in neuronal cells (Reiser and Bernstein, 2004).

Very interestingly, p42^{IP4} seems to be involved also in neuronal diseases, since p42^{IP4} was found to be up-regulated in neurons in the brain of Alzheimer's disease (AD) patients and is detected in AD plaques (Reiser and Bernstein, 2002, , 2004). It was hypothesized that p42^{IP4} might be a pivotal signalling protein in determining neuronal survival in the pathogenesis of AD, by interacting with CK I and nucleolin–RNA complexes (Reiser and Bernstein, 2004).

1.2.5 The ligands of p42^{IP4}

Phosphoinositides and inositol polyphosphates are central players in intracellular signal transduction (Prestwich, 2004). Receptor-regulated PI 3-K phosphorylates phosphatidylinositol(4,5)bisphosphate on position 3, yielding PIP₃, which is involved in many cellular responses including membrane vesicle trafficking, protein sorting, cytoskeletal rearrangement, apoptosis and chemotaxis (Toker and Cantley, 1997).

Receptor-activated phospholipase C isoforms hydrolyse phosphatidylinositol(4,5)bisphosphate, yielding inositol (1,4,5) trisphosphate (IP₃) and diacylglycerol (Berridge, 1993). The signal of IP₃ is terminated either by specific enzymatic dephosphorylation in position 5 or phosphorylation in position 3 by the IP₃ 3-kinase to IP₄ (Berridge, 1993; Stephens et al., 1993). IP₄ has attracted particular attention as a putative second messenger. Its physiological role, however, is not yet understood. For instance, IP₄ has been reported to regulate the frequency of Ca²⁺ oscillations (Zhu et al., 2000), and to facilitate store-operated calcium influx by inhibition of IP₃ 5-phosphatase (Hermosura et al., 2000).

PIP₃ mediates its effects by recruiting proteins to the membrane that are capable of binding tightly and, at least in some cases, specifically to the lipid through phosphoinositide binding domains, most commonly PH domains (Ferguson et al., 2000; Lemmon and Ferguson, 2000). Thus, an artificially plasma membrane-targeted p42^{IP4} bypasses the requirement of PIP₃ for its involvement in ARF6 inactivation, suggesting that PIP₃ is required for recruitment of p42^{IP4} to the plasma membrane but not for its activity (Venkateswarlu et al., 2004).

However, it was shown that phosphorylation of the second messenger IP₃ to inositol IP₄ establishes another mode of PH domain regulation through a soluble ligand. At physiological concentrations, IP₄ promoted PH domain binding to PIP₃. In primary mouse thymocytes, this was required for full activation of a protein tyrosine kinase called Itk after T cell receptor engagement. Thus, IP₄ acts as an important “third messenger” *in vivo* (Huang et al., 2007).

In neutrophils, chemoattractant stimulation triggered rapid elevation in IP₄ concentration. Depletion of IP₄ enhanced membrane translocation of the PIP₃-specific PH domain. This led to enhanced sensitivity to chemoattractant stimulation, elevated superoxide production, and enhanced neutrophil recruitment to inflamed peritoneal cavity. On the contrary, increase of intracellular IP₄ concentration blocked PH domain-mediated membrane translocation of target proteins and dramatically decreased the sensitivity of neutrophils to chemoattractant stimulation (Jia et al., 2007). Furthermore, IP₄ was shown to play a role in maintaining neutrophil survival. Depletion of IP₄ leads to accelerated neutrophil spontaneous death. Finally, it was established that IP₄ is essential modulators of neutrophil function and innate immunity (Jia et al., 2008).

In neurons, as a consequence of the elongation of one neurite, the axon is specified and the cell acquires its polarity. In developing hippocampal neurons, PIP₃ was found that accumulates in the tip of the growing processes. Moreover, it was suggest that PIP₃ is involved in axon specification, possibly by stimulating neurite outgrowth (Menager et al., 2004). Later, it was proposed that the KIF13B - p42^{IP4} complex transports PIP₃-containing vesicles from the cell body to the distal end of the neurites (Horiguchi et al., 2006).

It was shown that PI 3-K activation and subsequent generation of PIP₃ are responsible for membrane translocation of p42^{IP4}. Moreover, by activation of the phospholipase C-coupled thrombin receptor and subsequent activation of PI 3-K via epidermal growth factor in HEK 293 cells it was demonstrated that *in vivo* cellular trafficking of the human p42^{IP4} is dependent on products of both PI 3-K and IP₃ 3-kinase, PIP₃ and IP₄ (Sedehizade et al., 2005).

Interestingly, cognate cellular ligands of p42^{IP4}, PIP₃ and IP₄, control the interaction of p42^{IP4} with the peptidase nardilysin. Moreover, it was suggested that PIP₃ and IP₄ can modulate the recruitment of proteins, which are docked to p42^{IP4}, to specific cellular compartments (Stricker et al., 2006). IP₄ is also a concentration-dependent and stereoselective inhibitor for the interaction of p42^{IP4} with RanBPM (Haase et al., 2008).

1.3 2',3'-Cyclic nucleotide-3'-phosphodiesterase (CNP)

CNP is a myelin-associated protein, an enzyme abundantly present in the central nervous system of mammals and some vertebrates. *In vitro*, CNP specifically catalyzes the hydrolysis of 2',3'-cyclic nucleotides to produce 2'-nucleotides, but the physiologically relevant *in vivo* substrate is still unknown. The purified protein from brain is highly basic, with an isoelectric point close to 9.

1.3.1 Two isoforms of CNP

Oligodendrocytes, Schwann cells, and myelin from all species examined manifest two isoforms, designated CNP1 (~ 46 kDa) and CNP2 (~ 48 kDa). These have identical amino acid sequences except for a 20-residue extension at the N-terminus that is exclusive to CNP2 (Kurihara et al., 1990; Kurihara et al., 1992; Gravel et al., 1994). One gene (Douglas et al., 1992; Monoh et al., 1993) consisting of four exons and two promoters gives rise to two RNA transcripts, one of which can generate both proteins. Both polypeptides are synthesized on free ribosomes (Gillespie et al., 1990), both are enzymatically active, and both are post-translationally modified by isoprenylation at the C-terminus (De Angelis and Braun, 1994; O'Neill and Braun, 2000).

1.3.2 Motifs in primary structure and modifications of CNP

The sequence identity or homology is relatively strong among amino acid sequences of CNP from different species, as deduced from cDNAs for bullfrog, chicken, mouse, rat, bovine, and human. All CNP species have strongly conserved consensus motifs for the potential binding of nucleotide phosphoryl groups in both the N-terminal and C-terminal domains.

ATPase motifs, along with the adenine recognition motif (YFGKRPPG), are common to many nucleotide binding proteins and enzymes. Interestingly, since they fall outside the essential catalytic domain of CNP (Lee et al., 2001), they must serve another nucleotide-related function. ATPase activity has not been detected in purified preparations of CNP or in the recombinant protein. Although some preliminary experiments suggest that ATP (and other nucleoside triphosphates) may bind to CNP, definitive experiments have not yet been done.

By alignments of nucleotide binding motifs with other enzymes, it was noted that CNP shares modest sequence similarities with polynucleotide kinase (Koonin and Gorbalenya, 1990; Gravel et al., 1994), and it was suggested that CNP might also possess this

activity. This possibility was subsequently tested with catalytically active recombinant CNP in a polynucleotide kinase assay, with no such activity being evident (Prinos et al., 1995).

The **C-terminal isoprenylation motifs**, present in CNP of all species, have been the focus of some attention. Prenylated proteins are posttranslationally modified by formation of cysteine thioethers with the isoprenoid lipids farnesyl (C-15) or geranylgeranyl (C-20) at or near the carboxy terminus. Most of these proteins are members of signal-transducing pathways. CNP is typical of a large category of proteins bearing a cys-A1, A2-X motif in which A1 and A2 are aliphatic amino acids and X is any amino acid; these are removed once the cys has become isoprenylated. The terminal carboxyl end then may become modified by methylation (Sinensky, 2000). It was shown that isoprenylation mediates the binding of CNP to membranes, explaining the avid association with myelin in the absence of a protein transmembrane domain (Braun et al., 1991; De Angelis and Braun, 1994). It was determined that the isoprenylated cysteine in CNP undergoes the additional carboxymethylation step (Cox et al., 1994). The consequences of this for CNP biology were not established, but a body of evidence suggests that there is biological importance of this modification for some proteins, and that methylation greatly enhances the association of farnesylated peptides with lipid bilayers (Sinensky, 2000).

More recently, the prenylation was determined to be a process necessary to permanently anchor CNP to the plasma membrane (Esposito et al., 2008). A 13 residue, C-terminal CNP fragment, C13, was demonstrated to be directly responsible for CNP membrane anchoring. Furthermore, a general model was proposed, in which the post-translational lipidation is an important biomolecular trick to enlarge the hydrophobic surface and to enable the contact of the protein with the membrane (Esposito et al., 2008).

Modification of CNP by fatty acylation (palmitoylation) has also been demonstrated, although the site for palmitoylation (a cysteine residue) has yet to be identified (Agrawal et al., 1990b). Further, acylation occurs independently of isoprenylation, since the C397S mutant CNP is just as strongly palmitoylated as the wild-type protein (De Angelis and Braun, 1994). The addition of these hydrophobic groups has significance for the targeting of proteins to specific membrane microdomains (“lipid rafts”). Lipid rafts are rich in glycosphingolipids and cholesterol and are believed to have important roles in the organization of signalling complexes (Kim and Pfeiffer, 1999).

The 20 amino acid domain at the N-terminus of CNP2 (referred to as N2 for N-terminal domain of CNP2) is highly conserved among all species studied. Its structure meets the basic requirements for a mitochondrial targeting signal in that it has a net positive charge,

some hydroxylated and hydrophobic residues, lacks acidic residues, and is predicted to form an α -helix (von Heijne et al., 1989; Neupert, 1997). The N2 domain is capable of being phosphorylated on serines 9 and 22 (O'Neill and Braun, 2000). In oligodendrocytes phosphorylation of serine 9 occurs after treatment with phorbol ester, a known activator of PKC, whereas serine 22 (putative protein kinase A phosphorylation site) is constitutively phosphorylated. CNP2 may either be phosphorylated by PKC and/or protein kinase A (Bradbury et al., 1984; Bradbury and Thompson, 1984; Vartanian et al., 1988; Agrawal et al., 1990b; Vartanian et al., 1992; Agrawal et al., 1994).

1.3.3 Mitochondrial localization of CNP

Previously CNP had been observed associated with mitochondria in adrenal cells (McFerran and Burgoyne, 1997). Recently, it was demonstrated that CNP2 is translocated to mitochondria by virtue of a mitochondrial targeting signal at the N-terminus (Lee et al., 2006). It was established that the N2 domain of CNP2 was sufficient for mitochondrial localization. This was determined by finding that a fusion protein of N2 with green fluorescent protein (GFP) was efficiently targeted to mitochondria. PKC-mediated phosphorylation of the targeting signal at Ser22, and, to a smaller extent, Ser9, inhibits CNP2 translocation to mitochondria, thus retaining CNP in the cytoplasm. CNP2 is imported into mitochondria and the targeting signal cleaved, yielding a mature, truncated form similar in size to CNP1. CNP2 is entirely processed in adult liver and embryonic brain, indicating that it is localized specifically to mitochondria in non-myelinating cells. Therefore, a broader biological role for CNP2 in mitochondria during myelination was suggested. The biochemical analysis and electron microscopy of immunogold-labeled CNP demonstrate that CNP2 is peripherally and tightly associated with the mitochondrial inner membrane on the side facing the intermembrane space (Lee et al., 2006). Furthermore, in amoeboid microglial cells in developing rat brain, CNP was associated primarily with the plasma membrane, filopodial projections and mitochondria (Wu et al., 2006).

All these data indicate that a mitochondrial role for CNP is likely to be different from its specific role in the cytoplasm. However, there were no data on the function of CNP in mitochondria so far.

1.3.4 Enzymatic characteristics of CNP

All 2',3'-cyclic mono-nucleotides can be hydrolyzed by CNP to yield 2'-nucleotides exclusively. CNP does not act upon 3', 5'-cyclic mononucleotides (cAMP, cGMP). This enzyme does not cleave other cyclophosphate rings. Although physiologically relevant substrates with 2',3'-cyclic termini have not yet been reported, numerous cyclic phosphate-

containing RNAs that are generated as intermediate products of splicing reactions are present in most cells.

Although a range of kinetic parameters have been reported, the most rigorous study of CNP to date shows that purified recombinant CNP1 hydrolyzes cyclic NADP (in the assay of (Sogin, 1976)) with a K_m of 0.26 mM and a k_{cat} of 836 s^{-1} at $25\text{ }^{\circ}\text{C}$ (Lee et al., 2001). The catalytic domain resides in the C-terminal region comprising two-thirds of the protein. Mapping of the catalytic domain by deletion mutant analysis, by chemical modification studies of specific amino acids and by site-directed mutagenesis have provided new insights. Contrary to earlier reports, cysteine residues have nonessential roles for enzymatic activity. On the other hand, two specific histidines (positions 230 and 309 in CNP1) are essential for catalytic activity (Lee et al., 2001); they are part of two tetrapeptide motifs, H-X-T/S-X (where X is often a hydrophobic residue), that are essential for the enzymatic activity of the other three classes of related enzymes (Hofmann et al., 2002).

1.3.5 Three-dimensional structural features of CNP and link to RNA metabolism

The solution structure of the catalytic core fragment of CNP (residues 163 to 378 of rat CNP1) has been determined by NMR (Kozlov et al., 2003). Interestingly, the folded structure is remarkably similar to known structures of two other proteins. The first protein is cyclic nucleotide phosphodiesterase from the plant *Arabidopsis thaliana*. This is an enzyme involved in the tRNA splicing pathway, known to hydrolyze ADP-ribose 1',2'-cyclic phosphate (Hofmann et al., 2000). The second protein is bacterial 2'-5' RNA ligase from *Thermus thermophilus*, which is an enzyme that ligates tRNA half-molecules containing 2', 3'-cyclic phosphate and 5'-hydroxy termini (Kato et al., 2003).

Collectively, this group of enzymes appears to constitute a super-family of proteins, with enzymatic activities not yet well understood in a physiological context, but with an apparent link (inferred for CNP) to RNA metabolism. This inference for CNP is further strengthened by the observation that the β -sheet surface in the active site has an abundance of positively charged and aromatic residues, a common feature of RNA-binding proteins. Coupled with a large binding cavity, this suggests that RNA could be a substrate for CNP (Kozlov et al., 2003).

Indeed, very recently, it was shown that CNP is an RNA-binding protein (Gravel et al., 2009). Furthermore, by using precipitation analyses, it was demonstrated that CNP associates with poly(A)(+) mRNAs *in vivo* and suppresses translation *in vitro* in a dose-dependent manner. Isolated RNA aptamers can suppress the inhibitory effect of CNP on translation. It was also demonstrated that CNP1 could bridge an association between tubulin

and RNA. It was suggested that CNP1 may regulate the expression of mRNAs in oligodendrocytes of the central nervous system (Gravel et al., 2009).

1.3.6 Interaction partners of CNP

In earlier studies of cultured oligodendrocytes, CNP appears to co-localize with both actin and tubulin-based cytoskeletal networks (Dyer and Benjamins, 1988, , 1989; Dyer and Matthieu, 1994; Dyer et al., 1995). Later, CNP was shown to bind to the actin-based cytoskeleton (De Angelis and Braun, 1996).

Initial work showed detailed confocal images of CNP and tubulin colocalized in primary cultures of differentiated oligodendrocytes (Dyer and Benjamins, 1989). The colocalization was particularly along the microtubular veins in the membraneous sheets and in numerous discrete large “cuff-like” punctate structures that dot the microtubule network.

Further biochemical evidence for CNP-tubulin interaction was derived from observations that MT in cultured rat thyroid cells became dissociated from the plasma membrane after treatment with lovastatin, a drug that blocks isoprenylation. Since tubulin lacks the motif for isoprenylation, it was reasoned that an isoprenylated linker protein was responsible for membrane attachment of MT. A 48kDa isoprenylated protein was later identified to be CNP (Laezza et al., 1997).

Subsequently, CNP was found not only to be associated with MT in cultured rat thyroid cells and brain tissue, but was also co-purified with MT by successive cycles of polymerization and depolymerization. Thus, CNP was identified as a microtubule-associated protein, which furthermore possesses microtubule polymerization activity *in vitro* (Bifulco et al., 2002). The domain responsible for this activity, but not for tubulin binding, was identified as the last 13 amino acids at the C terminus of CNP. This peptide containing C-terminal 13 residues caused MT to polymerize *in vitro*. Moreover, preliminary *in vitro* data suggested that CNP phosphorylation by PKC negatively regulates microtubule polymerization. Submembranous colocalization of the proteins and CNP-dependent microtubule organization suggest that CNP is a membrane-bound microtubule-associated protein that can link tubulin to membranes and may regulate cytoplasmic microtubule distribution (Bifulco et al., 2002).

Oligodendrocytes extend arborized processes that are supported by MT and microfilaments. CNP was shown to mediate process formation in oligodendrocytes (Lee et al., 2005). It was reported that tubulin is a major CNP-interacting protein. *In vitro*, CNP binds preferentially to tubulin heterodimers compared with MT and induces MT assembly by copolymerizing with tubulin. Moreover, CNP overexpression induces dramatic morphology changes in both glial and non-glial cells, resulting in MT and F-actin reorganization and

formation of branched processes. These morphological effects are attributed to CNP-MT assembly activity. Accordingly, cultured oligodendrocytes from CNP-deficient mice extend smaller outgrowths with less arborized processes. Therefore, it was proposed that CNP is an important component of the cytoskeletal machinery that directs process outgrowth in oligodendrocytes (Lee et al., 2005).

Recently, substantial colocalization of CNP with Juxtanodin in the myelin sheath was shown. Juxtanodin is an oligodendroglial protein featuring a putative C-terminal actin-binding domain. Furthermore, expression of Juxtanodin promoted arborization of cultured OLN-93 cells and CNP trafficking to the process arbors of cultured primary oligodendrocyte precursors (Zhang et al., 2005).

1.3.7 Functions of CNP

Numerous studies were performed to link CNP to any inherited diseases of myelin and neurological mutations in mice, which can cause an assortment of demyelinating and dysmyelinating pathologies. In studies of encephalitogenic proteins that could function as self-antigens in inflammatory demyelinating diseases, CNP has been considered as a potential autoantigen. However, CNP was found not to be encephalitogenic in rodents, although a heat-shock protein related peptide domain of CNP was shown to alter the course of experimental autoimmune encephalomyelitis (Birnbbaum et al., 1996). Later it was confirmed that CNP was non-encephalitogenic in several mouse strains, even though several CNP epitopes could induce T-cell responses in these mice (Maatta et al., 1998; Morris-Downes et al., 2002).

Several studies implicated CNP as an autoantigen in multiple sclerosis. It was reported that antibodies to CNP were detected in sera of 74% of patients with multiple sclerosis (Walsh and Murray, 1998). These antibodies were present as IgM in high titer also in cerebrospinal fluid. Further, CNP-containing immune complexes were found in brain tissue of some patients. Curiously, the antibody response was against CNP1 and not CNP2. However, both isoforms were reported to bind the C3 complement, fueling speculation about a role for CNP in the pathogenesis of multiple sclerosis (Walsh and Murray, 1998).

CNP has been considered as a potential antigenic target for a T-cell response in the pathogenesis of demyelinating diseases. A recombinant human CNP was used to isolate several specific T-cell lines from a patient with multiple sclerosis, as well as from a healthy control (Rosener et al., 1997). Further, human CNP from brain as well as specific CNP peptides were used to screen for human T-cell responses. Primary proliferative responses were detected in some patients with multiple sclerosis as well in healthy controls. The T-cell responses were directed mainly to the CNP1 polypeptide region 343–373. Despite a detailed

analysis of their findings, an unambiguous involvement of CNP-specific T cells in multiple sclerosis could not be established (Muraro et al., 2002).

Expression of CNP in amoeboid microglial cells in developing rat brain from prenatal day 18 to postnatal day 10 was demonstrated *in vivo* and *in vitro*, respectively. The functional role of CNP in amoeboid microglial cells remains speculative. Given its expression in amoeboid microglial cells transiently occurring in the perinatal brain and that it is markedly elevated in activated microglia, it is suggested that the enzyme may be linked to the major functions of the cell type such as release of chemokines and cytokines. In relation to this, CNP may play a key role associated with transportation of cytoplasmic materials (Wu et al., 2006).

Converging evidence from imaging, microarray, genetic, and other studies suggests that abnormalities in myelin may play a role in schizophrenia. The expression of CNP has been reported to be reduced in the schizophrenic brain (Peirce et al., 2006). Further confirmation implicating myelin abnormalities in the etiology of schizophrenia has been revealed. A genetic variation in the *Cnp* gene, rs2070106, has recently been shown to be associated with schizophrenia in Caucasians (Voineskos et al., 2008). However, no association between genetic variations in the *Cnp* gene and schizophrenia in the Han Chinese population was found (Tang et al., 2007).

In a molecular genetic approach to CNP function, the expression of CNP in oligodendrocytes was increased by introduction of the human gene into mice (Gravel et al., 1996). A transgenic line expressing a six-fold increase of CNP protein developed abnormalities suggestive of a gain of function due to the extra CNP. In adult mice, large vacuoles were observed, surrounded by myelin membranes that extended from myelin internodes. Further, an absence of the major dense lines from compact myelin was seen in about half of the myelin sheaths. Oligodendrocytes cultured from these adult animals manifested a more robust and aggressive regrowth of cellular processes. This was consistent with other studies, which connected CNP to the cytoskeleton and to process extensions. Further observations on these CNP overexpressing mice revealed aberrant oligodendrocyte and myelin membrane formation during early stages of oligodendrocytes differentiation (Yin et al., 1997).

Generation of *Cnp1*-null mutant mice (Lappe-Siefke et al., 2003) has thus far provided little insight into CNP function in myelinogenesis. In these animals that lack CNP protein, myelination appears to follow a normal course and is morphologically normal. However, the adult mice manifest a severe neurodegenerative disorder, with axonal swellings

and Wallerian degeneration causing a large microglial response, hydrocephalus and premature death. Therefore, it was suggested that CNP is essential for axonal survival.

Later it was reported that *Cnp1*-null mice have disrupted axoglial interactions, which underlie the clustering of ion channels and of cell adhesion molecules, regulate gene expression, and control cell survival in the central nervous system (Rasband et al., 2005). Nodal sodium channels and paranodal adhesion proteins are initially clustered normally, but become progressively disorganized with age. This disorganization is prominent in older *Cnp1*-null mice and occurs before axonal degeneration and microglial invasion. Disrupted axoglial signalling underlies progressive axonal degeneration, observed later in the central nervous system of *Cnp1*-null mice. Thus, it was suggested that CNP is a glial protein required for maintaining the integrity of paranodes (Rasband et al., 2005).

Changes in brain white matter are prominent features of the aging brain. These include glial cell activation, disruption of myelin membranes with resultant reorganization of the molecular components of the node of Ranvier, and loss of myelinated fibers associated with inflammation and oxidative stress. Overexpression of CNP was already implicated in age-related changes in myelin and axons (Gravel et al., 1996; Yin et al., 1997; Lappe-Siefke et al., 2003).

Very recently it was shown that with age, excess CNP which is found in myelin and throughout brain white matter accompanied by proteolytic fragments of CNP (Hinman et al., 2008). It was suggested that incomplete degradation of CNP due to failure of the proteasomal system and aberrant degradation by calpain-1 leads to age-related CNP accumulation and proteolysis. Moreover, it was proposed that these phenomena result in age-related dysfunction of CNP in the lipid raft, which may lead to myelin and axonal pathology (Hinman et al., 2008).

1.4 Aims of this study

1.4.1 Motivation

Previously, expression of the p42^{IP4} protein in chinese hamster ovary (CHO) cells stably transfected with pcDNA-p42^{IP4} was shown in cytosol, membranes and nucleus (Sedehizade et al., 2002). The membrane fraction in that study also contained mitochondria. Moreover, the yeast protein Gcs1p, which is structurally and functionally related to p42^{IP4}, is localized in mitochondria and is involved in maintenance of mitochondrial morphology (Huang et al., 2002). Finally, a high probability for mitochondrial localization of p42^{IP4} had been predicted by the program PSORT II (<http://psort.nibb.ac.jp/>; Nakai and Kanehisa, 1992). Therefore, we hypothesized localization of p42^{IP4} in mitochondria.

Previously, CNP was found in mitochondria of adrenal medullary chromaffin cell cultures (McFerran and Burgoyne, 1997), amoeboid microglial cells (Wu et al., 2006) and oligodendrocyte cell line (OLN93 cells) (Lee et al., 2006), but the role of CNP in mitochondria is still obscure. We found localization of both, p42^{IP4} and CNP, in the inner membrane fraction of mitochondria. This indicates some unknown functions for these proteins in mitochondrial physiology.

1.4.2 Main aims and goals of study

The main aim of this investigation was to study as possible mitochondrial function the participation of p42^{IP4} and CNP in Ca²⁺-induced PTP. Cellular Ca²⁺ signals are crucial in the control of cell death. Mitochondria dampen cytosolic Ca²⁺ loads and support cellular Ca²⁺ homeostasis. However, mitochondria take up a limited amount of calcium up to a certain threshold. Accumulation of Ca²⁺ above this threshold leads to increased permeability of the inner mitochondrial membrane due to formation of an unselective pore, which is called the PTP.

Since Ca²⁺-induced PTP opening is important in mitochondrial events leading to programmed cell death, we investigated whether p42^{IP4} and CNP are involved in Ca²⁺-induced PTP functioning in mitochondria and therefore control pore-dependent apoptosis. The results of our investigation might be helpful for understanding the death response of mitochondria leading to neurodegeneration, based on the action of the PTP complex.

To improve the understanding of p42^{IP4} and CNP functions in mitochondria, we planned in the current study to establish the possible p42^{IP4} /CNP interaction and to identify further interacting proteins.

1.4.3 Strategy

To establish exact mitochondrial localization of p42^{IP4}, CHO cells and N2a (mouse neuroblastoma) cells stably transfected with pcDNA-p42^{IP4} were analysed by subcellular fractionation, confocal microscopy and submitochondrial fractionation.

To find out protein partners of p42^{IP4} and CNP in RBM, GST pull-down binding assay and immunoprecipitation were used.

To perform functional studies of mitochondria, we established the method of isolation of functionally active mitochondria from cultured cells. The effect of the Ca²⁺-induced PTP opening on functional state of isolated mitochondria from different types of cells and tissues in different conditions was examined.

The influence of overexpression of p42^{IP4} in N2a cells and the influence of CNP knock-down in OLN-93 cells on mitochondrial functions during Ca²⁺-induced PTP opening were investigated.

2. Materials and Methods

2.1 Materials

2.1.1 Chemicals and Reagents

| Chemicals | Manufacturer |
|---|---|
| IP ₄ (D-myo-inositol 1,3,4,5-tetrakisphosphate, tetrapotassium salt) | Alexis, Gruenberg, Germany |
| Bacto Agar | BD Bioscience (Clontech), Heidelberg, Germany |
| Bacto Tryptone | |
| Bacto Yeast extract | |
| G418 Sulphate | |
| Dulbecco's Modified Eagle's Medium (DMEM) | Biochrom, Berlin, Germany |
| HAM'S F12 | |
| Fetal calf serum (FCS) | |
| Penicillin and Streptomycin | |
| Ampicillin | |
| Rotenone | Biomol |
| Bio-Rad protein assay dye reagent concentrate | Bio-Rad Laboratories, München, Germany |
| Immersol TM 518N (Immersion oil for microscopy) | Boehringer, Mannheim, Germany |
| PIP ₃ (phosphatidylinositol 3,4,5-Trisphosphate diC8) | Echelon Biosciences Incorporated, Salt Lake City, UT, USA |
| Ammonium peroxodisulfate | Fluka |
| Sodium azide | |
| Paraformaldehyde (PFA) | |
| Protein A Sepharose CL-4B | GE Healthcare, Munich, Germany |
| Glutathione-Sepharose 4B | |
| Magnet assisted transfection | IBA GmbH |
| TEMED | Roche, Mannheim, Germany |
| FuGENE 6 | |

| | |
|---|-----------------------------|
| protease inhibitor cocktail tablets | |
| trypsin | |
| ponceau S solution (0.2% in 3% acetic acid) | |
| Acrylamide | SERVA, Heidelberg, Germany |
| N, N'-Methylenbisacrylamide | |
| Protein G agarose | Sigma, Taufkirchen, Germany |
| Dimethyl sulfoxide (DMSO) | |
| TEMED | |
| β-mercaptoethanol | |
| Igepal CA630 | |
| Bromphenol blue | |
| PAP pen for immunostaining | |
| poly-L-lysine | |
| Isopropyl b-D-thiogalactoside | |
| 2',3'cyclic AMP | |
| 2',3'cyclic GMP | |
| 2',3'cyclic NADP | |

All other chemical reagents from Carl Roth

2.1.2 Antibodies

2.1.2.1 Primary antibodies

| Antibody | Manufacturer |
|---|-------------------------------------|
| Rabbit anti-CNP (antibody 27695) | Abcam, Cambridge, UK |
| Rabbit anti-SOD 2 (Mn-superoxide dismutase 2, antibody 13533) | |
| Mouse monoclonal anti-Nucleoporin p62 | BD Biosciences, Heidelberg, Germany |
| Mouse monoclonal anti-Cyt c (cytochrome c, clone 6H2.B4) | |
| Mouse monoclonal anti-plasma membrane calcium ATPase (clone 5F10) | Biozol, Eching, Germany |
| Mouse monoclonal anti- Cyt c (cytochrome c, clone 7H8.2C12) | |
| Rabbit anti-VDAC (voltage-dependent anion | Calbiochem, Schwalbach, Germany |

| | |
|---|---------------------------------------|
| channel, Ab-5) | |
| Mouse monoclonal anti-GAPDH (glyceraldehyde 3-phosphate dehydrogenase, clone 6C5) | Chemicon, Martinsried/Munich, Germany |
| Mouse monoclonal against Myc | Invitrogen, Karlsruhe, Germany |
| Mouse monoclonal against ANT (adenine nucleotide translocator) | MitoSciences, Eugene, Oregon, USA |
| Mouse monoclonal against COXIV (Cytochrome oxidase subunit IV, clone 20E8C12) | Sigma, Taufkirchen, Germany |
| Mouse monoclonal against β -tubulin I | |
| Mouse monoclonal against α - tubulin | |
| Mouse monoclonal anti-Synaptotagmin I (clone 41.1) | Synaptic Systems, Gottingen, Germany |
| mouse monoclonal against CNP | Published |
| Mouse monoclonal against p42 ^{IP4} (Mab117-2) | Published |
| rabbit polyclonal against p42 ^{IP4} (AS1516g) | Published |
| Normal mouse IgG | Santa Cruz |
| Normal rabbit IgG | Santa Cruz |

2.1.2.2 Secondary antibodies

| Antibody | Manufacturer |
|--|--|
| peroxidase-conjugated goat anti-mouse IgG | Dianova, Hamburg, Germany |
| peroxidase-conjugated goat anti-rabbit IgG | |
| Alexa Fluor® 555 goat anti-mouse IgG | Molecular Probes, MoBiTec, Göttingen, Germany |
| Alexa Fluor® 488 goat anti-rabbit | |

2.1.3 Cells, medium and related reagents

2.1.3.1 Mammalian cells

Cell lines

- a) CHO631 (Hamster ovary cells)
- b) N2a (Mouse neuroblastoma)

c) OLN93 (Rat oligodendrocytes)

d) HEK293 (Human embryonic kidney)

Cell culture medium and solvents

CHO631 cells - HAM'S F-12: 1.17 g/L NaHCO₃, 1.802 g/L D-glucose, 0.146 g/L L-glutamine, 100U/ml Penicillin, 100 µg/ml Streptomycin

N2a cells - DMEM: 3.7 g/L NaHCO₃, 4.5 g/L D-glucose, 1.028 g/L N-Acetyl L-alanyl-L-glutamine, 10% FCS, 100U/ml Penicillin, 100 µg/ml Streptomycin

OLN93 cells - DMEM: 3.7 g/L NaHCO₃, 4.5 g/L D-glucose, 1.028 g/L N-Acetyl L-alanyl-L-glutamine, 10% FCS, 100U/ml Penicillin, 100 µg/ml Streptomycin

HEK-293 cells- DMEM/HAM'S F12 (1:1) with 2mM Glutamine, 10% FCS, 100U/ml Penicillin, 100 µg/ml Streptomycin

HBSS (Hanck's balanced salt solution) without Ca²⁺ and Mg²⁺ from PAA.

G418 sulphate was from Calbiochem. stock: 500 mg/ml, working concentration: 500 µg/ml

2.1.3.2. Bacterial cells:

Bacteria strains: DH5a, XL1-Blue, BL21

LB medium

10 g/l Bacto-tryptone (BD Bioscience), 5 g/l Bacto-yeast extract (BD Bioscience),

10 g/l NaCl, pH 7.0

LB agar plates

LB medium, 18 g/l Bacto-agar (BD Bioscience), appropriate antibiotic (100 µg/ml ampicillin)

2.1.4 Animals

Male Sprague Dawley rats from Harlan-Winkelmann GmbH, Borcheln, Germany

2.1.5 Plasmid vectors:

pcDNA3.1+ from Invitrogen

pcDNA3.1/Myc-His (B) from Invitrogen

pGEX 5X-2 from GE Healthcare

pEGFP-C2 from BD Bioscience (Clontech)

2.1.6 Small interfering RNAs (siRNAs)

ON-TARGETplus SMARTpool of 4 siRNAs targeting rat CNP1 from Dharmacon, Chicago, IL, USA

| siRNA name | siRNA sequence |
|---|---|
| siGENOME ON-TARGETplus SMARTpool duplex (9), J-080116-09, CNP1 | Sense Sequence GCACAAGCUUUGCCCGAAAUU |
| | Antisense Sequence 5'-PUUUCGGGCAAAGCUUGUGCUU |
| siGENOME ON-TARGETplus SMARTpool duplex (10), J-080116-10, CNP1 | Sense Sequence CCGAGGAGUACAAGCGUCUUU |
| | Antisense Sequence 5'-PAGACGCUUGUACUCCUCGGUU |
| siGENOME ON-TARGETplus SMARTpool duplex (11), J-080116-11, CNP1 | Sense Sequence GUGAGGAGAUCUUACGGCAUU |
| | Antisense Sequence 5'-PUGCCGUAAGAUCUCCUCACUU |
| siGENOME ON-TARGETplus SMARTpool duplex (12), J-080116-12, CNP1 | Sense Sequence GUUCCGAGACCCUCCGAAAUU |
| | Antisense Sequence 5'-PUUUCGGAGGGUCUCGGAACUU |

Non-silencing siRNA from Qiagen.

2.1.7 Enzymes

| Enzymes and buffer | Manufacturer |
|--|---|
| T4 DNA Ligase | Gibco BRL (Life Technologies), Karlsruhe, Germany |
| Eco RI | MBI Fermentas, St. Leon-Rot, Germany |
| NotI | |
| Tango ⁺ (yellow) (10X) buffer | |

2.1.8. Molecular weight markers

Nucleic acid standard markers

GeneRuler[™] 1 kb and 100 bp DNA ladders from MBI Fermentas.

Protein standard marker

Precision Plus Protein All Blue Standard (250-10 kDa) from Bio-Rad

2.1.9 Kits

| Type of kit | Usage | Manufacturer |
|---|--|---|
| BigDye Terminator Cycle Sequencing Ready Reaction kit | DNA sequencing | Applied Biosystems, Warrington, UK |
| ECL+Plus | detection of western blot | Amersham Pharmacia Biotech, Buckinghamshire, UK |
| ApoAlert Caspase-3 Colorimetric assay Kit | Detection of apoptosis | BD Bioscience (Clontech), Heidelberg; Germany |
| Concert Rapid PCR Purification system | Cleaning of PCR, restriction digestion product | Gibco BRL (Life Technologies), Karlsruhe, Germany |
| Concert Rapid Gel Extraction system | Cleaning of PCR product from gel | |
| Invisorb Spin Plasmid Mini kit | Plasmid isolation | Invitex, Berlin, Germany |
| HiSpeed Plasmid Midi kit | Plasmid isolation | Qiagen, Hilden, Germany |
| Hotstar Taq Master Mix kit | PCR | |
| Omniscript Reverse Transcription kit | Making of cDNA | |
| Flexi Gene DNA kit | Isolation of Genomic DNA from cell culture | |
| RNase-Free DNase Set | Removal of genomic DNA during RNA isolation | |
| RNeasy Maxi, Midi and Mini kit (Isolation of RNA) | Isolation of RNA | |
| Supersignal West Pico kit | Detection of western blot | Pierce, Rockford, IL, USA |

2.1.10 Laboratory instruments

| Instrument | Manufacturer |
|------------|--------------|
|------------|--------------|

| | |
|--|---|
| ABI PRISM™ 310 Genetic Analyzer | Applied Biosystems Division, Foster City, CA, USA |
| Mighty Small II (for western blotting electrophoresis) | Amersham Pharmacia Biotech, Buckinghamshire, UK |
| Ultrasonic homogenizer | Bandelin electronic, Berlin, Germany. |
| T3 Thermocycler | Biometra, Göttingen, Germany |
| Electrophoresis power supply | Bio-Rad Laboratories, Munich, Germany |
| Gel electrophoresis system | |
| Semi-dry Transfer Cell | |
| Mini PROTEAN II (Tankblot) | |
| GS-800 Calibrated Densitometer | |
| LSM510 laser scanning confocal microscope | Carl Zeiss, Jena, Germany |
| Thermomixer comfort | Eppendorf, Hamburg, Germany |
| Biofuge pico and 13 R centrifuges | Kendro, Hanau, Germany |
| Megafuge 1.0 R centrifuge | |
| Sorvall [®] RC-5B Refrigerated Superspeed Centrifuge | |
| Sorvall [®] discovery [™] 90 ultraspeed centrifuge | |
| Heraeus cell culture incubator | |
| Heraeus refrigerator (-80 °C) | |
| LaminAir [®] (clean bench) | |
| Millipore purification system | Millipore, Schwalbach, Germany |
| Ultra-pure water system | |
| Rotator | Labinco BA, Netherlands |
| Microplate reader | Molecular Devices |
| Microplate reader Spectramax M5 | |
| Innova 4230 Refrigerated incubator shaker | New Brunswick Scientific, Nürtingen, Germany |
| TPP ⁺ -selective electrode | Nico, Moscow, Russia |
| Ca ²⁺ -sensitive electrode | |
| UV/visible Spectrophotometer | Pharmacia Biotech |
| Balance (analytical and preparative) | Sartorius, Göttingen, Germany |

| | |
|--|---------------------------------------|
| Gel-blotting-papers | Schleicher & Schuell, Dassel, Germany |
| Protran BA83 Cellulosenitrat (E) (0.2 µm) | |
| Protran BA79 nitrocellulose transfer membrane (0.1 µm) | |
| Eagle Eye Still video system | Stratagene, Heidelberg, Germany |
| Vivaspin 6 filter concentrator | Vivascience AG, Hannover, Germany |
| pH Meter (pH526) | WTW |

2.1.11 Buffers and solvents

All buffers were prepared with distilled water.

2.1.11.1 Buffers and solvents

1x HBSS : 145 mM NaCl, 5.4 mM KCl, 1mM MgCl₂, 1.8 mM CaCl₂, 25 mM glucose, 20 mM HEPES, pH 7.4 adjusted with 1.67 M Tris (hydroxymethyl)-aminomethane

1x PBS: 137 mM NaCl, 2.6 mM KCl, 8.1 mM Na₂PHO₄, 1.4 mM KH₂PO₄, pH 7.4

E. coli-lysis buffer (PBS+ 1% Triton X- 100):137 mM NaCl, 2.6 mM KCl, 8.1 mM Na₂PHO₄, 1.4 mM KH₂PO₄, pH 7.4, 1% Triton X- 100

Storage buffer: 50 mM Tris/HCl pH 8,0, 100 mM NaCl, 1 mM mercaptoethanol, 20% glycerol

1xTBE: 89 mM Tris, 89 mM Boric acid, 2 mM EDTA, pH 8.0

1xTE: 10 mM Tris/HCl, pH 7.4, 1 mM EDTA, pH 8.0

Ethidium bromide solution: 10 mg/ml

TCM: 10 mM Tris/HCl, pH 7.5, 10 mM CaCl₂, 10 mM MgCl₂

4% PFA (Paraformaldehyde) solution: 4% PFA, 120 mM sodium phosphate, pH 7.4, 4% Saccharose

FTP: Blocking and Washing buffer (immunostaining):

17% (v/v) fetal calf serum, 20 mM Na₂HPO₄, 450 mM NaCl, 0.3% Triton X- 100

Lysis buffer: 50 mM Tris/HCl pH 7.4, 150 mM NaCl, 1% Igepal CA630, 0.25% Na-deoxycholate, 1 mM EDTA and 1 mM NaF

60% Acrylamid/Bis: 58.4% Acrylamide, 1.6% N,N'-Methylen-bisacrylamide

Resolving buffer: 750 mM Tris/HCl, pH 8.8

Stacking buffer: 250 mM Tris/HCl, pH 6.8

SDS solution: 10% (w/v) SDS in H₂O

PER solution: 10% (w/v) Ammoniumperoxodisulfat in H₂O

4x Laemmli Sample buffer: 500 mM Tris/HCl, pH6.8, 8% SDS, 40% Glycerol

5x Laemmli Running buffer: 125 mM Tris, 960 mM Glycine, 0.5% SDS, pH 8.5

1x Transfer buffer: 25 mM Tris, 192 mM Glycine, 20% (v/v) Methanol

Membrane Stripping buffer: 62.5 mM Tris, pH 6.8, 100 mM β-Mercaptoethanol, 2% SDS

PBST: 137 mM NaCl, 2.6 mM KCl, 8.1 mM Na₂PHO₄, 1.4 mM KH₂PO₄, pH 7.4

0.1% Tween 20

50% Protein G agarose slurry or 50% Protein A sepharose slurry: 1 ml 1x PBS and 4 µl 10% sodium azide

2.1.11.2 Buffers for mitochondria studies

All buffers for mitochondria studies were prepared with bidistilled water

Buffer A: 0.32 M sucrose, 0.5 mM EDTA, 0.5 mM EGTA, and 10 mM Tris-HCl, pH 7.4

Buffer for mitochondria isolation:

0.32 M sucrose, 0.5 mM EDTA, 0.5 mM EGTA, 0.5% bovine serum albumin (BSA; fraction V) and 10 mM Tris-HCl, pH 7.4

Buffer for washing of mitochondria:

0.32 M sucrose, and 10 mM Tris-HCl, pH 7.4

Incubation medium:

100 mM KCl, 100 mM sucrose, 10 mM Tris-HCl, 0.4 mM K₂HPO₄, 5 mM potassium succinate, 1.5 µM oligomycin and 2 µM rotenone, pH 7.4

2.1.12. Oligonucleotides for PCR and sequencing.

(Synthesized by MWG, Biotech, Ebersberg, Germany)

| cDNA | Primer name | Primer sequence | Tm (°C) | application |
|---------------|-------------|--|---------|-------------|
| mice GAPDH | THGAPDHFV | 5'- ATGGTGAAGGTCGGTGTGAACGGATTT GG-3' | 58° | PCR |
| | THGAPDHRV | 5'- TTACTCCTTGGAGGCCATGTAGGCCAT GAG-3' | | |
| mice | THMMP42F1 | 5'-TTCTCCGACTGCCAACTCCTAC-3' | 58° | PCR |

| | | | | |
|--------------------|---------------------|-------------------------------|-----|------------|
| p42 ^{IP4} | THMMP42R6 | 5'-GACAATGGTTATGCCATGAGG-3' | | |
| | pGEX 5' Seq. Fw | 5'-GGGCTGGCAAGCCACGTTTGGTG-3' | 55° | Sequencing |
| | pGEX 3' Seq. Rev | 5'-CCGGGAGCTGCATGTGTCAGAGG-3' | 55° | Sequencing |
| | T7 promoter | 5'-GTAATACGACTCACTATAGGGC-3' | 55° | Sequencing |
| | BGH seq | 5'-CTAGAAGGCACAGTCGAGG-3' | 55° | Sequencing |

2.2 Methods

2.2.1 RT-PCR

Total RNA was extracted from cultured cells using RNeasy Mini kit (Qiagen). One microgram of RNA was reverse-transcribed using Omniscript™ Reverse Transcription kit (Qiagen), and the resulting cDNA was amplified in the presence of appropriate primers for 30 cycles by PCR using HotStarTaq™ Master Mix kit (Qiagen) for 15 min at 95°C, followed by repeated cycles of 30 s at 94°C, 90 s at 58° C, 60 s at 72°C, then a final 10 min extension at 72°C. The reaction products were analyzed by electrophoresis with 1% agarose gel containing ethidium bromide, and visualized by Bio-Rad gel document system (Bio-Rad).

2.2.2 Plasmid constructs

A NotI DNA fragment coding the full length p42^{IP4} was excised from pBluescript⁺-p42^{IP4} (Sedehizade et al., 2002) and sub-cloned into pGEX-5X-2 vector (GE Healthcare, Munich, Germany). An EcoRI DNA fragment with the full length p42^{IP4} cDNA was excised from pBluescript⁺-p42^{IP4} and sub-cloned into the EcoRI site of pcDNA3.1Myc vector (Invitrogen, Karlsruhe, Germany). At first, the original pBluescript⁺-p42^{IP4} construct was digested with the NotI or EcoRI to obtain DNA fragments encoding for the p42^{IP4}. Then the fragments obtained were ligated into the linearized pGEX-5X-2 and pcDNA3.1Myc vectors respectively. The ligated product was purified using the DNA purification kit from Gibco/BRL. The purified DNA was checked for the presence of the inset by digestion of the ligated DNA using NotI or EcoRI, respectively. The successfully ligated DNA constructs were transformed into E.coli using the heat-shock method (CaCl₂ based). The E.coli were plated and allowed to grow for 24 hours at 37°C on LB-agar plates containing 100 mg/ml ampicillin, as a selection marker. The positive clones were picked, and cultivated in 5 ml of LB medium containing ampicillin for 24 h. DNA was prepared from the above cultures using the DNA-Mini-prep kit (Qiagen). The DNA obtained from the mini prep was digested with

NotI or EcoRI to recheck for the presence of the inset of the DNA encoding p42^{IP4} in the appropriate construct. The DNA from the positive clones was sequenced using the DNA sequencing kit from ABI PRISM, using the appropriate set of primers.

The clones that expressed the complete p42^{IP4} without any point mutations and frame shift, were retransformed in E.coli using heat-shock method (CaCl₂ based), and the DNA was isolated using the DNA Midi-Prep kit (Qiagen).

The construct p42^{IP4}-pcDNA3 and CHO cells, stably transfected with pcDNA3-p42^{IP4} were described before (Sedehizade et al., 2002). The sequence of all constructs used was verified by sequencing on automated sequencer (ABI PRISMTM 310 Genetic Analyzer) with the dye terminator cycle sequencing kit (ABI-Prism, Applied Biosystems) according to the manufacturer's instructions in both directions prior to use.

2.2.3 Agarose gel electrophoresis of DNA

To check the quality of DNA (PCR product, recombinant plasmid DNA, restriction analysis) 1% agarose (Sigma, Taufkirchen, Germany) gel and 1.5% gel for DNA laddering assay in 0.5x TBE buffer were made. Gel was pre-stained in ethidium bromide (10 mg/ml) (Sigma). DNA samples were prepared in 6x loading buffer (containing bromophenol blue dye) (MBI Fermentas). Gel was run in 0.5x TBE for 60 min at 80 V for PCR samples, at 100 V for plasmid DNA and 3 h at 30V for genomic DNA. Depending on the fragment size either GeneRuler 100bp DNA Ladder (1 kb) or GeneRuler DNA Ladder Mix (10 kb) (MBI Fermentas) used. DNA bands were visualised under UV-Transilluminator in an Eagle Eye II video system (Stratagene, Heidelberg, Germany).

2.2.4 Transformation of E. coli with plasmid DNA by heat-shock method (CaCl₂ based)

To make competent cells, single colony of E.coli was grown in 5 ml LB media overnight at 37°C with shaking at 250 rpm. 1 ml of overnight bacterial culture was then transferred to 100 ml of fresh LB media and continued to grow at 37°C with shaking till the cells reached their logarithmic phase i.e, OD₆₀₀= 0.3-0.4. Then the bacterial suspension was centrifuged at 3,000 g for 5 min at 4°C. Supernatant was discarded and cell pellet was resuspended in 10 ml of ice-cold 100 mM CaCl₂ solution. The cell suspension was then incubated on ice in cold room (4°C) for 1 h and centrifuged for 5 min at 3,000 g at 4 °C. Supernatant was discarded carefully and pellet was resuspended in 1 ml of ice-cold 100 mM CaCl₂ containing 30% glycerine (1 ml solution= 700 µl 100 mM CaCl₂+ 300µl of 100% glycerine). From this competent cell suspension aliquots of 200 µl were made, frozen in liquid nitrogen and stored at -80°C.

To transform bacteria, 200 μ l of CaCl_2 competent cells for each reaction were thawed on ice. To the cells we added 100 μ l of cold TCM buffer and either 10-20 ng of super-coiled plasmid DNA or 20 μ l of ligation mix. Cells were incubated on ice for 20 min and then heat – shock given for 90 s at 42°C. Transformation reaction mix was immediately incubated on ice for 1 min, then 700 μ l of LB media (pre-warmed at 37°C and without any antibiotic) was added to transformation mix and incubated for 30-60 min with shaking at 37°C. 100 μ l of the transformation mixture in case of super-coiled DNA was plated on the LB-agar plate containing suitable antibiotic. For ligation transformation, reaction mix was centrifuged briefly, supernatant was discarded and pellet was resuspended in the residual volume and plated on LB-agar containing suitable antibiotic. LB-agar plates were incubated up-side down at 37°C to facilitate growth of transformants under appropriate antibiotic selection pressure.

2.2.5 Expression and purification of glutathione S-transferase (GST) and GST-p42^{IP4} constructs from E. coli.

For expression in E. coli, the pGEX-5X-2 constructs were transformed in BL21 (GE Healthcare). The expression and purification of the fusion protein was performed in the presence Triton-X 100 (Roth, Karlsruhe, Germany) according to a published procedure (Stricker et al., 2006) with modifications. In brief, E. coli transformed with the pGEX-5X-2-p42^{IP4} construct were grown in LB medium containing ampicillin to absorbance at 600 nm, $A_{600} = 0.6-0.8$ and expression of the fusion protein was induced by the addition of 0.1 mM isopropyl b-D-thiogalactoside (Sigma). The cells were grown for an additional 3 h at 25 °C, collected by centrifugation, and stored at 80°C until use. Frozen E. coli pellets were solubilized in E. coli-lysis buffer (137 mM NaCl, 2.6 mM KCl, 8.1 mM Na_2PHO_4 , 1.4 mM KH_2PO_4 , pH 7.4, 1% Triton X-100) containing a cocktail of protease inhibitors (Roche, Mannheim, Germany) by sonication (5x10 s). After centrifugation (10,000 g for 10 min at 4°C), glutathione-sepharose slurry was added to the supernatant and incubated on a rotator (60 min at 4°C). The beads were sedimented by centrifugation (500 g for 5 min at 4°C) and washed three times with E. coli-lysis buffer. To remove non-specifically bound proteins, the beads were incubated in lysis buffer supplemented with 1 M NaCl (15 min at 4°C) and after centrifugation the beads were resuspended in storage buffer (50 mM Tris/HCl pH 8,0, 100 mM NaCl, 1 mM mercaptoethanol and 20% glycerol).

The beads and lysates were analyzed by SDS-PAG electrophoresis. The purified fusion proteins were stored as a 50% (v/v) beads suspension and used for GST pull-down assay.

2.2.6 Cell culture and transfection

CHO cells were maintained in Hams' F12 medium supplemented with 10% fetal calf serum (Biochrom, Berlin, Germany) and 100 µg/ml penicillin, and 100 µg/ml streptomycin in a humidified 5% CO₂ atmosphere at 37 °C. N2a cells were maintained under the same conditions with the exception that Dulbecco's Modified Eagle's Medium was used.

OLN93 cells, an oligodendrocyte cell line (Richter-Landsberg and Heinrich, 1996), kindly provided by Prof. C. Richter-Landsberg (University of Oldenburg, Germany), were grown at 37°C in a 5% CO₂ atmosphere in Dulbecco's modified Eagle's medium (Biochrom KG) supplemented with 10% fetal calf serum (Biochrom KG, Berlin, Germany) containing 2 mM glutamine, 100 µg/ml penicillin, and 100 µg/ml streptomycin.

Transfections were carried out using FuGENE 6 (Roche) according to manufacturer's instructions. The cells were stably transfected with the respective plasmid DNA (2 µg). Before transfection the cells were grown in 10-cm dishes to 60% confluency. The transfected cells were kept for 8–10 h in serum- and antibiotic-free medium. After 24-48 h, the transfected cells were cultivated in selection medium containing 400 µg/ml G418 (Calbiochem, Schwalbach, Germany). Single cell colonies were isolated after 3 weeks by cloning rings, verified at the transcription and translation level by RT-PCR and western blot and used for further experiments.

2.2.7 Confocal microscopy

For immunofluorescence, N2a cells stably transfected with p42^{IP4}-pcDNA3.1Myc and CHO cells, stably transfected with pcDNA-p42^{IP4} were grown on poly-L-lysine-coated coverslips. Cells were fixed in 4% paraformaldehyde, blocked and permeabilized in blocking buffer (17% (v/v) fetal calf serum, 20 mM Na₂HPO₄, 450 mM NaCl, 0.3% Triton X- 100) and incubated with rabbit polyclonal anti-Myc antibody (Invitrogen, Karlsruhe, Germany; 0.8 µg/µl) or rabbit polyclonal anti-p42^{IP4} antibody (AS1516g) and mouse monoclonal anti-Cyt c antibody (clone 6H2.B4; BD Bioscience; Heidelberg; Germany) overnight at 4°C, as described in the respective figure legends. After washing, the secondary antibody was applied (Alexa Fluor® 555 goat anti-mouse IgG antibody at 1:100; Alexa Fluor® 488 goat anti-rabbit at 1:200 Molecular Probes, MoBiTec, Göttingen, Germany) for 2 h at 25°C. Mounted slides were observed with a confocal laser scanning microscope LSM510 (Carl Zeiss, Jena, Germany).

2.2.8 Subcellular fractionation by differential centrifugation

Subcellular fractionation and organelle isolation techniques were done by modification of previously reported procedures (Sharer et al., 2002; Leissring et al., 2004). All steps were carried out at 4°C. N2a cells were washed two times in phosphate-buffered saline, collected in ice-cold buffer A (0.32 M sucrose, 0.5 mM EDTA, 0.5 mM EGTA, and 10 mM Tris-HCl, pH 7.4) containing cocktail of protease inhibitors (Roche) and gently disrupted using a Potter-Elvehjem homogenizer. The cell homogenate was then subjected to centrifugation at 500 g for 10 min, yielding a nuclear pellet and supernatant. The mitochondrial fraction was obtained from this supernatant after centrifugation at 12,000 g for 10 min. Finally, the 12,000 g supernatant was further fractionated at 49,000 g for 30 min, yielding the soluble cytosolic fraction and membrane pellet. After each centrifugation step, the resulting pellets were washed by resuspension in an excess of buffer A, followed by centrifugation at the appropriate relative centrifugal force.

The protein concentration was determined by the Bradford method (Bio-Rad Protein assay, Bio-Rad, Munich, Germany) using bovine serum albumin as standard.

2.2.9 Preparation of mitochondrial lysate and cytosolic fraction from rat brain

Rat brains were rapidly removed and placed within 30 s in ice-cold buffer A containing 0.02% bovine serum albumin (fatty acid free, fraction V). All manipulations were carried out at 4°C. The tissue was homogenized in a Potter-Elvehjem homogenizer; the ratio of brain tissue to buffer used for isolation was 1:10 (w/v). The homogenate was centrifuged at 2,000 g for 3 min. The pellet of mitochondria was obtained by centrifugation of the 2,000 g supernatant at 12,000 g for 10 min. RBM were suspended in ice-cold solution, containing 0.32 M sucrose and 10 mM Tris-HCl (pH 7.4) and were additionally washed by centrifugation at 12,000 g for 10 min.

For preparation of mitochondrial lysate, RBM aliquots (4 mg of protein) were suspended in lysis buffer (50 mM Tris/HCl pH 7.4, 150 mM NaCl, 1% Igepal CA630, 0.25% Na-deoxycholate, 1 mM EDTA and 1 mM NaF) containing a cocktail of protease inhibitors (Roche). Then suspensions were rotated on a rotation wheel for 30 min at 4°C, solubilized by ultrasonic treatment and centrifuged at 14,000 g for 15 min. The 14,000 g supernatant gives the mitochondrial lysate.

For preparation of brain cytosolic fraction, the brain tissue was homogenized using an Ultraturrax three times for 20 s at 4°C in buffer A containing a cocktail of protease inhibitors (Roche). The homogenates were then centrifuged at 400 g for 5 min at 4°C. The supernatant

obtained was centrifuged at 100,000 g for 30 min at 4°C. The 100,000 g supernatant gives the cytosolic fraction.

2.2.10 Isolation of mitochondria from cultured cells

Isolation of mitochondria from cells was carried out at 4°C according to a published procedure (Leissring et al., 2004) with modifications. Confluent monolayers of N2a or CHO cells, cultured in 15 cm dishes, or confluent monolayers of OLN93 cells, cultured in T-75 flasks, were washed with phosphate-buffered saline, collected by scraping in buffer A, containing 0.02% bovine serum albumin (fatty acid free, fraction V), and pelleted at 500 g for 5 min. Cells were re-suspended in the same ice-cold buffer and disrupted with a Potter-Elvehjem homogenizer. The cell homogenate was centrifuged twice at 500 g for 5 min to remove unbroken cells and nuclei, and twice at 3,000 g for 4 min to remove trapped peroxisomes and other organelles. The supernatant obtained was centrifuged at 12,000 g for 10 min. The mitochondrial pellet was suspended in ice-cold medium containing 0.32 M sucrose and 10 mM Tris-HCl (pH 7.4) and centrifuged at 12,000 g for 10 min. The mitochondria isolated were re-suspended in the same ice-cold medium. Mitochondria from N2a and OLN93 cells were used for functional studies.

2.2.11 Subfractionation of mitochondria

Mitochondria isolated from CHO cells were subfractionated by using a phosphate swelling-shrinking method described previously (Bijur and Jope, 2003), with minor modifications. Briefly, mitochondria were subjected to swelling by the addition of swelling buffer (10 mM KH₂PO₄, pH 7.4) containing a cocktail of protease inhibitors, and incubated for 20 min at 4°C with gentle mixing. An equal volume of shrinking buffer (10 mM KH₂PO₄, pH 7.4, 32% sucrose, 30% glycerol, 10 mM MgCl₂, and protease inhibitors) was added and samples were incubated for an additional 20 min at 4°C. The suspension was centrifuged at 10,000 g for 10 min, yielding a supernatant containing the outer membrane and the intermembrane space fractions, which was saved as mixture 1, and a pellet comprised of mitoplasts. The mitoplasts were washed three times in the mixture of swelling and shrinking buffer (1 : 1), then resuspended in 500 µl of swelling buffer and sonicated 10 s x 3 with a 1-min interval on ice by 40% of maximal power. This suspension containing the inner membrane and matrix fractions was saved as mixture 2. Mixtures 1 and 2 were centrifuged at 150,000 g for 1 h. The supernatant from mixture 1 was saved as the intermembrane space fraction and the supernatant from mixture 2 was saved as the matrix fraction. Proteins from the intermembrane space fraction were concentrated using a Vivaspin 6 filter concentrator (Vivascience AG, Hannover, Germany). The outer membrane pellet in mixture 1 and the

inner membrane pellet in mixture 2 were washed once in swelling buffer and centrifuged at 150,000 g for 1 h. The outer and inner membrane pellets were solubilized in lysis buffer containing protease inhibitors, as described above.

Mitoplast and outer membranes of rat brain mitochondria were obtained according to previously reported procedures (Rice and Lindsay, 1997).

2.2.12 Electrophoresis and immunoblotting

For immunoblotting, proteins solubilized in Laemmli buffer were separated under denaturing conditions on sodium dodecyl sulphate (SDS)-polyacrylamide gel electrophoresis (PAGE) using 10% or 12.5% gels and transferred to nitrocellulose membranes (Protran BA83 or BA79, Whatman, Dassel, Germany). Precision Plus Pre-stained Standards (Bio-Rad) were used as markers. Equal transfer was controlled by Ponceau red staining of the membrane. After overnight blocking, the membrane was incubated with the appropriate primary antibody. The monoclonal anti-CNP antibody was described before (Reiser et al., 1994). A polyclonal rabbit serum raised against p42^{IP4} (AS1516g) and monoclonal antibody, Mab117-2, were described before (Haase et al., 2008). Anti-Cyt c (cytochrome c, clone 7H8.2C12, Biozol, Eching, Germany), pan anti-plasma membrane calcium ATPase (clone 5F10, Biozol), anti-Cytochrome oxidase subunit IV (clone 20E8C12, MitoSciences, Eugene, Oregon), anti-ANT (adenine nucleotide translocator, MitoSciences), anti-SOD 2 (Mn-superoxide dismutase 2, antibody 13533, Abcam Cambridge, UK), anti-CNP (antibody 27695, Abcam), anti-VDAC (voltage-dependent anion channel, Ab-5, Calbiochem), anti Synaptotagmin I (clone 41.1, Synaptic Systems, Gottingen, Germany), anti-Nucleoporin p62 (BD Biosciences, Heidelberg, Germany), anti-GAPDH (glyceraldehyde 3-phosphate dehydrogenase, clone 6C5, Chemicon, Martinsried/Munich, Germany), anti- β -tubulin I (Sigma) and anti- α -tubulin (Clone B-5-1-2, Sigma) antibodies were used for immunoblotting. Immunoreactivity was detected using the appropriate secondary antibody conjugated to horseradish peroxidase (Dianova; Hamburg, Germany). Peroxidase activity was detected with enhanced chemiluminescence reagents (Super-Signal West Pico; Pierce, Rockford IL).

Quantification of the band densities from western blots was carried out using a GS800 calibrated densitometer and QUANTITY ONE software (Bio-Rad, Munich, Germany). Films were scanned and the intensities of the bands were quantified.

2.2.13 GST-pull-down assay

For the GST pull-down, mitochondrial lysate was precleared by rotation 4 - 8 h with glutathione-Sepharose beads at 4°C. After centrifugation (500 g 5 min at 4°C) glutathione-

Sepharose beads were discarded and precleared lysate was used for binding. To determine protein-protein interaction *in vitro*, equal amounts of GST and GST-p42^{IP4} fusion proteins immobilized on glutathione-Sepharose beads were incubated with brain cytosolic fractions or precleared mitochondrial lysates (4 mg of protein) overnight on a rotating wheel at 4°C. After centrifugation (1000 g for 5 min at 4°C) the beads were washed five times with 1 ml of lysis buffer described above. The proteins were eluted from the beads with 10 µl of 2× Laemmli buffer, separated by SDS-PAGE, transferred to nitrocellulose membranes and immunoblotted as described above.

2.2.14 Immunoprecipitation and co-immunoprecipitation

For immunoprecipitation, RBM lysates were precleared by protein G-agarose (Sigma) or A-sepharose beads (GE Healthcare), depending on the primary antibody used, for 2 h at 4°C. Cytosolic fractions and precleared RBM lysates were incubated with primary antibody, *i.e.* monoclonal anti-CNP antibody (described before in (Reiser et al., 1994), monoclonal anti- α -tubulin antibody (Clone B-5-1-2, Sigma), or polyclonal rabbit antiserum against p42^{IP4} (AS1516g, described before in (Haase et al., 2008) for 2 h on ice. Then it was mixed with 20 µl of suspension of protein G-agarose or A-sepharose beads, respectively, for overnight incubation at 4°C under rotation with a following centrifugation at 500 g for 5 min. The immunoprecipitated complexes were washed with lysis buffer (described above) five times. Samples were eluted in 10 µl of 2× Laemmli buffer and used for electrophoresis and immunoblotting as described above.

2.2.15 Isolation of rat brain mitochondria for functional study

Rat brains were rapidly removed (within 30 s) and placed in ice-cold buffer A, containing 0.02% bovine serum albumin (fatty acid free, fraction V). All solutions used were ice-cold; all manipulations were carried out at +4°C. The tissue was homogenized in a Potter-Elvehjem homogenizer; the ratio of brain tissue to isolation medium was 1:10 (w/v). The homogenate was centrifuged at 2000 g for 3 min. The pellet of mitochondria was obtained by centrifugation of the 2000 g supernatant at 12,500 g for 10 min. At the next step, in representative experiments, mitochondria were purified on Percoll gradient (15%-23%-40%) according to published procedures (Sims, 1990). Rat brain mitochondria were suspended in ice-cold solution, containing 0.32 M sucrose and 10 mM Tris-HCl (pH 7.4) and were additionally washed by centrifugation at 11,500 g for 10 min. The protein concentrations in the stock mitochondrial suspensions were 25-30 mg/ml.

2.2.16 Evaluation of mitochondrial functions

Mitochondrial functions were measured, as described earlier (Azarashvili et al., 2007). RBM (1.0 mg protein/ml) or mitochondria from cultured cells (0.7 mg of protein/ml) were incubated in respiration buffer containing 100 mM KCl, 100 mM sucrose, 10 mM Tris-HCl, 0.4 mM K₂HPO₄, in the presence of 2 μM rotenone and 1.5 μM oligomycin, pH 7.4 at 25°C, in an open chamber. Succinate (5 mM potassium succinate) was used as mitochondrial respiratory substrate. PTP opening was induced by threshold Ca²⁺ load. For Ca²⁺ loading, additions of Ca²⁺ per mg of protein: 70 or 200 nanomoles for mitochondria isolated from N2a, 80-120 nanomoles for RBM and 70 nanomoles for mitochondria isolated from OLN93 cells were used. All experiments were performed in an open chamber.

Extramitochondrial Ca²⁺ was determined with a Ca²⁺-sensitive electrode (Nico, Russia). The mitochondrial membrane potential was determined by measuring tetraphenylphosphonium (TPP⁺) in the incubation medium with a TPP⁺-sensitive electrode. Oxygen consumption rate was detected with a Clark-type O₂ electrode.

Changes in Ca²⁺ and TPP⁺ concentration, as well as in oxygen consumption were simultaneously monitored in the incubation medium. Parameters of Ca²⁺ transport, rate of Ca²⁺ influx, Ca²⁺ capacity (amount of Ca²⁺ taken up by mitochondria before PTP opening), lag time for Ca²⁺ efflux after Ca²⁺ addition under PTP opening were evaluated, as described earlier (Azarashvili et al., 2007).

In some experiments mitochondria were pre-incubated with IP₄ (D-myo-inositol 1,3,4,5-tetrakisphosphate, tetrapotassium salt, Alexis, Gruenberg, Germany) or PIP₃ (phosphatidylinositol 3,4,5-Trisphosphate diC8, Echelon Biosciences Incorporated, Salt Lake City, UT, USA) for 20 min before loading with Ca²⁺.

Swelling of RBM was measured as a change in scattering of the mitochondrial suspension absorbance at 540 nm (A₅₄₀) using Microplate reader Spectramax M5 (Molecular Devices) at 30°C. Standard incubation medium for swelling assay contained 125 mM KCl, 10 mM Tris, 2 mM KH₂PO₄, 10 mM succinate, 0.5 μM oligomycine, 0.5 μM rotenone. The concentration of protein in the cuvette was 0.45 mg protein/ml. The swelling was initiated by addition of 450 μM Ca²⁺.

2.2.17 Detection of CNP activity in isolated mitochondria

CNP activity was detected according to published procedure (Bradbury and Thompson, 1984). Aliquots of the mitochondrial suspension (rat brain mitochondria or OLN93 cells) containing 40 μg of protein were taken from the chamber under control

conditions and after PT opening and were then solubilized in Laemmli buffer. Solubilized mitochondria were separated by electrophoresis in a 12.5% polyacrylamide gel and were transferred to nitrocellulose membranes. CNP activity was detected on membrane after blotting. The membrane was pre-incubated for 1 h in 50 mM MES (4-morpholine-ethanesulfonic acid) buffer, pH 6.1, containing 30 mM MgCl₂, 0.1% Triton X-100, 3 M guanidinium chloride, 1 mM EDTA, 1 mM dithiothreitol and 5% glycerol, then for 1 h in the same buffer without guanidinium chloride. The pre-incubation stage is essential for recovery of enzyme activity after SDS- electrophoresis. The blot was then stained for activity by using Nitro Blue Tetrazolium [3,3'-(3,3'-dimethoxy-4,4'-diphenylene)2,2'-di-*p*-nitrophenyl-5,5'-diphenylditetrazolium] chloride and phenazine methosulphate to detect NADPH produced in enzyme-linked reaction for CNP. The coloured reaction product was immobilized with diluted agarose. Equal volumes of 1% agarose in water at 55°C and reaction medium (200 mM MES buffer pH 6.1, containing 60 mM MgCl₂, 0.2 % Triton X-100, 0.1 mM 2',3'-cyclic NADP and 4 mg/ml glucose-6-phosphate, 0.4 mg /ml Nitro Blue Tetrazolium, 0.04 mg/ml phenazine methosulphate and 0.7 units of glucose-6-phosphate dehydrogenase) were rapidly mixed and poured on the nitrocellulose membrane. Coloured reaction was visible within 15 min and was stopped with 10% acetic acid. CNP activity in the bands (intensity of coloured band) on the blot was evaluated by determining the optical density of the coloured product.

2.2.18 Small interfering RNA (siRNA)

Chemically synthesized pool of siRNAs targeting CNP was obtained from Dharmacon, Chicago, IL. To knockdown the endogenous CNP, OLN93 cells were transiently transfected with rat CNP siRNAs by using magnet assisted transfection, according to the manufacturer's protocol (IBA GmbH, Germany). Briefly, one day before transfection cells were plated on a T-75 flasks. On the following day, the cells (50% confluent) were incubated for 15 min with CNP siRNAs or scrambled siRNA and magnet assisted transfection reagents mixture on the magnet plate. Afterwards, transfected cells were cultured for 48 h under normal conditions. Non-silencing siRNA served as a scrambled siRNA control (Qiagen). CNP knockdown was assessed by Western blot at 48 h after transfection.

2.2.19 Apoptosis detection

For inducing apoptosis N2a cells were exposed to 300 nM wortmannin, 10 nM and 100 nM staurosporine or/and 100 µM LY 294002. Detection of apoptosis was checked using DNA- laddering and caspase-3 assays.

For DNA laddering analysis, genomic DNA from 5×10^6 cells was isolated using Flexi Gene DNA kit (Qiagen) after 6 and 24 h incubation with the apoptotic-inducing drugs in

serum-free medium. DNA was treated with RNase and analysed by agarose gel electrophoresis as described above.

For Caspase-3 activity assay, 2×10^6 cells were harvested after 24 h incubation with the apoptotic-inducing drugs in serum-free or serum containing medium, and caspase-3 activity in cell lysate was measured using ApoAlert Colorimetric assay kit (BD Bioscience).

2.3 Statistical analysis

For statistical analysis, relative values of mitochondrial functions and relative levels of protein density were expressed as mean \pm SD from at least 3 independent experiments with samples from individual preparations of mitochondria. Statistical significance was evaluated using the Student's t- test. A value of $p < 0.05$ was accepted as significant.

3. Results

3.1. Possible role of p42^{IP4} in cell protection or cell death

The protein p42^{IP4} was suggested to be involved in neurodegenerative processes (Reiser and Bernstein, 2004). However, its exact physiological role is still unknown. Earlier, it has been shown that the p42^{IP4} ligand, IP₄, is able to play a key role in the induction of Ca²⁺ accumulation, which led to neuronal cell death (Tsubokawa et al., 1996). Another ligand of p42^{IP4}, PIP₃, generated from PIP₂ by action of PI 3-K. PI 3-K activates serine/threonine protein kinase termed protein kinase B, which phosphorylates numerous regulatory proteins to enhance cell survival (Lawlor and Alessi, 2001). It was shown that p42^{IP4} binds to all members of the PKC family and is phosphorylated by isoforms from all PKC classes (Zemlickova et al., 2003). Among many other functions, PKC plays a vital role in cellular survival and apoptosis. It was suggested that PKC- α , PKC- ϵ , and the atypical PKC's, PKC- λ/ι and PKC- ζ , preferentially function to promote cell proliferation and survival, while the novel isoform, PKC- δ is an important regulator of apoptosis (Reyland, 2009).

Recently it was shown, that PKC- and PI 3-K-mediated pathways are necessary for survival of mouse neuroblastoma (N2a) cell line under apoptotic conditions (Bronisz et al., 2002). Therefore, we used staurosporine (STS) for selective inhibition of the PKC pathway and LY 294002 for inhibition of PI 3-K to induce apoptosis in N2a cells. We aimed to find out whether p42^{IP4} plays a role in neuroprotection or cell death. For these purposes we compared consequences of induced apoptosis in the control and p42^{IP4} overexpressing N2a cells.

3.1.1 Influence of p42^{IP4} overexpression on apoptosis induced in N2a cells.

To investigate the possible role of p42^{IP4} in neuroprotection or cell death, we first induced apoptosis in N2a cells, stably transfected with pEGFP-C2-p42^{IP4}. Nontransfected and EGFP- C₂-transfected N2a cells were used as control cells. We performed detection of apoptosis in N2a cells first in the early stage, using caspase-3 assay, secondly in the last step, using both DNA-laddering assay and flow cytometry analysis.

It has been already shown that pro-survival pathway is totally dependent on PKC activity under serum-free conditions, whereas in the presence of serum it can be alternatively activated by undefined trophic signal(s) involving protein kinase B (Bronisz et al., 2002). Therefore, to induce apoptosis in N2a cells, 10 nM or 100 nM STS were applied for 24 h in serum-free or complete medium. STS-induced apoptosis was confirmed by oligonucleosomal DNA fragmentation assay (Fig. 3.1.1). DNA-laddering was observed in N2a cells stably-

transfected with pEGFP-C2-p42^{IP4} and nontransfected N2a cells exposed to 10n M and 100 nM STS (STS 10 and STS 100, respectively) for 24 h in serum-free medium. However, only slight differences in oligonucleosomal DNA cleavage in N2a cells stably-transfected with EGFP-C₂-p42^{IP4} and control cells, which were exposed to STS, were detected.

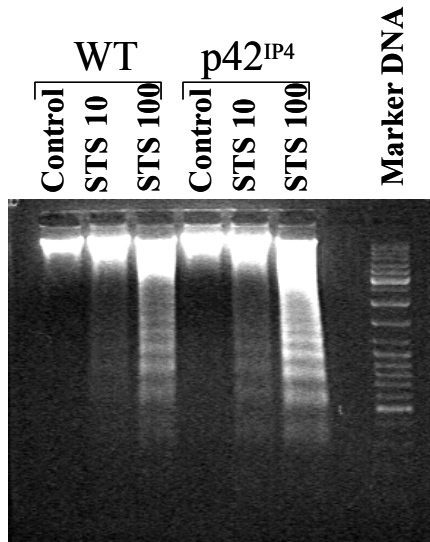


Fig. 3.1.1. Oligonucleosomal fragmentation of DNA isolated from N2a cells.

Cells were incubated in serum-free medium for 24 h with 10 nM staurosporine and 100 nM (STS 10 and STS 100 respectively).

Next, caspase-3 assay for detection of apoptosis in N2a cells in the early stage was used. Increase of caspase-3 activity was detected in N2a cells exposed to 100 nM STS or to 100 μ M LY 294002, or to combination of 10 nM STS and 50 μ M LY 294002 in serum-containing (Fig. 3.1.2) and serum-free medium (Fig. 3.1.3).

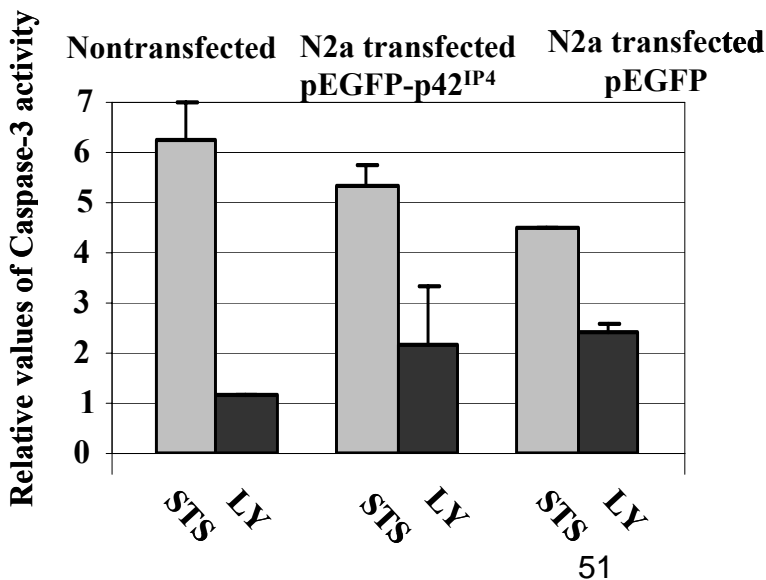


Fig. 3.1.2. Activity of caspase-3 in N2a cells after induction of apoptosis under serum-containing conditions.

Caspase-3 activity of N2a cells, exposed to 100 nM staurosporine and 100 μ M LY 294002 (STS and LY, respectively) for 24 h. Exposure were performed in media, containing 10% of serum. Relative values of caspase-3 activity versus respective control (without exposure) are presented.

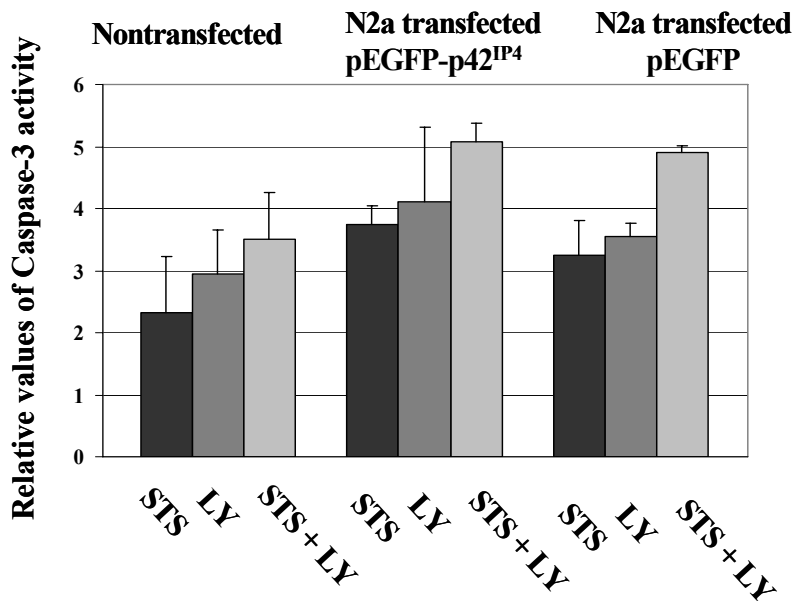


Fig. 3.1.3. Activity of caspase-3 in N2a cells after induction of apoptosis under serum-free conditions.

Caspase-3 activity of N2a cells, exposed to 100 nM staurosporine, 100 μ M LY 294002 or to combination of 10 nM STS and 50 μ M LY 294002 (LY and STS, respectively) for 24 h. Exposure was performed in serum-free medium. Relative values of caspase-3 activity versus respective control (without exposure) are presented.

There were no significant differences between levels of caspase-3 activity in N2a cells stably-transfected with EGFP-C₂-p42^{IP4} and control cells, which were exposed to either STS, LY 294002 or both inhibitors together (Fig. 3.1.3.). Thus, p42^{IP4} is not involved in caspase-3-mediated apoptosis induced by inhibition of PKC and PI 3-K pathways in N2a cells.

3.1.2 Influence of p42^{IP4} overexpression on cell cycle in N2a cells.

Since we could not see any significant effect of p42^{IP4} overexpression on the early apoptotic stage, using caspase-3 assay, we decided to use flow cytometry analysis to clarify whether p42^{IP4} is involved in the last step of apoptosis. N2a cells were grown to confluence, hence density arrested in G₀. Then cells were trypsinized and reseeded at a lower density to induce a synchronous entry into the cell cycle. Cells were allowed to grow 48 h before apoptotic treatment. Propidium iodide staining was applied to identify apoptotic cells by flow cytometry. Surprisingly, we observed a high level of apoptosis in EGFP-C₂-transfected N2a cells, which were used as a control (Fig. 3.1.4). Such toxic effects of empty EGFP vector in N2a cells made it impossible to use further flow cytometry for counting apoptotic cells.

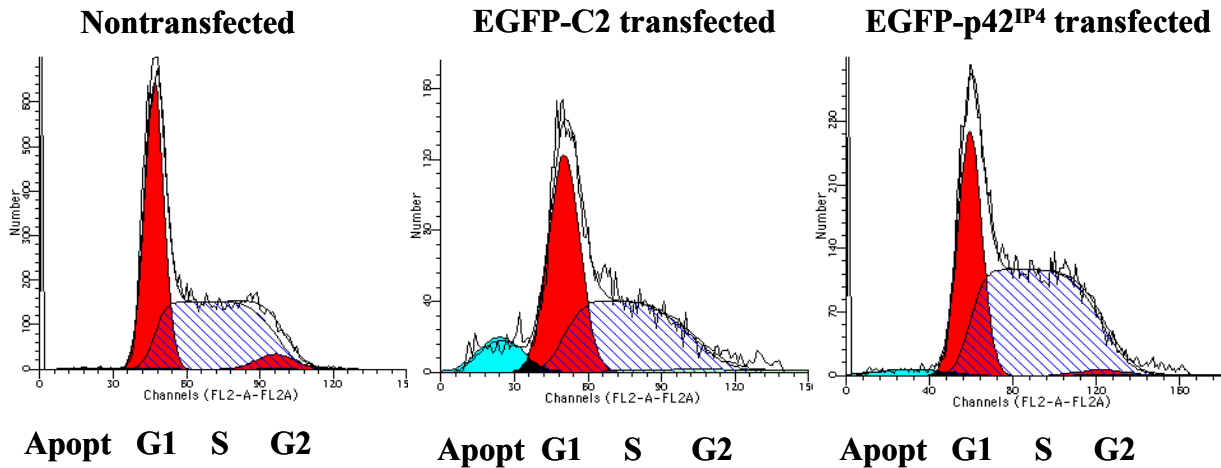


Fig.3.1.4. Analysis of N2a cells by flow cytometry.

Growth-arrested N2a cells were obtained by culture to confluence and then were released from contact inhibition by trypsinization. Cells were allowed to proceed 48 h, subjected to propidium iodide DNA staining and flow cytometry analysis. Peaks represent G1 phase cells and G2/M phase cells. Apopt - cells in apoptosis. For each sample 1×10^5 positive counts were monitored. FL2, fluorescence channel 2.

However, significant changes were observed in S/G2 phase in N2a cells overexpressing EGFP-p42^{IP4} (Fig. 3.1.4). The diagram of Fig. 3.1.5. represents the quantitative analysis showing the mean data from several experiments to demonstrate the effect of EGFP-p42^{IP4} on cell cycle in N2a cells. Interestingly, we observed that overexpression of EGFP-p42^{IP4} leads to a delay in exit from S-phase and a significant decrease in G2-phase (Fig. 3.1.5). So, we conclude that p42^{IP4} seems to have an effect on cell cycle. Since there are changes in S-phase and G2-phase, it might be possible that p42^{IP4} influences the level and activity of cyclin/ cyclin-dependent kinases, which are specific for these phases.

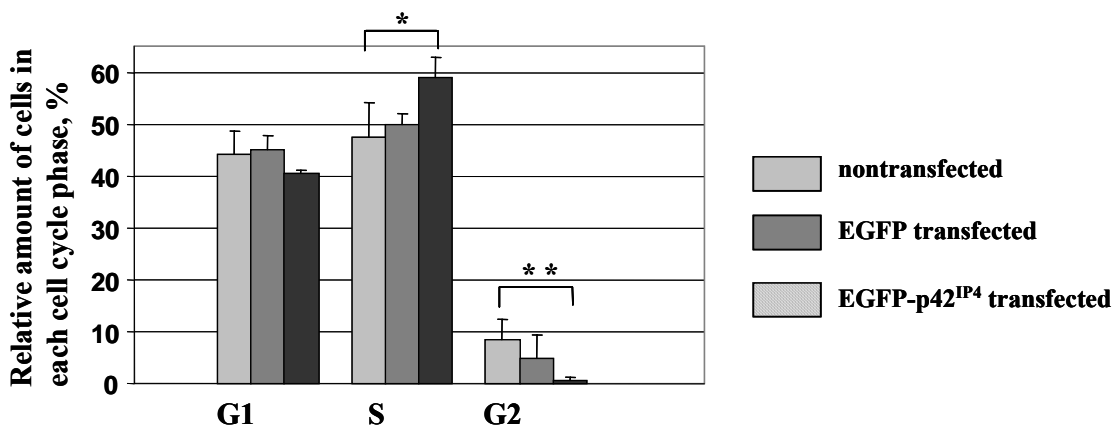


Fig.3.1.5. Effect of p42^{IP4} expression on cell cycle in N2a cells

Percentage of cells in the G1, S, and G2/M phases of the cell cycle without apoptotic treatment. The sum of total counted cells in G1, S and G2 phases represent 100%. Values represent the mean \pm SD from three independent experiments. * p < 0.05, ** p < 0.01 versus nontransfected control cells.

3.2. Novel localization of p42^{IP4}: mitochondrial localization

Previously, p42^{IP4} was identified in brain membranes from several species (Donie and Reiser, 1991). Expression of p42^{IP4} protein in non-neuronal CHO cells stably transfected with pcDNA-p42^{IP4} was shown in cytosol, membranes and nucleus (Sedehizade et al., 2002). The membrane fraction in that study also contained mitochondria.

p42^{IP4} associates with all PKC isoforms and is phosphorylated by PKC (Zemlickova et al., 2003). Additionally, protein kinase B is a target for PIP₃, the ligand of p42^{IP4}. Both, protein kinase B and PKC were found to be localized in mitochondria (Baines et al., 2003; Bijur and Jope, 2003).

Furthermore, the yeast protein Gcs1p, which is structurally and functionally related to p42^{IP4}, is localized in mitochondria and is involved in maintenance of mitochondrial morphology (Huang et al., 2002). Finally, a high probability for mitochondrial localization of p42^{IP4} was predicted by the program PSORT II (<http://psort.nibb.ac.jp/>; (Nakai and Kanehisa, 1992). All these data indicate possible localization of p42^{IP4} in mitochondria. Therefore, this question, which has not yet been investigated, was studied here.

3.2.1 p42^{IP4} is localized in mitochondria, isolated from transfected CHO cells

We used mitochondria isolated from CHO cells, stably transfected with pcDNA-p42^{IP4} to determine if the mitochondrial fraction contained p42^{IP4}. Immunoprecipitation of p42^{IP4} from the mitochondrial lysate was performed, and the precipitate was analyzed by immunoblotting. p42^{IP4} was detected using a monoclonal anti-p42^{IP4} antibody. Fig. 3.2.1 demonstrates that p42^{IP4}, which was present in the mitochondrial lysate, was highly concentrated in the immunoprecipitate.

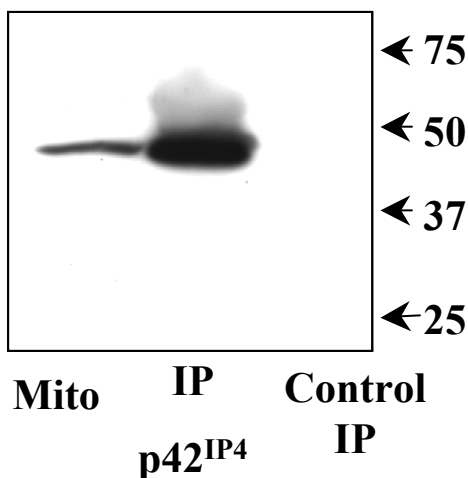


Fig. 3.2.1. Mitochondrial localization of p42^{IP4} in CHO cells.

Lysate of mitochondria from CHO cells, transfected with p42^{IP4} (2 mg of protein) was used for immunoprecipitation (IP) with control rabbit IgG antibody or anti-p42^{IP4} polyclonal rabbit antibody AS1516g, as described in "Materials and Methods". p42^{IP4} was visualized in the mitochondrial lysate (Mito) and precipitate by immunoblotting with monoclonal anti-p42^{IP4} antibody Mab117-2. Experiments were repeated three times with similar results.

3.2.2 p42^{IP4} is localized in inner mitochondrial compartments of transfected CHO cells

To investigate the compartmentalization of p42^{IP4} within mitochondria, mitochondria from CHO cells expressing p42^{IP4} were subfractionated into outer membrane, intermembrane space, inner membrane and matrix fractions. p42^{IP4} was found in all mitochondrial fractions of CHO cells (Fig. 3.2.2. A), but seems to be enriched in the intermembrane space. Separation of each mitochondrial compartment was verified by immunoblotting of the subfractions with mitochondrial compartment-specific proteins, VDAC (for outer membrane), Cyt c (for intermembrane space), cytochrome oxidase subunit IV (for inner membrane), and the Mn-superoxide dismutase (SOD2) for matrix, as shown in Fig. 3.2.2. A. VDAC, an outer membrane protein, is enriched at contact sites between the outer and inner membranes and is, therefore, typically detected in both outer membrane and inner membrane fractions (Bijur and Jope, 2003). SOD2 was stained not only in the matrix fraction. Probably due to the fragility of the inner membrane of mitochondria isolated from CHO cells SOD2 was also detected in the intermembrane space.

Mitochondrial compartments contain different amounts of protein. Therefore, to calculate the total p42^{IP4} content in each fraction, we had to take into account the whole protein amount in each subfraction of mitochondria. The relative distribution of p42^{IP4} was obtained by calculating the ratio between the total p42^{IP4} protein content in each submitochondrial fraction over the sum of p42^{IP4} contents of all fractions. The result shown in Fig. 3.2.2. B reveals that p42^{IP4} is localized predominantly at the inner membrane and in the intermembrane space of mitochondria, which is similar to the localization of Cyt c. p42^{IP4} is detectable only to a small degree in matrix and outer membrane fractions.

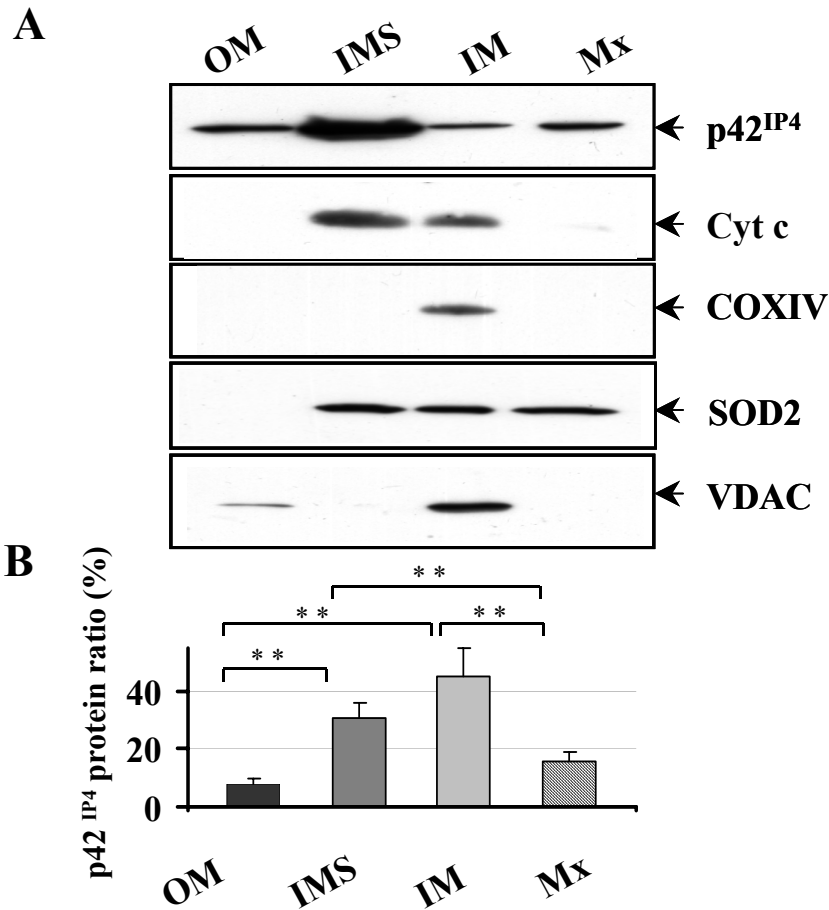


Fig. 3.2.2. Sub-mitochondrial distribution of p42^{IP4} in CHO cells.

(A) Isolated mitochondria from CHO cells were sub-fractionated as described in “Materials and Methods”. As indicated in the figure, the isolated outer membranes (OM), intermembrane space (IMS), inner membrane (IM) and matrix (Mx) fractions were separated by electrophoresis in 15% SDS-PAGE (20 μ g of protein per lane in each fraction) with following Western blot. The membrane was probed with anti-p42^{IP4} antibody Mab117-2. The same membranes were stained with antibodies for the compartment-specific proteins voltage-dependent anion channel (VDAC), cytochrome c (Cyt c), cytochrome oxidase subunit IV (COX IV), and Mn-superoxide dismutase (SOD2), respectively. (B) Relative distribution of p42^{IP4} given as the percent ratio. The ratio was calculated, as described in the text, taking the total p42^{IP4} content in each fraction over the sum of p42^{IP4} protein contents of all fractions. Data shown are the mean \pm S.D. obtained from three mitochondrial preparations. ** $p < 0.01$.

3.2.3 p42^{IP4} is localized in mitochondria, isolated from transfected N2a cells

p42^{IP4} is mainly expressed in neurons. Therefore, we chose mouse neuroblastoma N2a cells as a model for functional studies of p42^{IP4} in mitochondria. N2a cells endogenously express p42^{IP4} at a very low level, which is detectable by RT-PCR (Fig. 3.2.3 A) but hardly by Western blotting (data not shown).

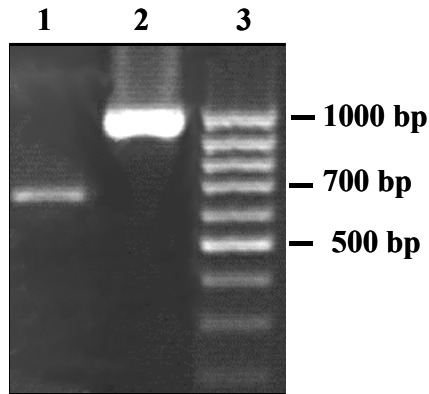


Fig. 3.2.3. The endogenous expression of p42^{IP4} in N2a cells.

Determination of p42^{IP4} mRNA by RT-PCR in N2a cells. Fragments were amplified by RT-PCR with specific primers, separated on 1% agarose gel, and stained with ethidium bromide. p42^{IP4} (691 bp, lane 1) mRNA is detected in N2a. GAPDH (984 bp, lane 2) served as an internal control. Lane 3 represents 100-bp DNA standard. Data are representative of three independent experiments.

To determine mitochondrial localization of p42^{IP4} in the neuroblastoma cell line, we stably transfected N2a cells with pcDNA-p42^{IP4} construct and performed subcellular fractionation of these cells. As shown in Fig. 3.2.4, p42^{IP4} is localized in mitochondria as well as in nuclear, cytosolic, and membrane fractions. VDAC antibody (for the outer mitochondrial membrane) was used to verify the mitochondrial fraction. Glyceraldehyde 3-phosphate dehydrogenase (for cytosol fraction) was stained not only in the cytosol but also in nuclear fraction possibly due to a contamination of nuclei with some unbroken cells. Nevertheless, we were not interested in purity of all subcellular fractions. It is important that staining with nucleoporin antibody (for nuclear fraction), glyceraldehyde 3-phosphate dehydrogenase antibody and plasma membrane calcium ATPase antibody (for plasma membrane fraction) shows that mitochondria are not contaminated with other subcellular fractions. Therefore, p42^{IP4} is indeed localized in mitochondria.

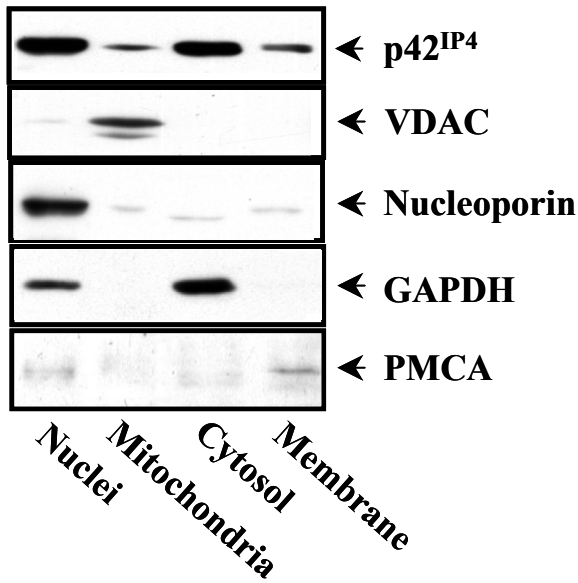


Fig. 3.2.4. Mitochondrial localization of p42^{IP4} in N2a cells.

Nuclear, cytosolic, mitochondrial and membrane fractions were obtained from N2a cells stably transfected with pcDNA- p42^{IP4}. The fractions were separated by electrophoresis in 10% SDS-PAGE (20 µg of protein per lane in each fraction) with following Western blot. The membrane was probed with monoclonal anti-p42^{IP4} antibody. The same membranes were stained with anti-VDAC (voltage-dependent anion channel) antibody (for mitochondria), anti-Nucleoporin antibody (for nucleus), anti-GAPDH (glyceraldehyde 3-phosphate dehydrogenase) antibody (for cytosol) and anti-PMCA (plasma membrane calcium ATPase) antibody (for plasma membrane). Experiments were repeated three times with similar results.

Additionally, we used confocal microscopy to confirm mitochondrial localization of p42^{IP4}. First, co-localization experiments were performed using N2a cells stably transfected with the p42^{IP4}-Myc construct. It should be noted that due to the high level of p42^{IP4} in the cytosol, mitochondrial localization is difficult to establish by this method. However, in the merged picture in Figure 3.2.5 A we could detect co-localization of p42^{IP4} with mitochondria of N2a cells stably transfected with p42^{IP4}-Myc by staining with antibodies against Myc and Cyt c.

Since N2a cells have a rather small size, we also performed staining of larger cells to detect more clearly the mitochondrial structures. For that purpose, CHO cells stably transfected with pcDNA-p42^{IP4} were double-stained with p42^{IP4} and Cyt c antibodies and analyzed by confocal microscopy. Although the p42^{IP4} protein is found to a large extent in the nucleus and cytosol, co-localization of p42^{IP4} with mitochondria of CHO cells was clearly determined, as can be seen in Figure 3.2.5 B. Graphs of profiles of fluorescence intensity indicate a coincidence between red (mitochondria) and green (p42^{IP4}) peaks (Fig. 3.2.5 B), confirming unequivocally the co-localization of p42^{IP4} with mitochondria. While p42^{IP4} is not restricted to mitochondria, there is a considerable overlap of green and red peaks in the profiles. Moreover, in the nuclear area a high intensity of green fluorescence (indicating p42^{IP4}) and a lack of red fluorescence (representing mitochondria) were detected. Altogether, these results show that p42^{IP4} is associated with mitochondria of both CHO and neuronal N2a cells.

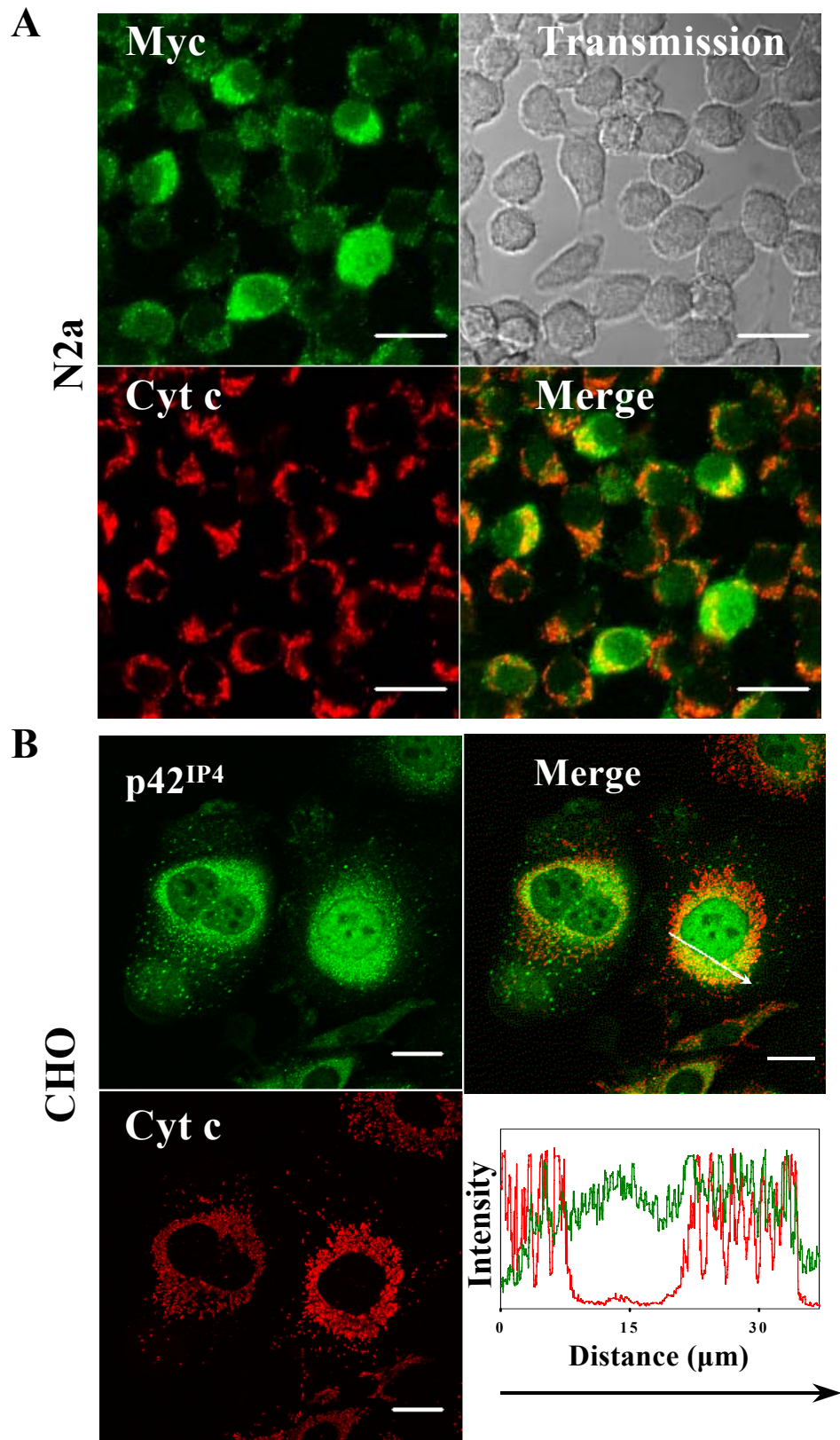


Fig. 3.2.5. Colocalization of p42^{IP4} with mitochondria.

(A) Confocal imaging of colocalization of p42^{IP4} with mitochondria in N2a cells. Stably transfected N2a cells expressing p42^{IP4} MycHis were fixed, permeabilized, double-stained with anti-myc and anti-Cyt c (cytochrome c) antibodies, and observed by confocal microscopy. Detection of p42^{IP4} MycHis (green) by polyclonal anti-myc antibody and Alexa Fluor 488 goat anti-rabbit IgG and detection of mitochondria (red) by monoclonal anti-Cyt c (cytochrome c) antibody and Alexa Fluor 555 goat anti-

mouse IgG was carried out. The merged picture in the lower right panel shows co-localization of p42^{IP4} with mitochondria (*yellow*). The right upper panel shows a transmission light picture. Scale bar indicates 20 μm . Pictures shown are representative of at least three independent experiments. **(B)** Confocal imaging of colocalization of p42^{IP4} with mitochondria in CHO cells. Stably transfected CHO cells expressing p42^{IP4} were fixed, permeabilized, double-stained with polyclonal rabbit serum raised against p42^{IP4} (AS1516g) and anti-Cyt c (cytochrome c) antibodies, and observed by confocal microscopy. Left upper panel shows detection of p42^{IP4} (*green*) by polyclonal rabbit serum and Alexa Fluor 488 goat anti-rabbit IgG, and the left lower panel shows detection of mitochondria (*red*) by monoclonal anti-Cyt c (cytochrome c) antibody and Alexa Fluor 555 goat anti-mouse IgG. The merged picture in the right upper panel shows co-localization of p42^{IP4} with mitochondria (*yellow*). Scale bar indicates 20 μm . The curves (right lower panel) represent the fluorescence intensity distribution determined for a cross-section of the cell, as indicated by the white arrow in the merged image. Arrow indicates the orientation of the section. Pictures shown are representative of at least three independent experiments.

3.3 p42^{IP4} is involved in regulation of mitochondrial Ca²⁺

The findings that p42^{IP4} is localized at the mitochondrial inner membrane and in the intermembrane space, raised the question of possible functions of this protein in mitochondria. To address this issue, we used a recently developed method of isolation of functionally active mitochondria from cultured cells and studied mitochondrial functions during Ca²⁺-induced PTP opening (Azarashvili et al., 2005; Azarashvili et al., 2007).

We investigated whether p42^{IP4} might be involved in the regulation of mitochondrial Ca²⁺ transport mechanisms. The PTP forms a Ca²⁺ efflux pathway from mitochondria through a large pore (Smaili et al., 2000). To study the influence of p42^{IP4} on mitochondrial functions during Ca²⁺-induced PTP opening in mitochondria, we compared the functional parameters of mitochondria, which were isolated from N2a wild type cells, or from cells transfected with p42^{IP4}, or transfected with empty vector. The effect of the over-expression of p42^{IP4} on Ca²⁺ transport, mitochondrial membrane potential ($\Delta\Psi_m$), and oxygen consumption rate were examined in isolated mitochondria upon Ca²⁺-induced PTP opening.

3.3.1 p42^{IP4} accelerates Ca²⁺-induced PTP opening in mitochondria from N2a cells

We used the open recording chamber with installed electrodes selective for O₂, Ca²⁺ and TPP⁺, as described in previous reports (Azarashvili et al., 2005; Azarashvili et al., 2007). The ability of mitochondria isolated from N2a wild type cells, or from cells transfected with p42^{IP4}, or transfected with empty vector to accumulate Ca²⁺ was investigated using two approaches.

First, Ca²⁺ was added in small bolus additions (70 nanomoles of Ca²⁺ per mg of protein per addition) to estimate the Ca²⁺ threshold (Ca²⁺ capacity) for each kind of mitochondria. Figure 3.3.1 A shows an experiment with mitochondria isolated from wild type N2a cells. After addition of the mitochondrial suspension into the chamber, the mitochondria

take up the membrane potential indicator TPP⁺ within 3 min, reflecting the amplitude of the mitochondrial membrane potential. Six pulses of Ca²⁺ were followed by rapid and complete accumulation of Ca²⁺ into the mitochondrial matrix. Each pulse was accompanied by a transient depolarization and restoration of $\Delta\Psi_m$, as shown by the TPP⁺ trace. The loading with Ca²⁺ was stopped, when the mitochondria were not able any more to accumulate the added Ca²⁺, as demonstrated by an increase in extramitochondrial Ca²⁺ in medium.

Addition of the last (seventh) pulse of Ca²⁺ resulted in a decreased rate of Ca²⁺ influx, which was correlated with membrane potential decrease. After a rather short time of retaining of Ca²⁺, rapid Ca²⁺ efflux from the mitochondrial matrix ensued. This efflux was associated by complete $\Delta\Psi_m$ dissipation. These events indicate increased permeability of the inner membrane and initiation of PTP opening. The precipitating Ca²⁺ release occurred after addition of threshold Ca²⁺ concentration. The Ca²⁺ threshold was above 420 nanomoles of Ca²⁺ per mg of protein for this kind of mitochondria. The same amount of Ca²⁺ had to be added to open PTP in mitochondria from N2a cells transfected with empty vector (Figure 3.3.1 B).

As shown in Fig. 3.3.1 C, mitochondria from N2a cells overexpressing p42^{IP4} were able to take up much less Ca²⁺ and thus had a lower Ca²⁺ threshold. In mitochondria isolated from N2a cells transfected with p42^{IP4} the Ca²⁺ efflux was observed already after the fourth addition of Ca²⁺. The Ca²⁺ threshold was above 210 nanomoles of Ca²⁺ per mg of protein. Moreover, the mitochondria accumulated TPP⁺ with a slower time course. This indicates that these mitochondria have a lower membrane potential.

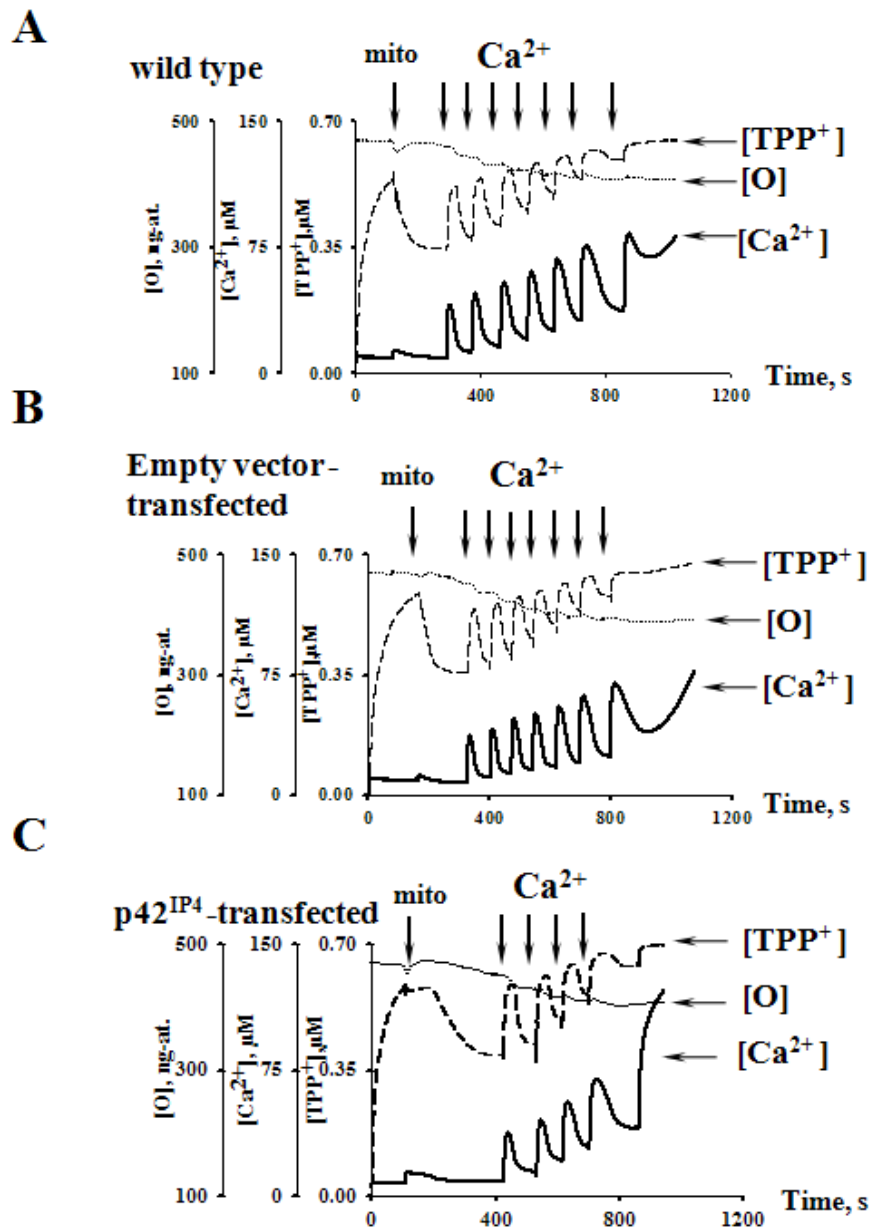


Fig. 3.3.1. *p42^{IP4} expression in mitochondria accelerates PTP opening induced by small bolus additions of Ca²⁺.*

Mitochondria (0.7 mg of protein per ml) isolated from N2a wild type cells (**A**), from N2a cells transfected with empty vector (**B**) and transfected with p42^{IP4} (**C**) were added (the first arrow, mito) to respiration buffer, as described in Methods. Oxygen consumption, transmembrane potential and extramitochondrial Ca²⁺ concentration were measured with O₂, TPP⁺ (tetraphenylphosphonium) and Ca²⁺-selective electrodes, respectively, upon Ca²⁺-induced PTP opening. Ca²⁺ arrows show additions of 70 nanomoles of Ca²⁺ per mg of protein. Mitochondria isolated from N2a wild type cells (**A**) and from N2a cells transfected with empty vector (**B**) were able to accumulate more Ca²⁺ and TPP⁺ before PTP opening in comparison with mitochondria transfected with p42^{IP4} (**C**).

Next, we used the second approach with big bolus additions (200 nanomoles of Ca²⁺ per mg of protein per addition) to determine the retention time of Ca²⁺, before initiation of its release (lag time) under PTP opening in each kind of mitochondria. There was a significant

decrease in the Ca^{2+} threshold and acceleration of PTP opening in mitochondria isolated from N2a cells transfected with p42^{IP4} in comparison with mitochondria from N2a wild type cells (Fig. 3.3.1). Therefore, we performed determination of lag time with the amount of Ca^{2+} which had to be added to open PTP in N2a cells transfected with p42^{IP4} . With this amount of Ca^{2+} we expected that in mitochondria from N2a cells transfected with p42^{IP4} the lag time would be shorter than in mitochondria from N2a wild type cells.

Figure 3.3.2 clearly shows the difference in lag time for PTP opening between mitochondria isolated from N2a wild type cells (A), and from N2a cells transfected with p42^{IP4} (C). The kinetics of Ca^{2+} uptake in these kinds of mitochondria were different, namely the rate of Ca^{2+} influx was decreased in mitochondria from N2a cells overexpressing p42^{IP4} in comparison with mitochondria from wild type. Lag time for PTP opening in mitochondria from N2a cells transfected with empty vector (Fig. 3.3.2 B) was the same as for mitochondria isolated from N2a wild type cells (Fig. 3.3.2 A).

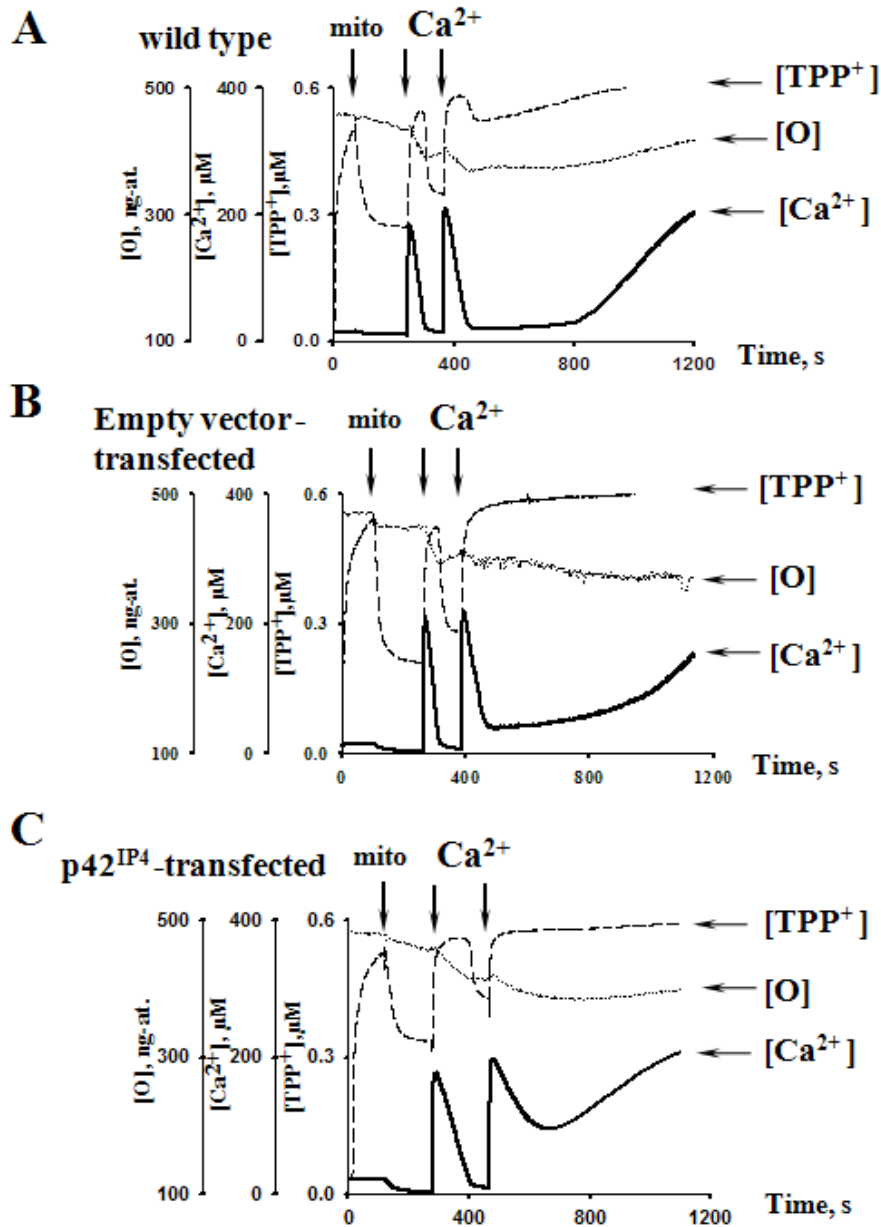


Fig. 3.3.2. *p42^{IP4} expression in mitochondria accelerates PTP opening induced by big bolus additions of Ca²⁺.*

Mitochondria (0.7 mg of protein per ml) isolated from N2a wild type cells (**A**), from N2a cells transfected with empty vector (**B**) and from N2a cells transfected with p42^{IP4} (**C**) were added (the first arrow, mito) to respiration buffer, as described in Methods. Oxygen consumption, transmembrane potential and extra-mitochondrial Ca²⁺ concentration were measured with O₂, TPP⁺ (tetraphenylphosphonium) and Ca²⁺-selective electrodes, respectively, upon Ca²⁺-induced PTP opening. Ca²⁺ arrows show additions of 200 nanomoles of Ca²⁺ per mg of protein. The difference in time before Ca²⁺ release (lag time) for PTP opening is illustrated between mitochondria isolated from N2a wild type cells (**A**), and from N2a cells transfected with p42^{IP4} (**C**). Lag time for PTP opening in mitochondria from N2a cells transfected with empty vector (**B**) was the same as for mitochondria isolated from N2a wild type cells (**A**). Results shown are representative of at least three independent experiments.

To exclude possible influence of traces of endoplasmic reticulum (ER) on results of Ca^{2+} measurement, we determined mitochondrial functions in the presence of thapsigargin, a specific inhibitor of the Ca^{2+} ATPase in the intracellular Ca^{2+} stores of the ER. The result that is shown in Fig. 3.3.3 reveals that thapsigargin did not influence the mitochondrial Ca^{2+} transport parameters measured. Therefore, we can rule out contamination of the mitochondrial fraction with ER.

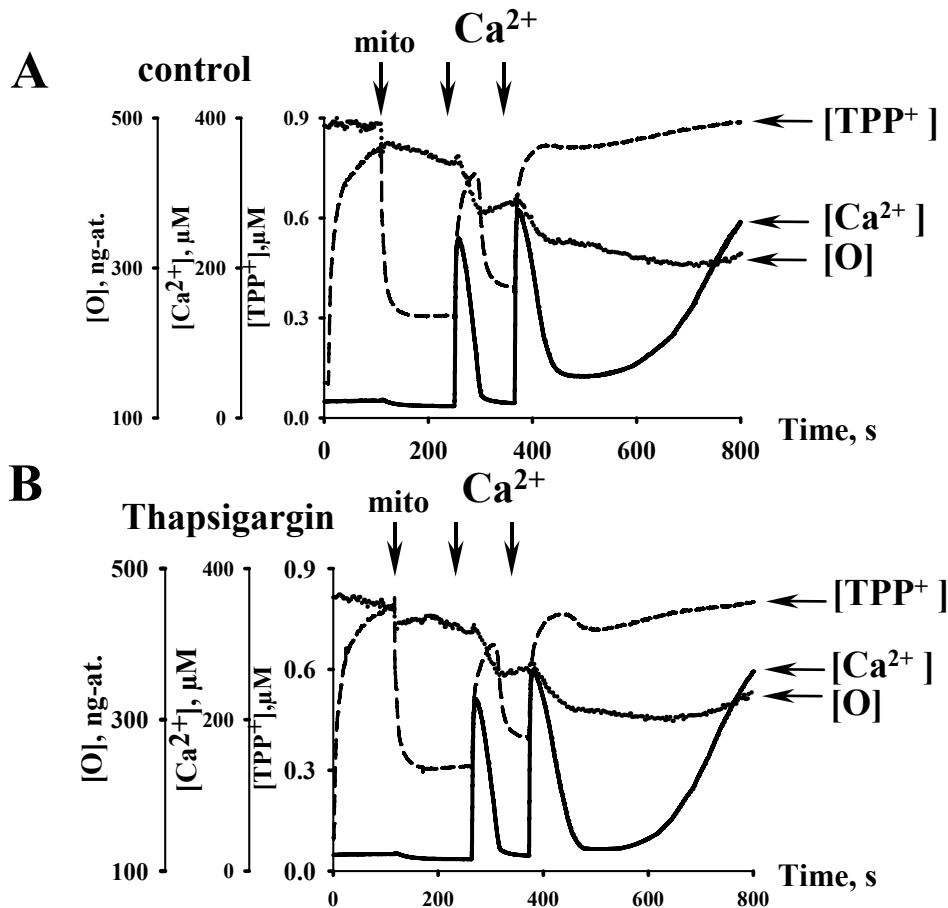


Fig.3.3.3. Lack of effect of thapsigargin on functions of mitochondria from N2a cells.

(A and B) Mitochondria (0.7 mg of protein per ml) isolated from wild type cells were added to respiration buffer, as described in Methods. Oxygen consumption, transmembrane potential and extra-mitochondrial Ca^{2+} concentration were measured with O_2 , TPP^+ and Ca^{2+} -selective electrodes, respectively, upon Ca^{2+} -induced PTP opening. Arrows show addition of 200 nanomoles of Ca^{2+} per mg of protein, each.

In the lower diagram (B) thapsigargin (a specific inhibitor of Ca^{2+} ATPase in the intracellular ER Ca^{2+} stores) ($0.5 \mu\text{M}$) was applied 20 s after the addition of mitochondria to the incubation medium. There were no differences in ability to accumulate Ca^{2+} and in time before Ca^{2+} release (lag time) under PTP-opening between mitochondria treated with thapsigargin and nontreated mitochondria. Therefore, there is no relevant contamination of ER in mitochondria.

It was discovered that PTP induction is inhibited by cyclosporin A (CsA) (Crompton et al., 1988; Broekemeier et al., 1989), an effect that has been attributed to a blockade of Cyp-

D association with ANT (Halestrap and Davidson, 1990). However, some studies on respiring isolated brain mitochondria have reported a limitation of CsA to inhibit PTP (Brustovetsky and Dubinsky, 2000; Kristal et al., 2000).

We investigated the influence of CsA on PTP induction in mitochondria isolated from N2a cells. As shown in Fig. 3.3.4. there were no differences in the Ca^{2+} -induced Ca^{2+} release and the accompanying decrease of the membrane potential between mitochondria isolated from N2a cells treated with CsA and nontreated mitochondria. Therefore, mitochondria isolated from N2a cells were CsA-insensitive (Fig. 3.3.4).

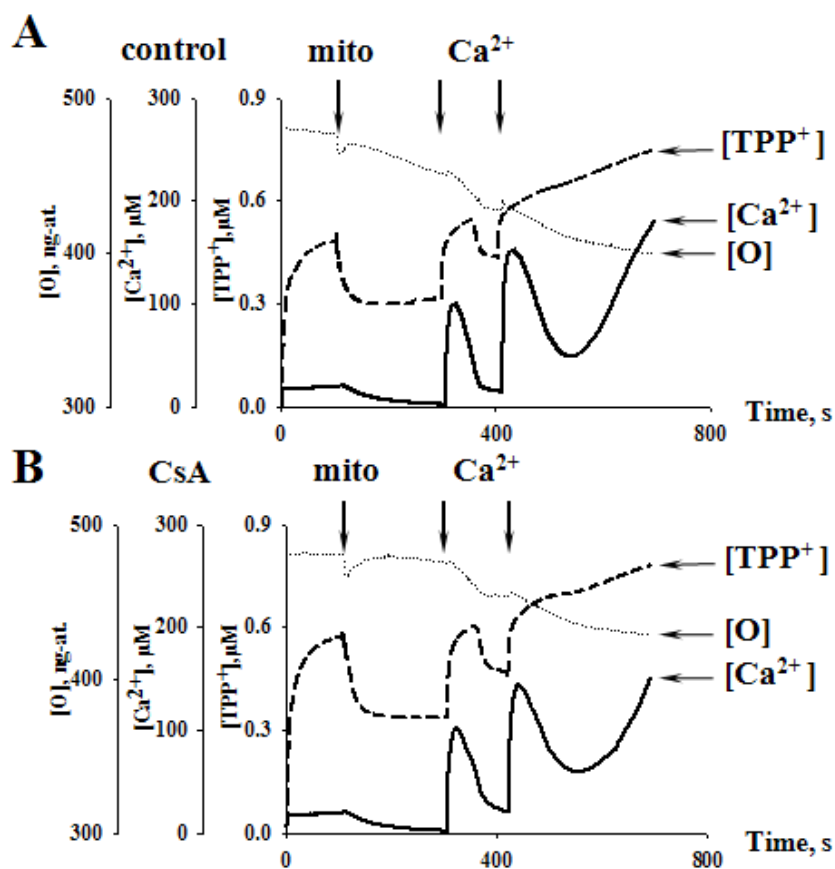


Fig. 3.3.4. Lack of effect of cyclosporine A (CsA) on functions of mitochondria from N2a cells.

(A and B) Mitochondria (0.7 mg of protein per ml) isolated from wild type cells were added to respiration buffer, as described in Methods. Oxygen consumption, transmembrane potential and extramitochondrial Ca^{2+} concentration were measured with O_2 , TPP^+ and Ca^{2+} -selective electrodes, respectively, upon Ca^{2+} -induced PTP opening. Arrows show addition of 200 nanomoles of Ca^{2+} per mg of protein, each.

In the lower diagram (B) 1 μM CsA, was applied 20 s after the addition of mitochondria to the incubation medium. There were no differences in ability to accumulate Ca^{2+} and in time before Ca^{2+} release (lag time) under PTP opening between control mitochondria and mitochondria treated with CsA.

Fig. 3.3.5 demonstrates an example, which shows how we evaluated the parameters of Ca^{2+} transport. To determine the lag time for Ca^{2+} release we first plot a tangential line at the point of inflection of the curve of Ca^{2+} influx (i), then a tangential line at the point of inflection of the curve of Ca^{2+} efflux (ii). The length of the segment of the tangential line on the lower peak of the Ca^{2+} trace, which intersects lines (i) and (ii), defines the lag time for Ca^{2+} release. The slope of tangential line (i) is the rate of Ca^{2+} influx.

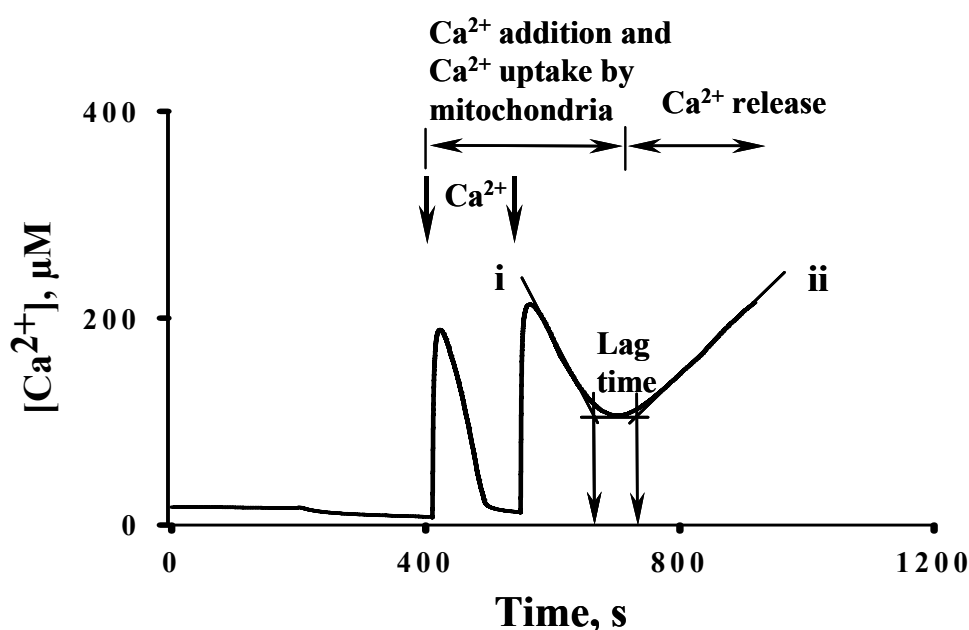


Fig. 3.3.5. Evaluation of the parameters of mitochondrial Ca^{2+} transport.

Isolated mitochondria were added to respiration buffer, as described in Methods. Extra-mitochondrial Ca^{2+} concentration was measured with Ca^{2+} -selective electrode upon Ca^{2+} -induced PTP opening. Ca^{2+} arrows show additions of 200 nanomoles of Ca^{2+} per mg of protein. Mitochondrial functions, rate of Ca^{2+} influx (slope of tangential line (i)), rate of Ca^{2+} efflux (slope of tangential line (ii)), lag time (length of segment of tangential line at lower peak of Ca^{2+} trace intersected by lines (i) and (ii)) were evaluated, as described in the text.

The amount of Ca^{2+} taken up by mitochondria before PTP opening is the Ca^{2+} capacity or Ca^{2+} threshold. The Ca^{2+} capacity was evaluated and is presented on the basis of small bolus Ca^{2+} additions. For the calculation, we used the sum of additions of Ca^{2+} , taking into account interpolation for the last addition, and then we determined the exact amount of Ca^{2+} load, which was accumulated before release of Ca^{2+} at PTP opening. That allowed presenting the statistical data.

Figure 3.3.6 represents the analysis of the functional Ca^{2+} parameters of mitochondria isolated from N2a wild type cells, mitochondria isolated from N2a cells transfected with empty vector, and mitochondria from N2a cells transfected with p42^{IP4} . Data from both approaches, small and big bolus Ca^{2+} additions, are presented. As shown in the diagram, overexpression of p42^{IP4} lead to a significant decrease in the rate of Ca^{2+} influx, probably associated with a lowered membrane potential. The lag time was shortened and the Ca^{2+} capacity (threshold Ca^{2+} concentration) was decreased. These data indicate that p42^{IP4} was able to promote pore formation and Ca^{2+} -induced PTP opening in mitochondria.

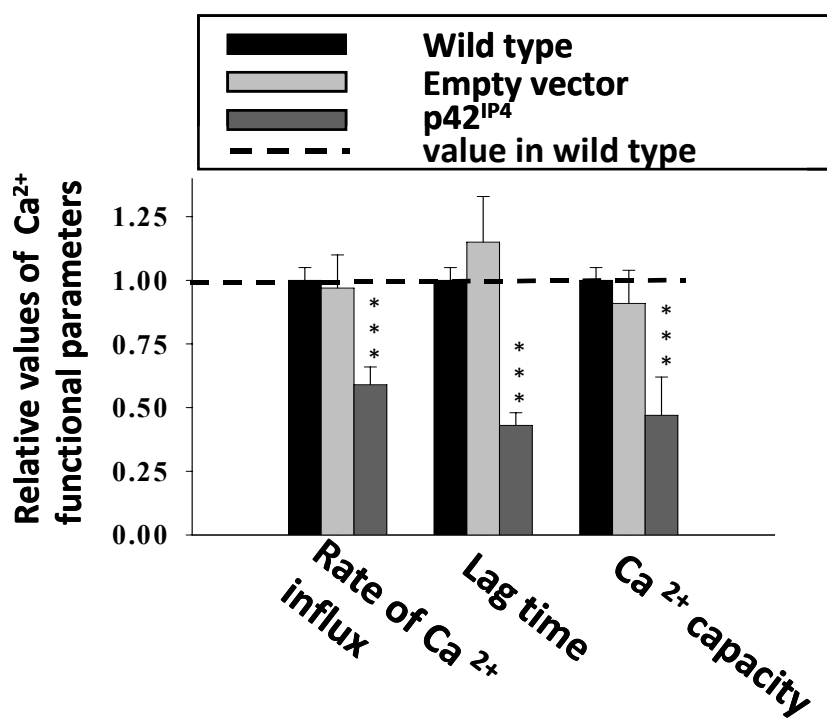


Fig.3.3.6. Influence of p42^{IP4} on mitochondrial functional parameters at Ca^{2+} -induced PTP opening. After loading with Ca^{2+} to induce PTP opening, the relative values of mitochondrial Ca^{2+} influx rate, lag time and Ca^{2+} capacity were evaluated for wild type N2a cells mitochondria, mitochondria from N2a cells transfected with p42^{IP4} , and from N2a cells transfected with empty vector. The levels of functional parameters of mitochondria isolated from wild type N2a cells loaded with threshold Ca^{2+} were taken as 1 (dashed line). Data shown are the mean \pm S.D. obtained from four mitochondrial preparations. *** $p < 0.001$ versus wild type control.

3.3.2 Effects of p42^{IP4} ligands, phosphatidylinositol(3,4,5)trisphosphate (PIP₃) and inositol(1,3,4,5)tetrakisphosphate (IP₄), on mitochondrial functions

The effects of PIP₃ and IP₄ on mitochondrial functions were also studied. Table 3.3.7. represents their influence on the functional Ca²⁺ parameters of PTP opening. The Ca²⁺ influx rate, lag time and Ca²⁺ capacity of mitochondria were reduced in the presence of 5 μM PIP₃ or 5 μM IP₄ in comparison with nontreated mitochondria from all three kinds of cells. The maximal decrease was observed in the lag time. Addition of IP₄ significantly shortened the lag time in comparison with nontreated mitochondria from all three kinds of cells. This means that IP₄ accelerates PTP opening. Also in the presence of 5 μM PIP₃ the reduction of the rate of Ca²⁺ influx, lag time and Ca²⁺ capacity was considerable for mitochondria isolated from all three kinds of cells in comparison with nontreated mitochondria.

Table 3.3.7.

| | Ca ²⁺ influx rate | | Lag time | | Ca ²⁺ capacity | |
|--------------------------------------|--------------------------------|--------------------------------|--------------------------------|--------------------------------|--------------------------------|--------------------------------|
| | IP ₄ | PIP ₃ | IP ₄ | PIP ₃ | IP ₄ | PIP ₃ |
| Wild type | 0.82 ± 0.04^b | 0.79 ± 0.01^c | 0.61 ± 0.11^c | 0.44 ± 0.08^c | 0.65 ± 0.05^a | 0.44 ± 0.06^c |
| Empty vector transfected | 0.90 ± 0.12 | 0.77 ± 0.10^a | 0.55 ± 0.08^c | 0.53 ± 0.12^a | 0.74 ± 0.06 | 0.68 ± 0.14^a |
| p42^{IP4} transfected | 0.86 ± 0.09^a | 0.71 ± 0.08^a | 0.53 ± 0.04^a | 0.51 ± 0.07 | 0.74 ± 0.11 | 0.49 ± 0.09 |

^a p < 0.05, ^b p < 0.01, ^c p < 0.001 versus respective control (without addition).

Table 3.3.7. The effects of IP₄ and PIP₃ on Ca²⁺ parameters of mitochondria from N2a cells.

Mitochondria isolated from N2a cells transfected with p42^{IP4}, transfected with empty vector and from N2a wild type cells were pre-incubated with 5 μM IP₄ (D-myo-inositol 1,3,4,5-tetrakisphosphate, tetrapotassium salt) or 5 μM PIP₃ (phosphatidylinositol 3,4,5-trisphosphate diC8) for 20 min. After that, the mitochondria were loaded with Ca²⁺ to induce PTP opening, as described in Fig. 3.3.2. Relative values of mitochondrial Ca²⁺ influx rate, lag time and Ca²⁺ capacity in the presence of IP₄ and PIP₃ versus respective control (without addition) are presented. Data shown are the mean ± S.D. obtained from three mitochondrial preparations.

To keep out the possibility that these effects observed were probably caused by the high number of negative charges present in PIP₃, we performed experiments with D-inositol(1,3,5,6) tetrakisphosphate. The latter has the same net charge, but is a poor ligand for p42^{IP4} (Hanck et al., 1999).

There were no differences between Ca^{2+} traces recorded for mitochondria in the chamber, when they were either treated with 5 μM D-inositol(1,3,5,6) tetrakisphosphate or not treated (control). Effects of D-inositol(1,3,5,6) tetrakisphosphate were not distinguishable from control (example is presented on Fig.3.3.3.), that was observed on at least two mitochondrial preparations. Therefore, we ruled out an influence of D-inositol(1,3,5,6) tetrakisphosphate on the mitochondrial Ca^{2+} transport parameters measured.

Thus, our results demonstrate that the ligands of p42^{IP4} , PIP_3 and IP_4 , destabilize mitochondria during Ca^{2+} -induced PTP opening specifically. Since the effects of PIP_3 and IP_4 on the rate of Ca^{2+} influx, lag time and Ca^{2+} capacity were considerable for mitochondria isolated from all three kinds of cells, we concluded that the action of the p42^{IP4} ligands on PTP opening was independent of the overexpression of p42^{IP4} .

3.4. Interaction of p42^{IP4} with CNP and α -tubulin in rat brain mitochondria

Since p42^{IP4} has been identified as a brain-specific protein (Hammonds-Odie et al., 1996; Stricker et al., 1997), it was important to examine in RBM the localization of p42^{IP4} and the possible association of p42^{IP4} with other mitochondrial proteins. Because we found p42^{IP4} mainly in the inner membrane fraction of mitochondria, it was reasonable to look for p42^{IP4} -interacting proteins within inner membrane and contact sites. One such protein was CNP.

CNP was found in mitochondria of adrenal medullary chromaffin cell cultures (McFerran and Burgoyne, 1997), amoeboid microglial cells (Wu et al., 2006) and oligodendrocyte cell line (OLN93 cells) (Lee et al., 2006). Recently, we described for the first time that CNP localizes in the mitochondrial membrane fractions and associates with VDAC of the outer membrane and ANT of the inner membrane of RBM (data shown below, in Fig. 3.5.1; Fig. 3.5.2). Moreover, the involvement of CNP in acceleration of Ca^{2+} release via PTP functioning, using mitochondria isolated from wild type OLN93 cells and CNP knock-down OLN93 cells was shown by us (data shown below, in Fig. 3.6.3; Fig. 3.6.4). Localization of both proteins, CNP and p42^{IP4} , in the inner membrane of mitochondria and their participation in Ca^{2+} -induced PTP opening allow us to hypothesize a possible interaction between these proteins.

Another protein possibly interacting with p42^{IP4} is α -tubulin. Microtubules (MTs) are a major component of cytoskeletal systems that are responsible for the regulation of the distribution of mitochondria in mammalian cells. Moreover, it was shown that α -tubulin is an inherent component of mitochondrial membranes specifically interacting with the VDAC (Carre et al., 2002). Kinesins are a superfamily of microtubule-associated motor proteins, and

some members of this family are responsible for the movement of mitochondria along microtubules. Recently, the kinesin-3 protein KIF13 B was found as interaction partner for p42^{IP4} (Venkateswarlu et al., 2005). Therefore, we supposed possible association between α -tubulin and p42^{IP4} in mitochondria.

3.4.1 Localization of p42^{IP4}, CNP and α -tubulin in rat brain mitochondria

At first, we determined whether p42^{IP4}, CNP and α -tubulin are localized in RBM. Since for these proteins cytosolic localization was shown before, we performed Western blot analysis of two brain fractions, mitochondria and cytosol. As shown in Fig. 3.4.1, p42^{IP4}, CNP and α -tubulin are detected in RBM. The mitochondrial fraction isolated from rat brain contained both nonsynaptic and synaptic mitochondria, as shown by staining with synaptotagmin I antibody (for the synaptic vesicles). VDAC and Cyt c antibodies were used to verify mitochondria. As shown by the lack of staining with the Cyt c antibody in the cytosol, mitochondria were not disrupted during the preparation. In addition, staining with GAPDH antibody confirmed that RBM were not contaminated with cytosolic fraction.

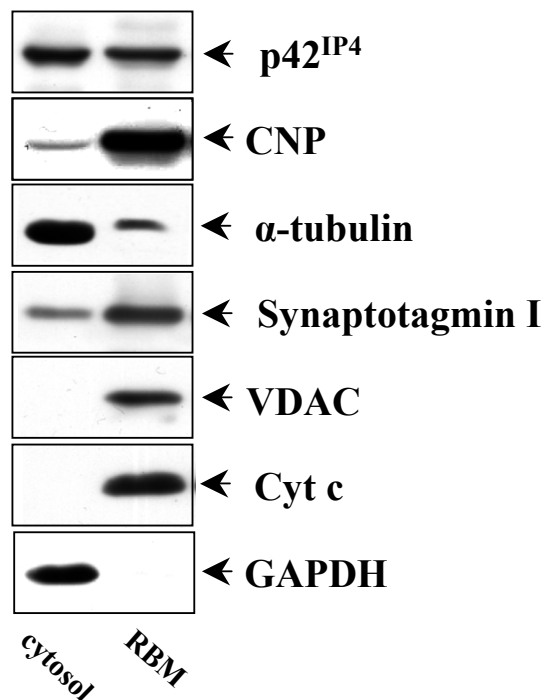


Fig. 3.4.1. p42^{IP4}, CNP, and α -tubulin are localized in RBM.

Mitochondria were isolated from rat brain without additional purification. Brain cytosolic fraction was used as positive control for p42^{IP4} expression. Aliquots of mitochondria or cytosol (30 μ g of protein per lane) were separated by 10% SDS-PAGE with following Western blot. The membrane was probed with the antibodies indicated on the right side, as described in Methods. RBM were positive for the mitochondrial markers VDAC (voltage-dependent anion channel; for the outer mitochondrial membrane) and Cyt c (cytochrome c; for intermembrane space), and the synaptosomal marker Synaptotagmin I. GAPDH (glyceraldehyde 3-phosphate dehydrogenase) antibody was used as marker for cytosolic fraction. Experiments were repeated three times with similar results.

3.4.2 p42^{IP4} interacts with CNP and α -tubulin *in vitro*

To check the association between p42^{IP4}, CNP and α -tubulin we performed pull-down assay using GST-p42^{IP4} fusion protein, expressed in bacteria. Since p42^{IP4}, CNP and α -tubulin localize to both cytosol and mitochondria, we used these two subcellular fractions for interaction studies. Cytosolic fraction or mitochondrial lysate were incubated with

immobilized GST-p42^{IP4}. Fig. 3.4.2. (I, II) demonstrates that CNP and α -tubulin from the mitochondrial fraction bind to GST-p42^{IP4}, but not to GST protein alone used as control. As shown in Fig. 3.4.2. (III, IV), α -tubulin and CNP from the cytosolic fraction bind to GST-p42^{IP4} as well.

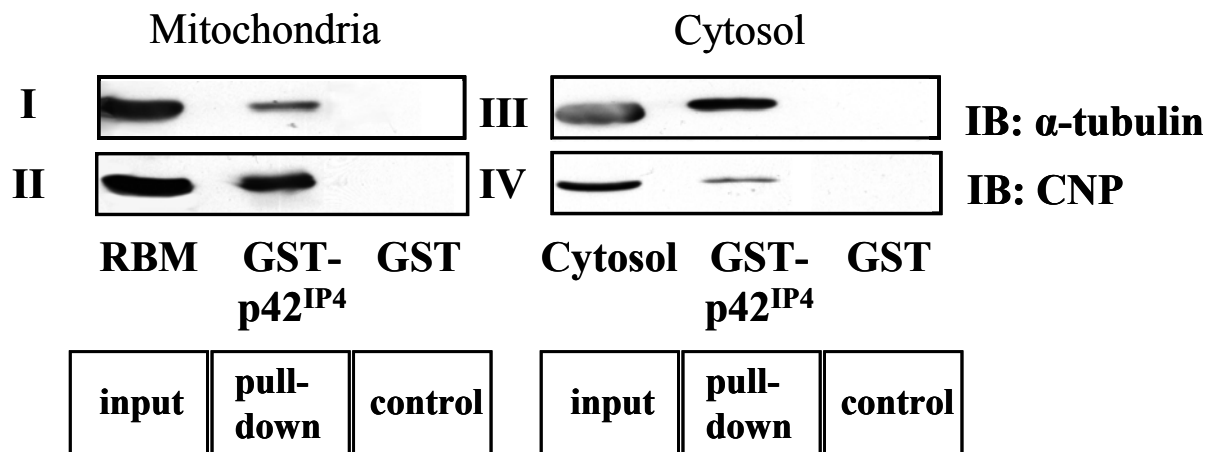


Fig. 3.4.2. p42^{IP4} interacts with CNP and α -tubulin *in vitro*, shown by pull-down binding assay. (I, II) Rat brain mitochondria (RBM) lysate or (III, IV) cytosol (2 mg of protein) (input) were incubated overnight with glutathione S-transferase (GST) protein alone (control) or GST-p42^{IP4} fusion protein (pull-down) immobilized on glutathione beads followed by SDS-PAGE (sodium dodecyl sulphate-polyacrylamide gel electrophoresis) and immunoblotting (IB) with the anti-CNP or anti- α -tubulin antibody. Experiments were repeated three times with similar results.

3.4.3 p42^{IP4} interacts with CNP and α -tubulin *in vivo*

To verify the interaction between p42^{IP4} and CNP *in vivo*, immunoprecipitation of p42^{IP4} from RBM and rat brain cytosol was performed, and the precipitate was analyzed for the presence of CNP by Western blot. Only CNP from the mitochondrial fraction was found to be co-immunoprecipitated with p42^{IP4} (Fig. 3.4.3. A). The CNP band can be detected in the mitochondrial precipitate also with control rabbit IgG, although to a much lesser extent than in the precipitate using the p42^{IP4} antibody. Therefore, we made the reverse co-immunoprecipitation with monoclonal CNP antibody. The p42^{IP4}-immunoreactive band was observed in the precipitate with CNP antibody from the mitochondrial fraction (Fig. 3.4.3. B), but not from cytosol, indicating that these two proteins interact only in RBM *in vivo*.

Next, to confirm that binding of p42^{IP4} to α -tubulin also occurs *in vivo*, we performed co-immunoprecipitation experiments. We found that p42^{IP4} could be specifically co-immunoprecipitated together with α -tubulin from RBM (Fig. 3.4.3. C).

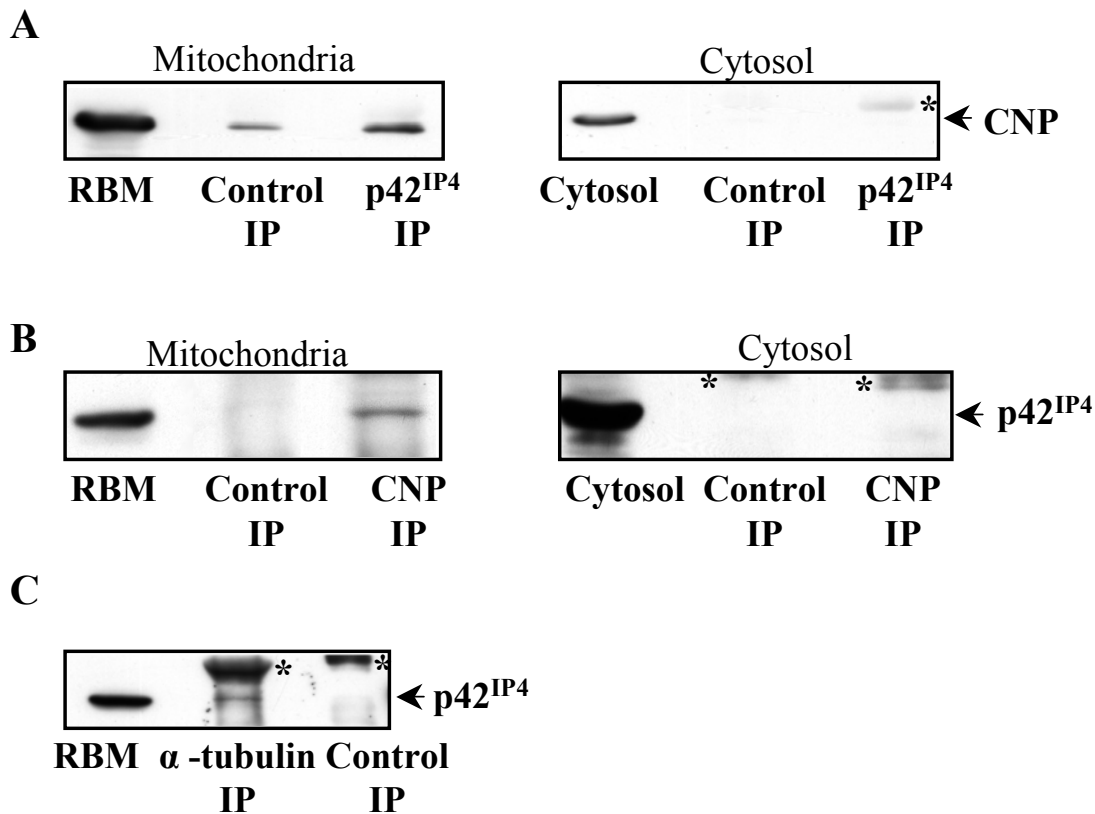


Fig. 3.4.3. In vivo interaction of p42^{IP4} with CNP and α -tubulin in RBM.

(A) Mitochondrial lysate from RBM or cytosol were immunoprecipitated (IP) with control rabbit IgG antibody or anti-p42^{IP4} antibody, and CNP was visualized in the precipitates and mitochondrial or cytosolic fractions by SDS-PAGE and immunoblotting with anti-CNP antibody. Here and in the following parts of the figure, the bands marked by (*) represent IgG heavy chains. (B) Mitochondrial or cytosolic fractions were immunoprecipitated with isotype-specific control antibody or anti-CNP antibody, and p42^{IP4} was detected in the precipitates and mitochondrial lysate by SDS-PAGE and immunoblotting using anti-p42^{IP4} antibody. (C) RBM lysates were immunoprecipitated with anti- α -tubulin antibody or isotype-specific control antibody and p42^{IP4} was visualized in the precipitates and mitochondrial lysate by SDS-PAGE and immunoblotting with anti-p42^{IP4} antibody. For all experiments, 2 mg of protein of mitochondrial or cytosolic fractions were used for IP. Experiments were repeated three times with similar results.

3.4.4 CNP interacts with α -tubulin *in vivo*

Since CNP is known to serve as a membrane anchor for tubulin (Bifulco et al., 2002), we also investigated the possible physical interaction of CNP and α -tubulin in RBM by co-immunoprecipitation study. As shown in Fig. 3.4.4. (I), α -tubulin was found in the precipitate using the CNP antibody. Vice versa, CNP was observed in the α -tubulin antibody immunoprecipitate, but CNP was not detected in that with the control IgG (Fig. 3.4.4., II). Altogether, these results indicate that there is *in vivo* formation of a complex between p42^{IP4}, CNP and α -tubulin in rat brain mitochondria.

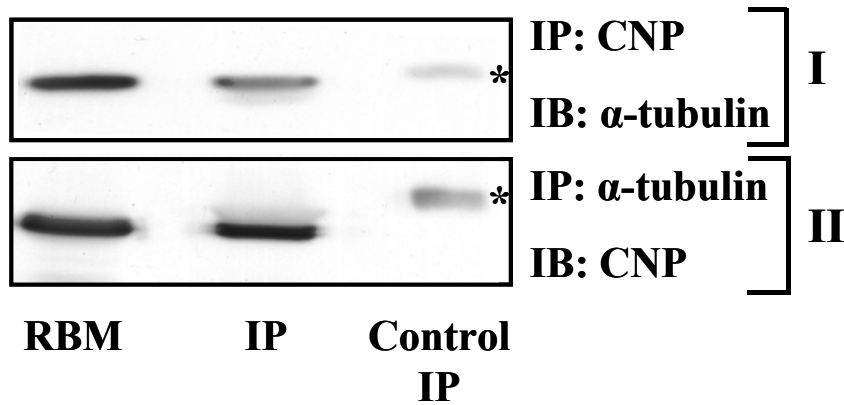


Fig. 3.4.4. In vivo interaction between CNP and α -tubulin in RBM

(I) RBM lysates (2 mg of protein) were immunoprecipitated with anti-CNP antibody (IP) or isotype-specific control antibody (control IP). α -Tubulin was visualized in the precipitates and mitochondrial lysate by immunoblotting (IB) with anti- α -tubulin antibody. Here and in the part II of the figure, the band marked by (*) represents IgG heavy chain (II) The lysates of RBM were immunoprecipitated with anti- α -tubulin antibody (IP) or isotype-specific control antibody (control IP), and CNP was detected in the precipitates and mitochondrial lysate by SDS-PAGE and immunoblot (IB) using anti-CNP antibody. Experiments were repeated three times with similar results.

3.5. Mitochondrial localization of CNP

3.5.1 CNP localization in sub-mitochondrial fractions of RBM

CNP was found to be located in mitochondria (McFerran and Burgoyne, 1997; Lee et al., 2006; Wu et al., 2006). We have shown here that CNP is localized in RBM (Fig. 3.4.1). However, there are no data on the function of CNP in mitochondria. At first we examined the localization of CNP in membrane fractions of RBM, such as mitoplasts (the inner membrane with matrix) and outer membranes. As shown in Fig. 3.5.1., CNP was found in both fractions. The fractions tested were also stained for SOD 2 (marker for mitoplasts) and for VDAC (marker for outer membranes). The faint staining of mitoplasts with VDAC antibodies revealing the presence of small amounts of VDAC in the mitoplast fraction can be explained by the presence of contact sites in the mitoplast that usually contain VDAC. SOD 2 was found mainly in mitoplasts and only a small trace amount of SOD 2 was detected in the outer membranes.

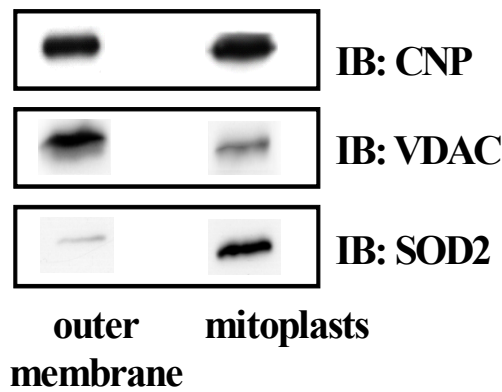


Fig. 3.5.1. CNP localization in sub-mitochondrial fraction

Isolated RBM were sub-fractionated, as described in Materials and Methods. Isolated outer membranes and mitoplasts were separated by electrophoresis in 12.5% SDS-PAGE (20 µg of protein per lane) with following immunoblotting (IB). The membrane was probed with CNP antibody. The same membranes were stained with antibodies for the compartment-specific proteins voltage-dependent anion channel (VDAC) and Mn-superoxide dismutase (SOD2), respectively.

3.5.2 CNP interaction with ANT and VDAC

The discovery of CNP in the inner and outer membranes forced us to look for CNP-interacting proteins within contact sites. ANT and VDAC are considered to be main regulators of the PTP complex, which comprises components in the inner as well as in the outer mitochondrial membrane. Therefore, we proposed interaction between these proteins and CNP. Thus, we performed immunoprecipitation of CNP, and the precipitate was analyzed by Western blot using ANT antibodies and VDAC antibodies. As shown in Fig. 3.5.2., the CNP antibodies immunoprecipitate contained immuno-reactive bands for ANT and VDAC antibodies. The immuno-reactive bands were not observed in the immunoprecipitate obtained with isotype-specific control antibodies. Co-immunoprecipitation of CNP specifically with ANT and VDAC was confirmed by immunostaining with SOD2 antibody. The results obtained indicate the interaction of CNP with regulatory components of PTP.

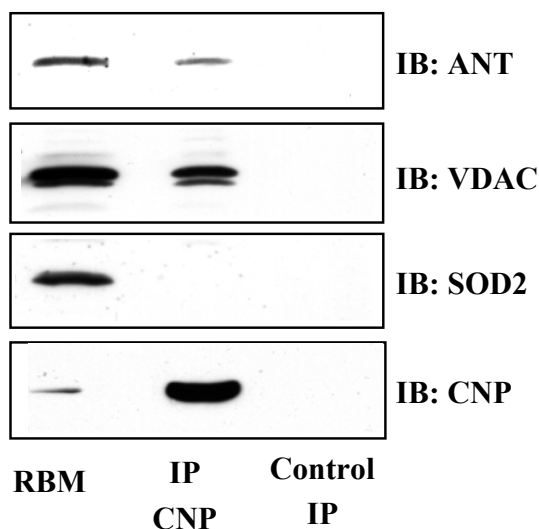


Fig. 3.5.2. CNP interaction with regulators of the PTP complex, ANT and VDAC.

Co-immunoprecipitation of CNP with ANT and VDAC. Experimental procedures are described in Materials and Methods. The lysates of RBM (2% of RBM lysate used for the IP experiments) and RBM immunoprecipitates with monoclonal CNP Ab (IP CNP), and with isotype-specific control antibody (control IP) were visualized by immunoblotting (IB) with ANT antibody, or with VDAC antibody. The same membranes were stained with SOD2 Ab and with polyclonal CNP Ab to show the specificity of co-immunoprecipitation and immunoprecipitation, respectively. Experiments were repeated three times with similar results.

3.6. CNP is involved in regulation of mitochondrial Ca²⁺

3.6.1 Influence of Ca²⁺-induced PTP on CNP activity in RBM

CNP activity was revealed in rat liver mitochondria, specifically in the outer and inner mitochondrial membranes (Dreiling et al., 1981). To investigate whether CNP activity might be changed during Ca²⁺-induced PTP opening, we used CNP enzyme activity assay published before (Bradbury and Thompson, 1984). Determination of the enzymatic CNP activity in isolated RBM after SDS-PAGE and Western blot on nitrocellulose membrane was performed. A suspension of purified RBM was added to the incubation medium in the chamber with installed electrodes to measure PTP development induced by threshold Ca²⁺ load. The samples were taken for CNP enzyme activity assay from the chamber before and after Ca²⁺-induced PTP. The enzymatic activity was decreased in the presence of threshold Ca²⁺ load as shown in Fig. 3.6.1., A and B. However, equal levels of CNP in RBM were found both in control condition and after Ca²⁺ threshold loading (Fig. 3.6.1., C and D).

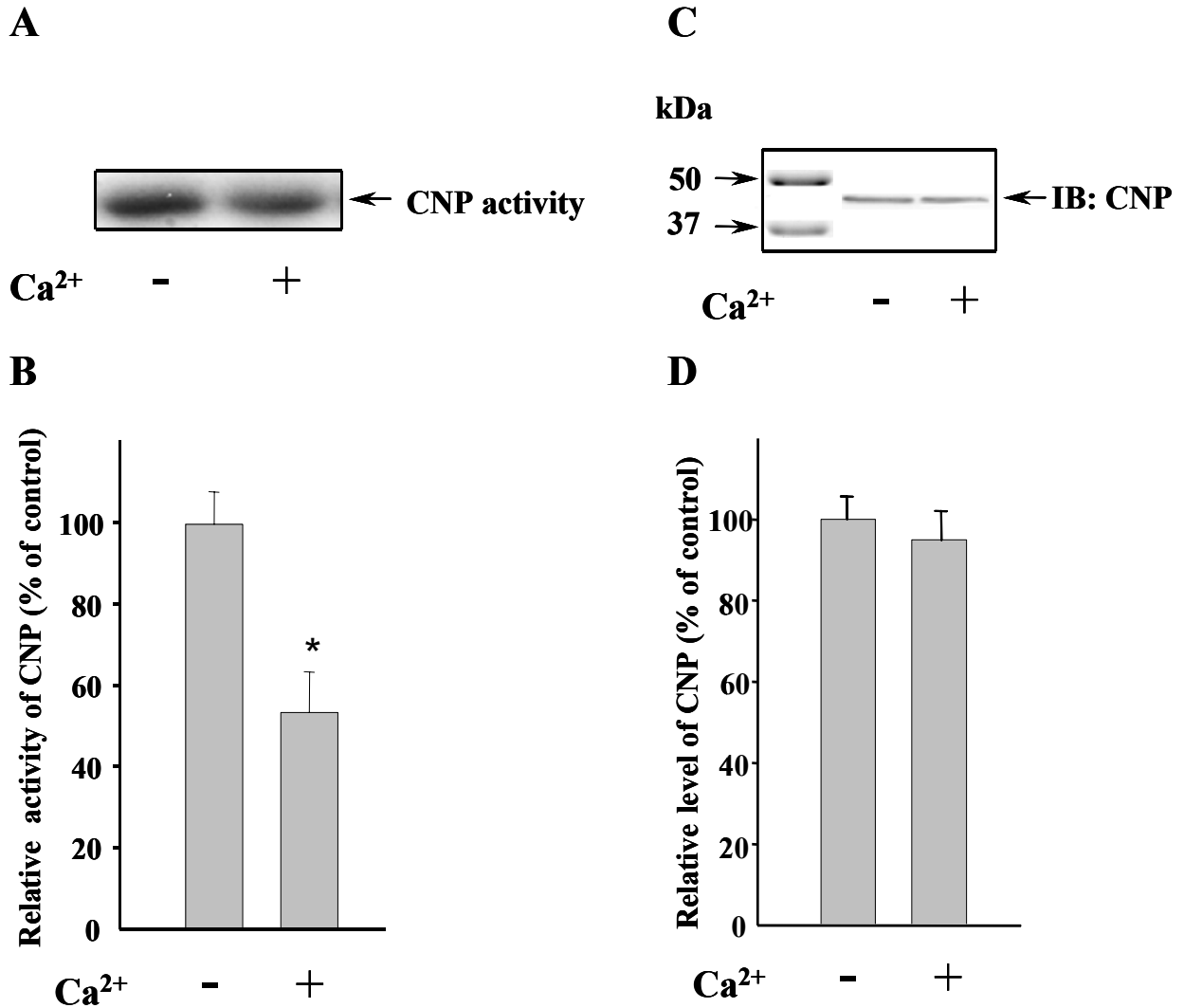


Fig. 3.6.1. Decrease of CNP activity in RBM under Ca²⁺-induced PTP

Detection of CNP activity (see Methods) in RBM is shown under control conditions and in the presence of threshold Ca²⁺ in the medium. (A) Detection of CNP activity on membrane, (B) Relative level of CNP activity under control conditions and in RBM loaded with threshold Ca²⁺. OD in control was taken as 100%. (C) Detection of CNP protein level by immunoblotting (IB) with monoclonal CNP Ab on the same membrane in control (in the absence of Ca²⁺ in the medium) or in the presence of threshold Ca²⁺ concentration. (D) Relative levels of CNP protein under control conditions and in Ca²⁺ overloaded RBM. Values represent the mean ± SD from three independent experiments. **p* < 0.05.

3.6.2 Effect of CNP knock-down on Ca²⁺-induced PTP

To obtain direct evidence supporting the involvement of CNP in Ca²⁺-induced PTP functioning in mitochondria, RNA interference studies were carried out. We studied the question of whether the CNP content was related to the induction of PTP. At first, we tested the expression of CNP in different types of cultured cells, such as human embryonic kidney HEK293, mouse neuroblastoma N2A and the rat oligodendrocyte line OLN93. As shown in Fig. 3.6.2. A, endogenous expression of CNP detected with the CNP Ab was highest in the

OLN93 cells. Thus, OLN93 cells were chosen for transfection with siRNA targeting CNP. Non-targeting scrambled siRNA served as a control. 48 h after transfection, the level of CNP expression was assayed by Western blot.

Transfection with CNP-targeting siRNA significantly reduced the CNP protein expression, as measured in total OLN93 cell lysate (Fig. 3.6.2. B). Next, mitochondria were isolated from OLN93 wild type cells as well as from CNP knock-down OLN93 cells. Scrambled siRNA did not affect CNP expression. In mitochondria isolated from CNP knock-down OLN93 cells the level of CNP was reduced to about 20% of control level (Fig. 3.6.2. C). Reduction of CNP expression in mitochondria correlated with decreased enzymatic CNP activity (Fig. 3.6.2. D). However, there was no effect on mitochondria isolated from OLN93 cells transfected with scrambled siRNA

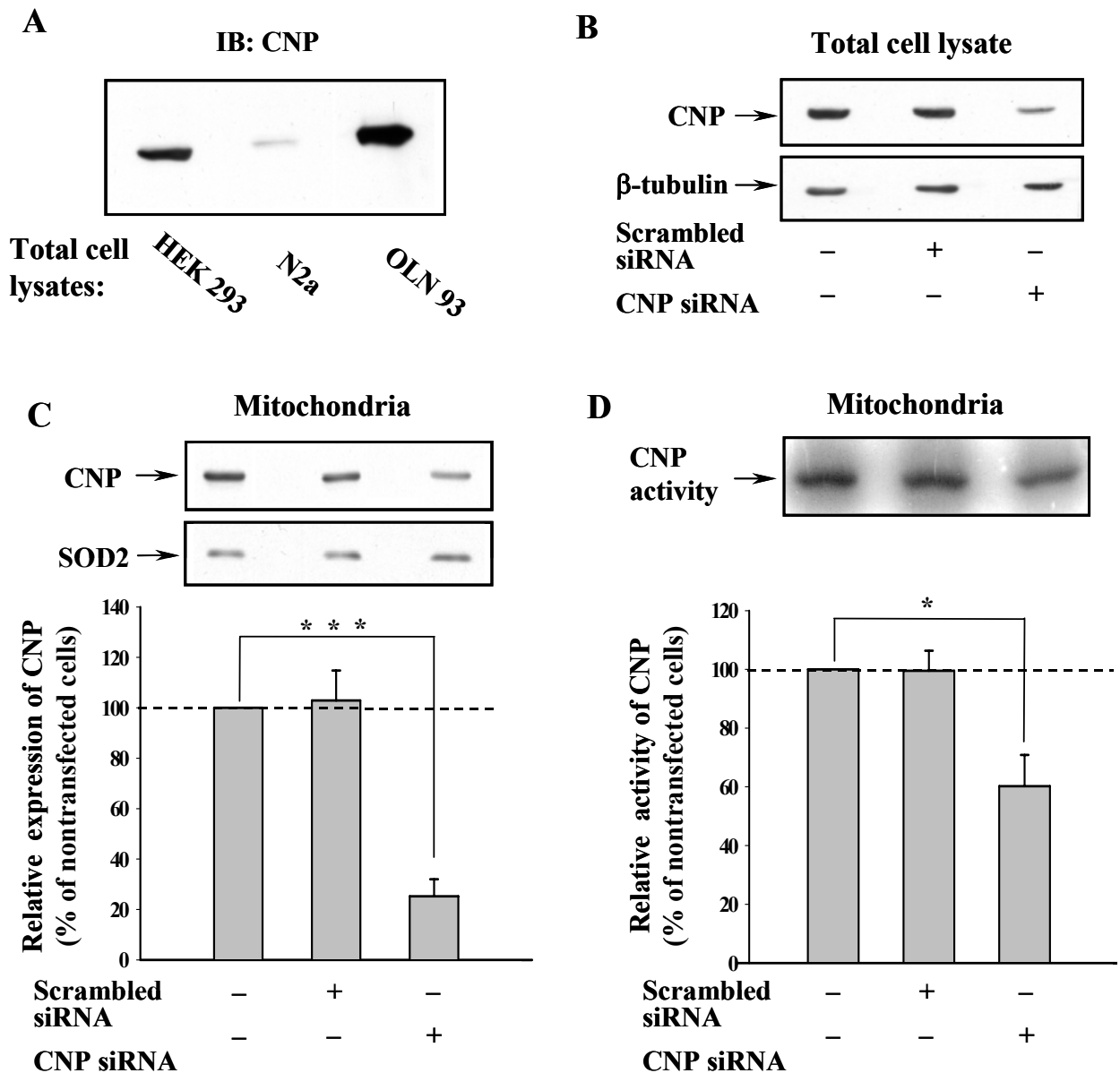


Fig. 3.6.2. CNP protein level in different types of cultured cells. CNP protein level and enzymatic activity in OLN93 mitochondria and OLN93 cells downregulated by siRNA.

(A) Endogenous expression of CNP protein in HEK 293, N2a and OLN 93 was evaluated by Western blotting, as described in Materials and methods. Experiments were repeated three times with similar results. Twenty-five μ g of total cell lysates were loaded. (B) OLN93 cells were transfected with either 50 nM scrambled siRNA (control siRNA) or CNP siRNAs. At 48 h after transfection, CNP protein level in total cell lysates was determined by Western blot analysis. Representative data from three independent experiments are given, and β -tubulin I served as control for specificity of knock-down. (C) OLN93 cells were transfected with either CNP siRNAs (50 nM) or scrambled siRNA (50 nM), after 48 h mitochondria were isolated. The reduction of CNP expression in mitochondria was evaluated by Western blotting. CNP and SOD2 protein bands were quantified by densitometry. The histogram shows relative units as ratio of CNP to SOD2. Mitochondria isolated from non-transfected OLN93 cells were used as reference and assigned the value of 100%. Values represent the mean \pm SD from three independent experiments. *** $p < 0.001$ (D) CNP activity in mitochondria isolated from OLN93 cells, transfected with siRNA or non-transfected, was detected, as described in Materials and methods. The activity of CNP in mitochondria isolated from non-transfected OLN93 cells was taken as 100%. Values represent the mean \pm SD from three independent experiments. * $p < 0.05$.

To investigate whether the reduction in CNP level in mitochondria could influence the Ca^{2+} -induced PTP opening, we measured the parameters of mitochondria isolated from wild type OLN93 cells, scrambled siRNA-treated OLN93 cells as well as cells, transfected with siRNA targeting CNP, as described above.

Fig. 3.6.3. A shows that threshold Ca^{2+} concentration in mitochondria isolated from wild type OLN93 cells was achieved after four additions of Ca^{2+} (70 nanomoles of Ca^{2+} per mg of protein each), giving a threshold Ca^{2+} for OLN93 mitochondria of 280 nanomoles per mg of protein in the given experiment. A similar threshold was found in mitochondria isolated from scrambled siRNA-treated OLN93 cells (Fig.3.6.3. B). Mitochondria isolated from CNP knock-down OLN93 cells released Ca^{2+} after the third addition (also 70 nanomoles of Ca^{2+} per mg of protein each), yielding a lower threshold calcium concentration which was equal to 210 nanomoles Ca^{2+} per mg of protein (Fig. 3.6.3. C).

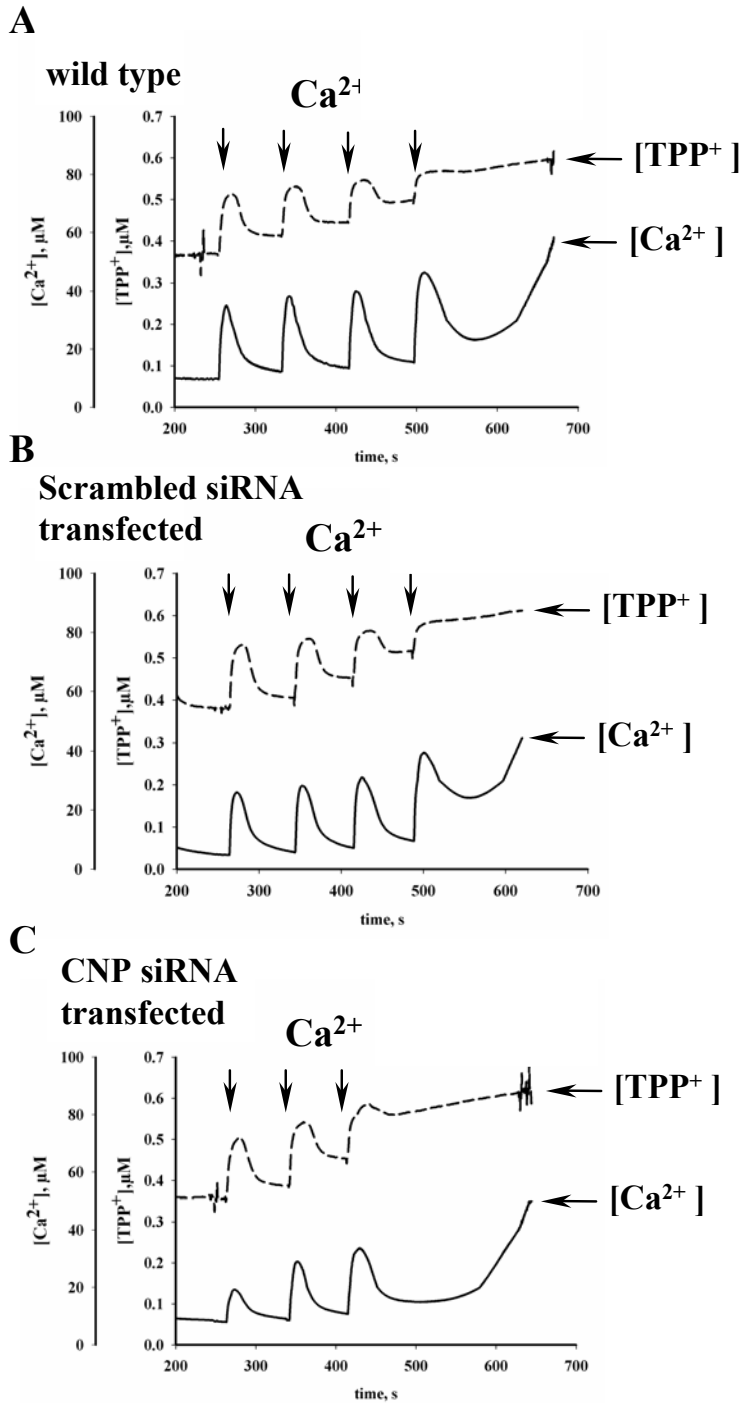


Fig.3.6.3. Reduction of CNP expression facilitates Ca^{2+} -induced PTP opening in mitochondria from OLN93 cells

Mitochondria isolated from wild type OLN93 cells (A) from scrambled siRNA-transfected OLN93 cells (B) and from CNP siRNA-transfected OLN93 cells (C) were incubated in the open chamber, as described in Materials and Methods. Changes of Ca^{2+} concentration in the incubation medium and of mitochondrial membrane potential are shown. The time scale represents the time after OLN93 mitochondria were added to the chamber. Ca^{2+} arrows show additions of 70 nanomoles of Ca^{2+} per mg of protein

The average data on Ca^{2+} -induced PTP opening in mitochondria isolated from wild type and CNP knock-down cells are shown in Fig. 3.6.4. No noticeable changes in Ca^{2+} influx

rate were observed in all kinds of isolated mitochondria. However, a reduced Ca^{2+} capacity and lag time were found for CNP knock-down mitochondria. These results demonstrate that reduction of CNP expression facilitates Ca^{2+} -induced PTP opening in mitochondria.

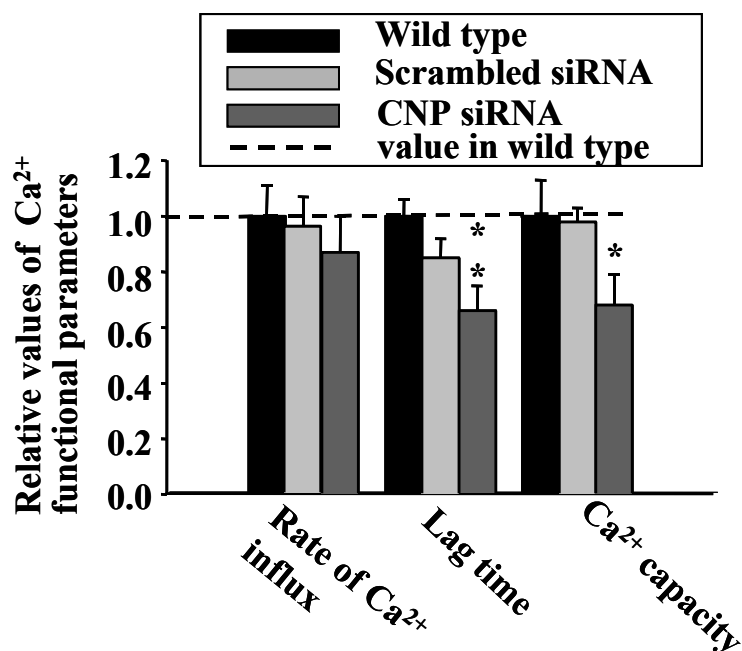


Fig.3.6.4. Influence of CNP knock-down on mitochondrial functional parameters at Ca^{2+} -induced PTP opening

After loading with Ca^{2+} to induce PTP opening, the relative values of mitochondrial Ca^{2+} influx rate, lag time and Ca^{2+} capacity were evaluated as described above in Fig 3.3.5. Values represent the mean \pm SD from three independent experiments. The levels of functional parameters of mitochondria isolated from wild type OLN93 cells loaded with threshold Ca^{2+} were taken as 1.0 (control). * $p < 0.05$, ** $p < 0.01$, versus control.

3.6.3 Effects of CNP substrates, 2',3'-cAMP, 2',3'-cNADP, on mitochondrial functions

It is known that 2',3'-cAMP as well as 2',3'-cNADP are CNP substrates (Vogel and Thompson, 1988; Sprinkle, 1989). Therefore, we also studied the effect of the substrates of CNP on mitochondrial functions. At first, we assayed the influence of 2',3'-cAMP on RBM functions in the open recording chamber with installed electrodes, as described above. Fig. 3.6.5. demonstrates typical results on Ca^{2+} -induced PTP in RBM in the absence and in the presence of 5 μM 2',3'-cAMP. In control RBM (Fig. 3.6.5. A), Ca^{2+} efflux was activated by two Ca^{2+} additions (80 nanomoles of Ca^{2+} per mg of protein). After the second, threshold Ca^{2+} addition the oxygen consumption rate returned to the resting state and added Ca^{2+} was almost fully accumulated. Subsequent Ca^{2+} efflux and activation of oxygen consumption indicated initiation of PTP opening that was observed after a lag time of about 3 min. Ca^{2+} efflux from

the mitochondrial matrix and membrane potential dissipation were fully developed after 6 min. In RBM treated with 5 μM 2',3'-cAMP (Fig. 3.6.5. B), PTP opening was accelerated. After the second Ca^{2+} addition the oxygen consumption rate did not return fully to the resting state and Ca^{2+} -induced Ca^{2+} efflux occurred faster with a very short lag time.

The diagram of Fig. 3.6.5. C represents the quantitative analysis showing the mean data from several experiments to demonstrate the action of 2',3'-cAMP on mitochondrial functions during Ca^{2+} -induced PTP opening. The lag time of PTP opening was decreased 2-fold, and the Ca^{2+} efflux rate was increased by 30%. These data demonstrate that 2',3'-cAMP was able to promote PTP opening.

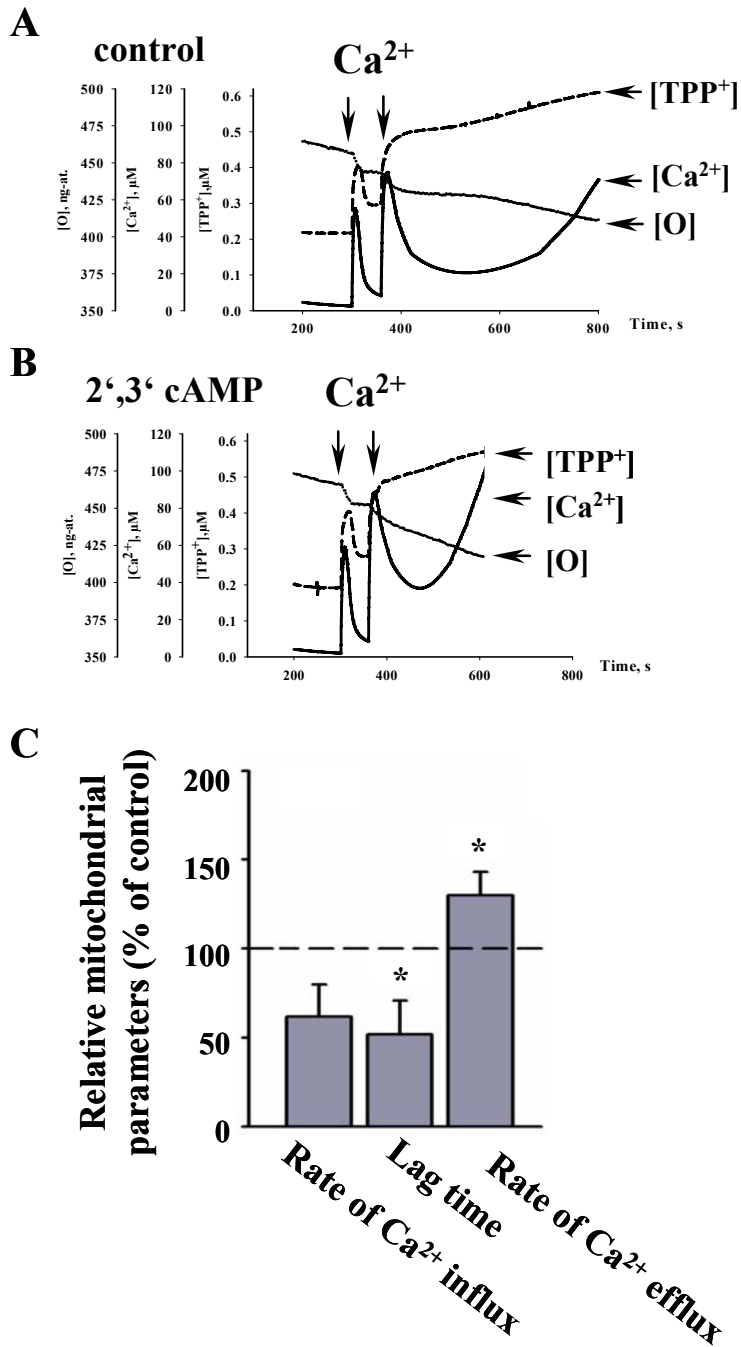


Fig. 3.6.5. Effect of 2',3'-cAMP on mitochondrial functions in RBM.

Isolated RBM (1.0 mg of protein per ml) were incubated in the electrode chamber in conditions described in Materials and Methods. Oxygen consumption rate, Ca^{2+} concentration in the incubation medium and changes in mitochondrial membrane potential are shown for control RBM (A), and RBM treated with 2',3'-cAMP (B). The time scale represents the time after RBM were added to the chamber. 2',3'-cAMP (5 μM) was applied 20 s after addition of RBM to the incubation medium. Two additions of Ca^{2+} (80 nanomoles of Ca^{2+} per mg of protein, each) shown by arrows, were applied to induce PTP opening. (C) Summary of effects of 2',3'-cAMP on RBM functions. The following parameters of Ca^{2+} -induced PTP opening were calculated from curves: Ca^{2+} influx rate, Ca^{2+} efflux rate and lag time for Ca^{2+} efflux. A detailed description of the parameter analysis is given in Fig 3.3.5. Values are given relative to the control value of 1.0 and represent the mean \pm SD from three independent experiments, * $p < 0.05$.

We also evaluated the effect of combined application of 2',3'-cAMP and CsA, as well as of 2',3'-cNADP and CsA. As shown in Fig. 3.6.6. A, with addition of CsA, inhibitor of PTP, no Ca²⁺-induced Ca²⁺ efflux was seen in the presence of 2',3'-cAMP. This inhibition of Ca²⁺ efflux by CsA supports the conclusion of participation of PTP.

Next, we checked whether 2',3'-cNADP, as well as 2',3'-cGMP were able to promote PTP opening. Figure 3.6.6. B demonstrates the effects of 2',3'-cNADP and 2',3'-cGMP used at the same concentration as 2',3'-cAMP (5 μM). In Fig. 3.6.6. B, trace 1 demonstrates Ca²⁺ fluxes in control RBM at threshold Ca²⁺ load. In the presence of 2',3'-cNADP, after the threshold Ca²⁺ load, a decreased rate of Ca²⁺ influx and a shortened lag time of Ca²⁺ efflux were seen (trace 2). The lag time in 2',3'-cNADP-treated RBM was about 2-times shorter than in control RBM (compare traces 1 and 2). No acceleration of Ca²⁺ efflux was observed in the presence of 2',3'-cGMP (trace 3). CsA was found to prevent the 2',3'-cNADP-induced stimulation of PTP opening (trace 4).

Fig. 3.6.6. C represents the average data obtained with 5 μM 2',3'-cNADP, 2',3'-cAMP and 2',3'-cGMP on the parameters of PTP opening, lag time and Ca²⁺ efflux. The effect of 2',3'-cAMP on PTP opening was not significant (data not shown), like that of 2',3'-cGMP. Thus, the efficiency of acceleration of Ca²⁺-induced PTP opening was decreasing in the following series: 2',3'-cAMP > 2',3'-cNADP >> 2',3'-cGMP, 2',3'-cAMP.

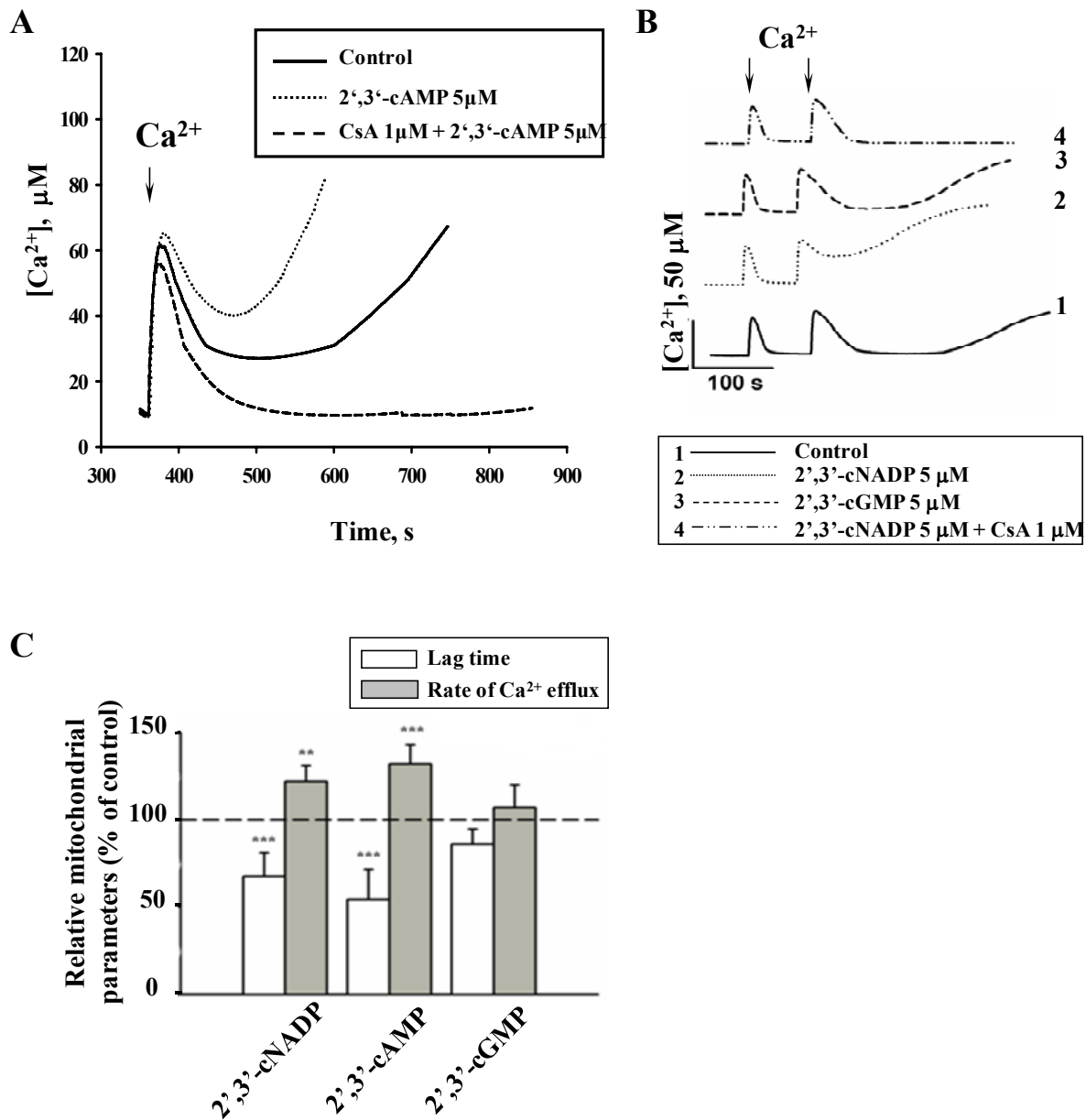


Fig. 3.6.6. Effect of 2', 3'-cAMP, 2',3'-cNADP and 2',3'-cGMP on Ca^{2+} -induced PTP opening in RBM.

(A) Effects of 2', 3'-cAMP and CsA on Ca^{2+} -induced PTP opening. Recordings represent Ca^{2+} fluxes in the presence of 2', 3'-cAMP (5 μM) and the combined application of 2', 3'-cAMP and CsA (1 μM). (B) Traces of the effect of 2',3'-cNADP (5 μM), in the absence and in the presence of CsA (1 μM), and 2',3'-cGMP (5 μM) on Ca^{2+} fluxes in RBM: trace 1 -control RBM, trace 2- RBM treated with 2',3'-cNADP, trace 3- RBM treated with 2',3'-cGMP, trace 4- RBM treated with CsA and 2',3'-cNADP. Experimental conditions as in Fig. 3.6.5. 2', 3'-cAMP, CsA, 2',3'-cNADP and 2',3'-cGMP were applied 20 s after the addition of RBM to the incubation medium. Arrows show the times at which Ca^{2+} (80 nanomoles of Ca^{2+} per mg of protein, each) was applied in the experiments. (C) Summary of effects of 5 μM 2',3'-cNADP, 5 μM 2',3'-cAMP, and 5 μM 2',3'-cGMP on Ca^{2+} -induced Ca^{2+} efflux and lag time in RBM. For analysis, of the parameters see Fig 3.3.5. Lag time before Ca^{2+} efflux was significantly decreased and Ca^{2+} efflux rate was significantly increased by 2',3'-cNADP and for 2',3'-cAMP, but not by 2',3'-cGMP. Values are given relative to the control value of 100 and represent the mean \pm SD from three independent experiments, * p < 0.05.

Induction of mitochondrial swelling is a prominent feature of PTP. Therefore, we examined the influence of 2',3'-cAMP and 2',3'-cNADP on Ca²⁺-induced swelling of isolated RBM to corroborate our hypothesis that the CNP substrates are involved in PTP regulation. Swelling was initiated by addition of Ca²⁺ to mitochondria incubated in standard medium (see Materials and Methods). Typical curves in Fig. 3.6.7. A demonstrate the decrease of light scattering at 540 nm, which indicates swelling. RBM swelling was accelerated in the presence of 5 μM 2',3'-cAMP or 5 μM 2',3'-cNADP.

We used the half time for reaching the maximum of the RBM swelling as characteristic parameter for quantification. The data in Fig. 3.6.7. B show that the swelling of RBM is significantly enhanced by 2',3'-cAMP and 2',3'-cNADP.

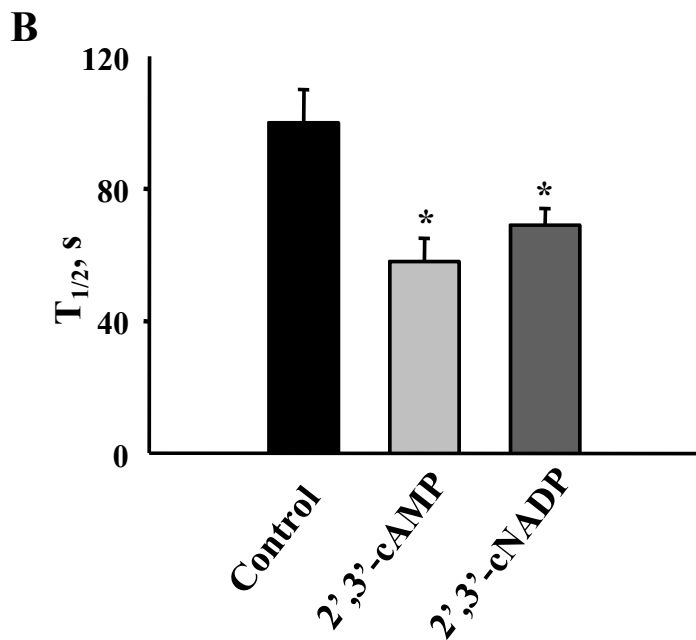
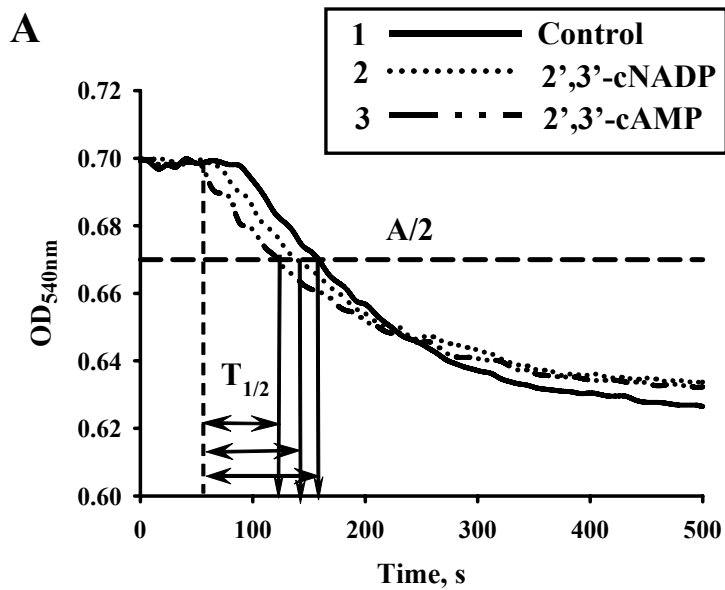


Fig. 3.6.7. Effect of 2',3'-cNADP, 2',3'-cAMP on RBM swelling

(A) Effect of 2',3'-cNADP, 2',3'-cAMP on RBM swelling. Swelling was initiated by addition of 100 μM Ca^{2+} to RBM incubated in standard medium (see Materials and Methods). Light scattering at 540 nm in RBM was measured. Trace 1- control- Ca^{2+} -induced swelling of RBM, trace 2 - effect of 5 μM 2',3'-cNADP, trace 3 - effect of 2',3'-cAMP. (B) Average results of half time for reaching the maximal swelling of RBM in the presence of 2',3'-cNADP and 2',3'-cAMP. Values are given relative to the control value of 100 and represent the mean \pm SD from three independent experiments, * $p < 0.05$, versus control

4. Discussion

4.1 The mechanism of mitochondrial Ca^{2+} -induced PTP opening remains unknown

Mitochondria are important regulators of cellular Ca^{2+} homeostasis, producers of ATP via oxidative phosphorylation, and regulators of cell death pathways (Sullivan et al., 2005). Mitochondria assist in maintaining Ca^{2+} homeostasis by sequestering and releasing Ca^{2+} . Isolated mitochondria in the presence of phosphate take up Ca^{2+} to a fixed capacity, in a membrane potential ($\Delta\Psi_m$)-dependent fashion (Chalmers and Nicholls, 2003). When the mitochondria become overloaded with Ca^{2+} , they undergo the cataclysmic mitochondrial permeability transition. Mitochondrial permeability transition is manifested as a sudden opening of a non-selective megachannel, PTP, in the inner mitochondrial membrane. The PTP opening increases the permeability to solutes with molecular mass up to 1500 Da in response to mitochondrial Ca^{2+} overload and/or oxidative stress (Bernardi, 1999; Halestrap, 2006). The Ca^{2+} -induced PTP opening is a complex process with many known inducers, modulators, and inhibitors. The PTP is a multi-protein complex formed in the contact sites between outer and inner membranes of mitochondria to increase the permeability of the inner membrane. Main events of PTP opening are collapse of the membrane potential, Ca^{2+} -induced Ca^{2+} efflux, induction of mitochondrial swelling and release of apoptotic factors (Bernardi, 1999; Halestrap et al., 2002; Zoratti et al., 2005). The quest for the pore identity has been ongoing for several decades. However, the PTP structure remains unknown (Juhaszova et al., 2008). Evidence has been accumulating that numerous signalling molecules and drugs affect the Ca^{2+} -induced PTP opening. Thus, it is important to explore fully the mechanism of mitochondrial Ca^{2+} -induced PTP opening and to search for new proteins involved in control of this complex process.

4.2 Known functions of p42^{IP4}

Different functions have been already proposed for p42^{IP4} . There were reports which showed the involvement of this protein in the activation of the mitogen-activated protein kinase cascade of the extracellular regulated kinase (Hayashi et al., 2006), in the ARF6 signalling pathway (Lawrence et al., 2005) or in the transcription factor activator protein-1 activation cascade (Chanda et al., 2003). p42^{IP4} was found to be involved in dendritic differentiation/synaptic plasticity and/or transport of PIP_3 -containing vesicles along axons to regulate neuronal cell polarity (Horiguchi et al., 2006; Moore et al., 2007). In neuronal cells,

p42^{IP4} regulates the actin cytoskeleton via ARF GAP-dependent and ARF GAP-independent mechanisms (Thacker et al., 2004; Venkateswarlu et al., 2004). p42^{IP4} has already been linked to short-term regulation of behavioural responses in rat brain (Reiser et al., 2004). Very interestingly, p42^{IP4} seems to be involved in neuronal diseases, since we found that p42^{IP4} is up-regulated in neurons in the brain of AD patients and is detected in AD plaques (Reiser and Bernstein, 2002, 2004). Although various functions of p42^{IP4} have been proposed, there were no data concerning a role of this protein related to mitochondria.

4.3 Novel localization and function of p42^{IP4}. Involvement of p42^{IP4} and its ligands in regulation of mitochondrial Ca²⁺-induced PTP opening

Previously, analysis of subcellular localization of the p42^{IP4} protein in non-neuronal CHO cells stably transfected with pcDNA-p42^{IP4} was performed. p42^{IP4} was found in membranes, cytosol, and nucleus (Sedehizade et al., 2002). In this study, we detected that p42^{IP4} is localized both in RBM and in mitochondria of the transfected cell lines CHO and N2a. Moreover, in mitochondria of CHO cells, p42^{IP4} was found predominantly at the inner membrane and in the intermembrane space of mitochondria, and to a lesser degree in the matrix and outer membrane. Such mitochondrial localization of the p42^{IP4} allowed us to suppose that p42^{IP4} might be involved in the regulation of mitochondrial Ca²⁺ transport mechanisms.

We used the mouse neuroblastoma N2a cells as an expression system as we have demonstrated that the N2a cells do endogenously express the p42^{IP4}. The neuronal nature of N2a cells and the endogenous expression of the p42^{IP4} make these cells an ideal system for studying the mitochondrial functions. Two approaches, where Ca²⁺ was added either in small or big bolus additions, were used to compare the ability of mitochondria to accumulate and retain Ca²⁺ before PTP opening. Study of the functional parameters of mitochondria isolated from N2a cells transfected with p42^{IP4} revealed that overexpression of p42^{IP4} accelerates Ca²⁺-induced PTP opening in mitochondria from these cells. In comparison with the mitochondria isolated from N2a cells transfected with p42^{IP4}, mitochondria from N2a wild type cells can accumulate significantly more Ca²⁺ before they undergo Ca²⁺-induced PTP. Thus, an important function of mitochondrial p42^{IP4} in neurons seems to be regulation of mitochondrial Ca²⁺ through PTP opening.

Moreover, in comparison with mitochondria from N2a wild type cells, mitochondria isolated from N2a cells transfected with p42^{IP4} have a lower membrane potential. This could cause p42^{IP4}-containing mitochondria to take up less Ca²⁺ and thus lead to destabilization.

It was found that CsA did not prevent PTP opening in mitochondria isolated from N2a cells. Tissue-specific differences in the nature of PTP induction are already well known. In liver mitochondria, CsA nearly completely inhibits PTP induction, whereas in nonsynaptosomal brain mitochondria CsA has very modest effects (Kristal et al., 2000). It was also reported that only in the presence of a low concentration of exogenous ADP, CsA fully inhibits PTP in brain mitochondria exposed to Ca²⁺ (Hansson et al., 2004). Thus, the inhibition of the PTP by CsA depends on the model, which is used.

Mitochondria isolated from brain represent a heterogeneous mixture from different cell types (Bambrick et al., 2006). Therefore, they have differing sensitivities to Ca²⁺ as inducer of PTP and to CsA as inhibitor of the PTP. It was shown that CsA increased the calcium uptake capacity of mitochondria isolated from astrocytes, while it had no effect on PTP in neuronal mitochondria. It was also observed that the astrocytes had a maximal mitochondrial calcium uptake capacity, which was twice as high as that of the neurons (Bambrick et al., 2006). Moreover, a difference in Ca²⁺ accumulation between synaptic and nonsynaptic mitochondria was shown (Brown et al., 2006). The reduced Ca²⁺ buffering capacity of synaptic mitochondria and their increased susceptibility to undergo PTP was proposed to contribute to synapse and neurite degeneration (Brown et al., 2006). Thus, the acceleration of Ca²⁺-induced PTP opening by overexpression of p42^{IP4}, which we describe here, may have pathological implications for neurons in the brain.

The function of “higher order” inositol phosphates, such as the ligand of p42^{IP4}, IP₄, in biological processes, has remained greatly a mystery (Miller et al., 2008). Early studies addressing the function of IP₄ examined Ca²⁺ responses, as it was initially thought that IP₃ 3-kinase functioned to regulate strictly the intracellular concentration of IP₃ by simply converting it to IP₄. Studies examining the function of IP₄ in endothelial and neuroblastoma cells demonstrated that IP₄ could directly activate Ca²⁺ channels in the plasma membrane (Luckhoff and Clapham, 1992; Tsubokawa et al., 1996; Szinyei et al., 1999). It was also described that IP₄ inhibited IP₃-activated Ca²⁺ permeable ion channels, which were purified from liver plasma membrane (Mayrleitner et al., 1995).

Other functions for IP₄ include the direct competitive inhibition of inositol phosphate 5-phosphatase in a mast cell line, thus preventing the conversion of IP₃ to IP₂ and facilitating store-operated Ca²⁺ entry (Hermosura et al., 2000). However, it was demonstrated in the same

report that at high levels, IP₄ inhibits IP₃ receptors. The net effect was an inhibition of the Ca²⁺ signal. The discrepancies between some of these reports may be explained by the differences in the role for IP₄ in specific cell types as well as the strength of IP₃ receptor stimulation (Miller et al., 2008).

Very recently a new function of IP₄ as a negative regulator of Ca²⁺ was described in immune B cells (Miller et al., 2008). While IP₃ was known to regulate positively ER-mediated Ca²⁺ release upon binding to the IP₃ receptor on the ER membrane, IP₄ possessed inhibitory functions. IP₄ inhibited store-operated calcium channels. IP₄ also negatively regulated the localization of signalling molecules in immune cells. Interestingly, it was proposed that IP₄ mediated its inhibitory function by competing with PIP₃ for PH domain-containing proteins, and p42^{IP4} is one of these proteins (Miller et al., 2008).

Moreover, the mechanism of feedback inhibition for regulating Ca²⁺ uptake was suggested to be a general for lymphocytes, as IP₄ was also capable of inhibiting store-operated Ca²⁺ channels in thymocytes, and peripheral T cells (Miller et al., 2007).

In this study, we have demonstrated the influence of p42^{IP4} ligands, IP₄ and PIP₃, on functions of mitochondria isolated from N2a cells under Ca²⁺-induced PTP opening. To check the possible influence of binding of the ligands to p42^{IP4} on mitochondrial functions, we compared the functional parameters of mitochondria, which were isolated from N2a wild type cells, or from cells transfected with p42^{IP4}, or transfected with empty vector. The Ca²⁺ influx rate, lag time, and Ca²⁺ capacity of mitochondria were reduced in the presence of PIP₃ or IP₄ in comparison with nontreated mitochondria from all three kinds of cells. The maximal decrease was observed in the lag time. Addition of IP₄ significantly shortened the lag time in comparison with nontreated mitochondria from all three kinds of cells. Also in the presence of PIP₃, the reduction of the rate of Ca²⁺ influx, lag time and Ca²⁺ capacity was considerable for mitochondria isolated from all three kinds of cells in comparison with nontreated mitochondria

Therefore, for the first time we have shown that IP₄ as well as PIP₃ destabilize mitochondria during Ca²⁺-induced PTP opening. However, the action of the p42^{IP4} ligands on PTP opening was found to be independent of the overexpression of p42^{IP4}.

4.4 Known functions of CNP

The majority of studies investigating the role of CNP were focused exclusively on the expression of CNP in oligodendrocytes and Schwann cells and the involvement of CNP in myelinogenesis. However, there is increasing evidence showing that this enzyme has possible

functions in mitochondria. Thus, CNP activity was revealed in rat liver mitochondria, specifically in the outer and inner mitochondrial membranes (Dreiling et al., 1981). CNP was found to be localized in mitochondria of adrenal medullary chromaffin cell cultures and in mitochondria of amoeboid microglial cells (McFerran and Burgoyne, 1997; Wu et al., 2006).

The *in vivo* biological roles of CNP are still largely unknown, and the possible function of CNP in mitochondria is even more enigmatic. Two CNP isoforms, CNP1 (46 kDa) and CNP2 (48 kDa), were found which are encoded by a single gene (Kurihara et al., 1992; Gravel et al., 1994). The two isoforms are due to the presence of two alternative translation start sites (O'Neill et al., 1997). Several posttranslational modifications of CNP, such as phosphorylation, isoprenylation and acylation, with unclear functional consequences are known (Vogel and Thompson, 1988; Sprinkle, 1989; Agrawal et al., 1990a, 1990b; De Angelis and Braun, 1994; Stricker et al., 1994). A recent study of transfected oligodendrocyte cells (OLN93), overexpressing CNP1 and CNP2 showed that CNP2 can be translocated to mitochondria due to the presence of a mitochondrial targeting signal at the N-terminus which is cleaved upon import into mitochondria (Lee et al., 2006). The translocation of CNP2 is regulated via phosphorylation of the targeting signal by PKC (Lee et al., 2006). Nevertheless, the definite functions of CNP in mitochondria were not understood.

4.5 Novel function of CNP. Involvement of CNP and its substrates in regulation of mitochondrial Ca²⁺-induced PTP opening

We have found that CNP localized in the inner and outer membranes of rat brain mitochondria. Such CNP localization in mitochondria indicates its possible concentration in contact sites, where the PTP complex is located. The PTP was previously considered as a complex formed by the association of ANT of the inner membrane and CyP-D of the matrix, the VDAC and PBR localized in the outer membrane and additional proteins such, as proteins of the Bcl-2 family, creatine kinase and hexokinase.

The two *Ant* genes in mice were knocked out in hepatocytes (Kokoszka et al., 2004). This led to a number of secondary responses such as the upregulation of Cyt c, the down-regulation of the uncoupling protein 2, the stimulation of the respiratory rate and an increased mitochondrial membrane potential. Experiments on the PTP revealed that its sensitivity for Ca²⁺ was reduced. Also, ANT ligands such as atractyloside and ADP had no modifying effect on the PTP anymore. Since PTP could still be induced, the authors of this study suggested that ANT is not essential for the PTP (Kokoszka et al., 2004). Nevertheless, the fact that the

deletion of the two mouse ANT forms led to only a minor effect on the PTP was surprising and caused several different interpretations. The first is a doubt that *Ant-1/2*-deficient tissues are indeed devoid of ANT activity. This possibility is supported by the recent discovery of ANT4 (Rodic et al., 2005). An alternative explanation is that other carriers of this gene family might substitute for ANT (Halestrap, 2004). Although recent experiments with mitochondria from *Ant*- and *Vdac*-deficient mice demonstrated that both proteins are not indispensable structural elements of the unselective pore, ANT and VDAC could still be considered as regulators or modulators of PTP (Baines et al., 2007; Juhaszova et al., 2008). We have shown the interaction of CNP with ANT and VDAC, which was the first indication of the involvement of CNP in regulation of mitochondrial PTP.

Furthermore, we revealed that the enzymatic activity of CNP in RBM was reduced under PTP opening, whereas the levels of CNP protein detected before and after PTP opening were unchanged. Earlier, CNP activity was discovered in rat liver mitochondria (Dreiling et al., 1981) and later, in mitochondria in cultured adrenal cells (McFerran and Burgoyne, 1997). The finding that CNP activity in RBM decreased under Ca^{2+} -induced PTP opening provided us additional evidence for CNP functioning in mitochondria.

The functional importance of CNP in mitochondria was unequivocally confirmed by RNA interference experiments using OLN93 cells. These cells contain a high endogenous level of CNP. OLN93 cells were transfected with siRNA targeting CNP. As a result, the endogenous CNP protein expression level was reduced. Mitochondria isolated from CNP knock-down OLN93 cells possessed reduced level of CNP and decreased enzymatic CNP activity in comparison with mitochondria isolated from wild type OLN93 cells. Mitochondria isolated from scrambled non-targeting siRNA OLN93 cells served as a control. The most important finding in this context is that lowered level of CNP and reduced CNP activity correlated with facilitation of Ca^{2+} -induced PTP opening. These results allow us to suppose that the CNP level and activity in mitochondria are important for the regulation of PTP development.

CNP hydrolyzes 2',3'-cyclic nucleotides and oligonucleotides containing a 2',3'-cyclic terminus to produce 2'-nucleotides. The influence of the CNP substrates, 2',3'-cyclic nucleotides, on the mitochondrial function has not yet been investigated. In our experiments, we for the first time studied the effect of the CNP substrates on mitochondrial functions. We found that 2',3'-cAMP and 2',3'-cNADP did not affect Ca^{2+} transport and other functions in mitochondria having the PTP closed. However, 2',3'-cAMP and 2',3'-cNADP enhanced PTP opening after Ca^{2+} loading. This effect was seen on Ca^{2+} transport, membrane potential

dissipation and swelling of rat brain mitochondria. Both CNP substrates were able to shorten the lag time and to increase the rate of Ca^{2+} efflux from rat brain mitochondria during Ca^{2+} -induced PTP opening. 2',3'-cGMP and 2',3'-cCMP were not effective in induction of Ca^{2+} -induced PTP opening. The potency sequence of 2',3'-cyclic nucleotides to stimulate Ca^{2+} -induced PTP opening in RBM was determined as: 2',3'-cAMP > 2',3'-cNADP >> 2',3'-cGMP, 2',3'-cCMP. Interestingly, the weak capacity of 2',3'-cCMP to activate Ca^{2+} -induced PTP opening is in parallel with the earlier reported lower capacity of CNP to hydrolyze 2',3'-cCMP compared to the cAMP analog (Drummond et al., 1962).

The enzymatic CNP activity was decreased under Ca^{2+} -induced PTP opening. Hence, hydrolysis of 2',3'-cyclic nucleotides was prevented. Consequently, this increases the efficiency of the action of 2',3'-cAMP and 2',3'-cNADP on stimulation of the Ca^{2+} -induced PTP opening in a feedback cycle. Therefore, we propose that in living cells inhibition of CNP activity under Ca^{2+} -induced PTP opening in mitochondria contributes to elevating the 2',3'-cyclic nucleotides level. An important question is still, what are the sources of the 2',3'-cyclic nucleotides in mitochondria. Oligonucleotides containing a 2',3'-cyclic terminus could be generated as 2',3'-cyclic intermediate in the enzymatic degradation of RNA as well as in processing and splicing reactions for mammalian RNA. On the other hand, we can suppose that at the conditions of our experiments, under threshold Ca^{2+} load the mitochondrial soluble adenylyl cyclase was activated by Ca^{2+} and 3',5'-cAMP was produced. 2',3'-cAMP could be created by transformation of the 3',5'-cyclic terminus to the 2',3'-cyclic one. This can occur in alkaline conditions, which are prevalent in mitochondria under threshold Ca^{2+} load.

Thus, CNP substrates, 2',3'-cAMP and 2',3'-cNADP, in turn seem to work as second messengers by promoting the mitochondrial PTP opening.

4.6 Hypothesis for functional importance of interaction between p42^{IP4}, CNP and α -tubulin in mitochondria.

Several protein interaction partners of p42^{IP4} were determined. Among these are protein kinases, such as casein kinase I (Dubois et al., 2001), and PKC (Zemlickova et al., 2003), several ARFs (Thacker et al., 2004; Venkateswarlu et al., 2004), F-actin (Thacker et al., 2004) and nucleolin (Dubois et al., 2003). More recently, further interesting protein interactions were reported for p42^{IP4}. Among these proteins were (i) the kinesin motor protein KIF13B/ GAKIN (Venkateswarlu et al., 2005; Horiguchi et al., 2006), (ii) the peptidase nardilysin, a N-arginine dibasic convertase (Stricker et al., 2006), and (iii) the Ran binding protein in microtubule-organizing centre, RanBPM (Haase et al., 2008). While a variety of

protein interaction partners of p42^{IP4} in different cellular compartments were determined, no proteins interacting with p42^{IP4} in mitochondria have been found so far.

In the present study, we demonstrated that p42^{IP4} is specifically associated with CNP and α -tubulin in mitochondrial and cytosolic fractions of rat brain by pull-down assay. Interestingly, the co-immunoprecipitation of p42^{IP4} and CNP was observed only in mitochondria but not in the cytosol. The co-immunoprecipitation can be taken as evidence for *in vivo* interaction between the respective proteins. Since technically it was not possible to show interaction all three proteins at the same time, therefore we demonstrated co-immunoprecipitation of p42^{IP4} with CNP, p42^{IP4} with α -tubulin, and CNP with α -tubulin in mitochondrial fraction. These co-immunoprecipitations led us to suggestion that *in vivo* complex formed between p42^{IP4}, CNP and α -tubulin in rat brain mitochondria.

CNP is one of the major proteins of myelin. Myelin-producing oligodendrocytes play an essential role in supporting normal neuronal functions of the mammalian central nervous system. *Cnpl*-null mice appeared to myelinate normally but suffered severe neurodegeneration from axonal loss with increasing age (Lappe-Siefke et al., 2003). Further analysis revealed that CNP deficiency caused major abnormalities to the structure of the paranodal loops of the optic nerves of mice as early as 3 months of age, which is before any visible onset of axonal degeneration (Rasband et al., 2005). Paranodal loops contact the axolemma for axon–glial signalling, which is critical for axonal integrity and organization (Salzer, 2003). Therefore, it was suggested that the loss of CNP from myelin disrupts axon–glial interactions which in turn causes many axons to degenerate (Rasband et al., 2005). Thus, in myelinating glia the function of CNP is crucial in maintaining axonal integrity. Moreover, expression of CNP in developing neuronal cells was revealed (Cho et al., 2003). These findings suggest significant contribution of CNP to the functioning of neurons.

Another protein that binds to p42^{IP4} is α -tubulin, protein belonging to MT. We hypothesize that an association between p42^{IP4}, CNP and α -tubulin in mitochondria can be implicated in the regulation of Ca²⁺ signalling by different cellular organelles. Fig. 4.1 shows our hypothesis based on present findings and data from the current literature.

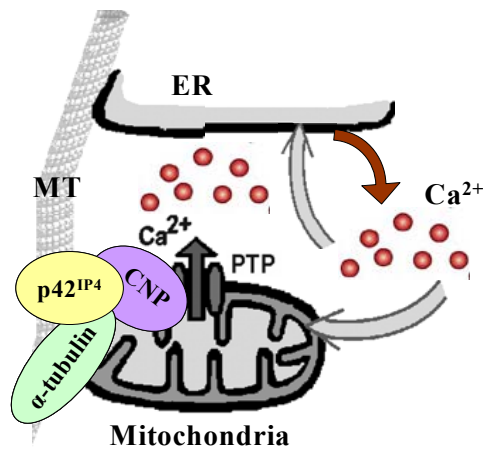


Fig. 4.1. Hypothesis for in vivo complex formation between $p42^{IP_4}$, α -tubulin and CNP in mitochondria and its possible involvement in intracellular regulation of Ca^{2+} signalling.

Mitochondria and ER take up cytoplasmic Ca^{2+} and can correspondingly release Ca^{2+} into the cytoplasm. MT, the self-assembly of α - and β -tubulin heterodimers, are additionally needed to keep ER and mitochondria together. For simplification of the figure, the second component of microtubules (MT), β -tubulin, is not shown. CNP interacts with regulatory components of PTP, VDAC and ANT, which are not shown here. α -Tubulin associates with CNP and VDAC. CNP interacts with α -tubulin and $p42^{IP_4}$ in mitochondria. $p42^{IP_4}$ binds to CNP and to α -tubulin in mitochondria. CNP and $p42^{IP_4}$ regulate the Ca^{2+} -induced opening of PTP. Complex formed between $p42^{IP_4}$, α -tubulin and CNP connects MT and mitochondria and possibly is involved in Ca^{2+} signalling between mitochondria and ER/cytosol through regulation of PTP. (Modified from (Mironov et al., 2005)).

Mitochondria and ER take up cytoplasmic Ca^{2+} and can correspondingly release Ca^{2+} into the cytoplasm. Indeed, a major functional interaction between mitochondria and the ER is the control of Ca^{2+} signalling. This is because Ca^{2+} exchange between the ER and mitochondria not only has a crucial role in regulating the physical interactions between the two organelles, but it also regulates a variety of physiological processes, including apoptosis and necrosis (Pizzo and Pozzan, 2007). Recently, a functional link between ER, Ca^{2+} and proapoptotic mitochondrial alterations was revealed. It was shown that ER stress results in the IP_3 receptor-mediated release of Ca^{2+} , which in turn causes mitochondrial membrane permeabilization. Thus, PTP opening was revealed to be required for ER stress-induced apoptosis (Deniaud et al., 2008).

MT, the self-assembly of α - and β -tubulin heterodimers, are additionally needed to keep ER and mitochondria together (Mironov et al., 2005). Close interactions of MT with mitochondria in living neurons and with isolated mitochondria were revealed. Moreover, the MT network was shown to play an important role in the maintenance of mitochondrial functions by regulating PTP opening and positioning of mitochondria close to the ER (Mironov et al., 2005). Coordination of basal cytoplasmic Ca^{2+} signalling between mitochondria and ER by MT can control neuronal functions. Among these functions, there were the temporal integration of cytoplasmic Ca^{2+} dynamics and long-term changes in Ca^{2+} that underlie synaptic plasticity (Levy et al., 2003; Loewenstein and Sompolinsky, 2003).

α -Tubulin was shown to be a component of mitochondrial membranes specifically interacting with the VDAC (Carre et al., 2002). VDAC mediates the complex interactions between mitochondria and other parts of the cell by transporting anions, cations, ATP, Ca^{2+} and metabolites. Thus, VDAC plays an important role in coordinating the communication between mitochondria and cytosol (Grimm and Brdiczka, 2007). Moreover, there were some indications that VDAC may be part of mitochondrial microdomains linking Ca^{2+} efflux from the ER to mitochondrial matrix Ca^{2+} influx, in itself a potent trigger of PTP (Szabadkai et al., 2006).

CNP interacts with regulatory components of PTP, VDAC and ANT. Thus, CNP and α -tubulin binding to each other also associate with PTP. p42^{IP4} binds to CNP and to α -tubulin in RBM. Therefore, the complex, which is formed by p42^{IP4} , CNP and α -tubulin, connects MT and mitochondria. Moreover, p42^{IP4} and CNP are involved in control of Ca^{2+} -induced PTP opening. Therefore, one of the important functions of this connection between MT and mitochondria could be the regulation of Ca^{2+} signalling between cellular organelles through regulation of PTP.

Thus, we hypothesize that in the brain p42^{IP4} possibly acts together with CNP and α -tubulin in order to regulate mitochondrial Ca^{2+} transport mechanisms. The reduction of mitochondrial Ca^{2+} buffering capacity induced by p42^{IP4} may increase the vulnerability of neurons to PTP and thereby contribute to processes leading to neurodegeneration.

This hypothesis could also be applied to AD development. Indeed, it was described that in neocortical areas of AD patients the neuronal expression of the protein p42^{IP4} is markedly increased, and the protein is associated with neuritic plaques (Reiser and Bernstein, 2002). Moreover, p42^{IP4} interacts with the protein kinase CK I α (Dubois et al., 2001), which hyperphosphorylates β -amyloid precursor protein in the brains of AD patients (Walter et al., 2000). Specific interaction of p42^{IP4} with nucleolin, another player in AD pathology, has also been revealed (Dubois et al., 2003). However, the significance of the increase in p42^{IP4} protein expression in terms of AD pathology is still unknown (Reiser and Bernstein, 2004). Our recent finding that nardilysin is an interacting partner for p42^{IP4} (Stricker et al., 2006) might also be of interest regarding the possible involvement of p42^{IP4} in AD pathology. Nardilysin enhances the cleavage of amyloid precursor protein by α -secretase through the activation of a disintegrin and metalloprotease proteases, which results in a decreased amount of amyloid- β peptide, the principal component of senile plaques in the brains of patients with AD (Hiraoka et al., 2007).

Involvement of CNP in AD was claimed in several studies. However, its role is still completely unclear. In AD patients, the activity of CNP was shown to be decreased in the hippocampus and putamen (Reinikainen et al., 1989). Another study showed a significant decrease in CNP protein in AD brain (Vlkolinsky et al., 2001), in contrast to a recent report, which demonstrated that the protein level of CNP in AD hippocampus was increased (Sultana et al., 2007).

Neurodegeneration in AD has been linked to dysregulation of intracellular Ca^{2+} (Giacomello et al., 2007). In an adult triple transgenic mouse model of AD that exhibits intraneuronal accumulation of amyloid- β proteins, the resting free Ca^{2+} concentration was shown to be greatly elevated in cortical neurons (Lopez et al., 2008). This Ca^{2+} deregulation in the AD brain may be associated with defective mitochondrial functions. Moreover, in neurons from AD brain, morphological alterations of mitochondria were revealed (Baloyannis, 2006).

4.7 Conclusions. Novel regulators of Ca²⁺-induced PTP opening.

In summary, the results obtained here suggest that p42^{IP4} and CNP in mitochondria play a role in regulation of mitochondrial Ca²⁺ transport mechanisms in the brain. The influence of p42^{IP4} and CNP as well as their substrates/ligands on Ca²⁺-induced PTP opening is summarized in Figure 4.2.

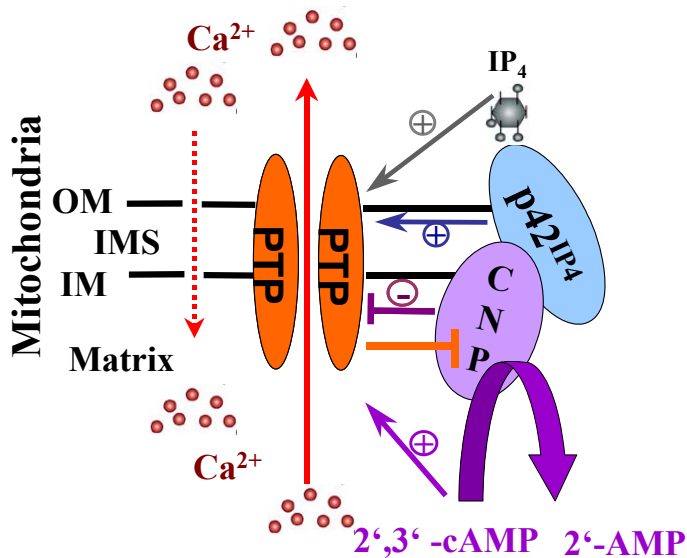


Fig. 4.2. The influence of the p42^{IP4} and its ligands on Ca²⁺-induced PTP opening. The influence of CNP and its substrates on Ca²⁺-induced PTP opening.

Overexpression of p42^{IP4} accelerate Ca²⁺-induced PTP opening. Ligands of p42^{IP4} (here only IP₄ is shown) stimulate PTP opening. CNP-knockdown stimulates PTP opening, thus we suppose that CNP suppresses PTP development. Inhibition of CNP activity under Ca²⁺-induced PTP leads to elevation of 2',3'-cyclic nucleotides levels (here only 2',3'-cAMP is shown), promoting PTP development. In addition, p42^{IP4} interacts with CNP *in vitro* and *in vivo* in mitochondria.

Importantly, here we have shown that p42^{IP4} stimulates Ca²⁺-induced PTP opening. The destabilization of mitochondria during Ca²⁺-induced PTP opening by overexpression of p42^{IP4} may have dramatic consequences for neuronal survival. Additionally, p42^{IP4} ligands, IP₄ and PIP₃, significantly accelerate Ca²⁺-induced PTP opening.

Furthermore, a regulatory role of CNP in PTP opening was established. This is derived from our findings that CNP knockdown facilitates Ca²⁺-induced PTP opening. Interestingly, CNP activity was reduced under Ca²⁺-induced PTP opening. Therefore, the intra-mitochondrial 2',3'-cyclic nucleotides level might be elevated due to inhibition of CNP activity under Ca²⁺-induced PTP opening. In addition, CNP substrates, 2',3'-cAMP and 2',3'-cNADP, enhanced PTP development. Thus, 2',3'-cAMP and 2',3'-cNADP might probably act as a second messengers.

Taken together, our results support the suggestion that p42^{IP4} and CNP are involved in regulation of Ca²⁺-induced PTP opening, important stage of initiation of cell death and, consequently, of the processes leading to neurodegenerative diseases.

5. Abstract

The neuronal protein p42^{IP4} was suggested to be involved in neurodegenerative processes. To find out a role of p42^{IP4} in cell death, we detected apoptosis in control and p42^{IP4} overexpressing mouse neuroblastoma (N2a) cells by caspase-3 assay, DNA-laddering assay and flow cytometry analysis. We have shown that p42^{IP4} is not involved in apoptosis. However, we observed that p42^{IP4} had an effect on cell cycle.

Cellular Ca²⁺ signals are crucial in the control of most physiological processes, cell injury and cell death. Mitochondria play a central role in cellular Ca²⁺ signalling. During cellular Ca²⁺ overload, mitochondria take up cytosolic Ca²⁺, which, in turn, can lead to opening of the permeability transition pore (PTP). Although Ca²⁺-dependent PTP has been implicated in a broad range of cell death pathways, the exact mechanism of the PTP opening remains elusive.

Previously, p42^{IP4} was identified in brain membrane fraction, which also contained mitochondria. Some other data indicate possible localization of p42^{IP4} in mitochondria. Therefore, this important question was studied here.

We determined for the first time mitochondrial localization of p42^{IP4}. Moreover, in rat brain mitochondria (RBM), we found interaction of p42^{IP4} with 2',3'-cyclic nucleotide 3'-phosphodiesterase (CNP) and α -tubulin by pull-down binding assay and by immunoprecipitation.

Localization of p42^{IP4} and CNP in the inner membrane fraction of mitochondria prompted us to study whether p42^{IP4} and CNP are involved in regulation of mitochondrial Ca²⁺-induced PTP. Simultaneous measurements of the respiratory rate, trans-membrane potential, and Ca²⁺ transport in the mitochondrial suspension were performed. We determined the rate of Ca²⁺ influx, Ca²⁺ capacity and lag time for PTP opening in mitochondria isolated from p42^{IP4}-transfected and from control N2a cells. Overexpression of p42^{IP4} led to promotion of Ca²⁺-induced PTP opening. Furthermore, p42^{IP4} ligands, phosphatidylinositol(3,4,5)trisphosphate and inositol(1,3,4,5)tetrakisphosphate, accelerated PTP opening in mitochondria isolated from N2a cells.

We found the interaction of CNP with modulators of PTP, adenine nucleotide transporter and voltage-dependent anion channel. The enzymatic activity of CNP was reduced under PTP opening. Involvement of CNP in PTP operation was confirmed in experiments using mitochondria isolated from CNP-knock-down oligodendrocyte cell line (OLN93). In mitochondria isolated from OLN93 cells transfected with CNP-targeting small interfering RNA, CNP reduction was correlated with facilitation of Ca²⁺-induced PTP opening. The CNP substrates, 2',3'-cyclic AMP and 2',3'-cyclic NADP, enhanced PTP development in RBM.

In summary, our results suggest that p42^{IP4} and CNP in mitochondria play a role in regulation of mitochondrial Ca²⁺ transport mechanisms in the brain. While Ca²⁺-induced PTP opening is important stage of initiation of cell death, consequently we hypothesize that in the brain p42^{IP4} and CNP contribute to processes leading to neurodegenerative diseases.

6. Zusammenfassung

Verschiedene in der Literatur beschriebene Befunde deuten auf die Bedeutung des gehirnspezifischen Proteins p42^{IP4} bei neurodegenerativen/neuroprotektiven Prozessen hin. p42^{IP4} wird auch als Centaurin α -1, und nach einem neueren Vorschlag als ADAP1 bezeichnet. Ein Ziel der vorliegenden Arbeit war aufzuklären, ob p42^{IP4} eine Rolle bei Neuroprotektion oder Zelltod spielt.

In einem ersten Ansatz wurden die Auswirkungen der Überexpression von p42^{IP4} auf die induzierte Apoptose untersucht. Dazu wurde die Mäuse-Neuroblastoma-Zelllinie N2a eingesetzt. Der Nachweis der Apoptose in den N2a-Zellen erfolgte mittels Caspase-3-Assay, DNA-Fragmentierung und Durchflusszytometrie. Hierbei ergaben sich keine Hinweise auf eine direkte Beteiligung von p42^{IP4} an der Apoptose. Wir konnten aber feststellen, dass die Überexpression von p42^{IP4} einen Effekt auf die Verteilung der Zellen im Zellzyklus hat. In den p42^{IP4} überexprimierenden Zellen kam es zu einer Verschiebung des Anteils der Zellen von der G2-Phase zur S-Phase.

Mitochondrien spielen eine zentrale Rolle in der zellulären Ca²⁺-Homöostase und beim Ca²⁺-Signalling. Bei der Überladung von Zellen mit Ca²⁺ können Mitochondrien große Menge an Ca²⁺ aufnehmen, was in der Folge zur Öffnung der Permeabilitätstransitions-pore (PTP) führen kann. Die Beteiligung einer Ca²⁺-abhängigen PTP an vielen zu Zelltod und Gewebsschädigungen führenden Vorgängen konnte gezeigt werden. Aber der genaue Mechanismus der PTP ist noch weitgehend unbekannt. Daher ist die Suche nach neuen Proteinen und Molekülen, die an der Kontrolle der Ca²⁺-induzierten PTP beteiligt sind äußerst wichtig.

p42^{IP4} wurde ursprünglich in Membranfraktionen aus Gehirn identifiziert, die auch Mitochondrien enthielten. Das Hefeprotein Gsc1p, das strukturell und funktionell mit p42^{IP4} eng verwandt ist, ist an der Aufrechterhaltung der mitochondrialen Morphologie beteiligt. p42^{IP4} interagiert mit Proteinkinase C Isoformen, für die ebenfalls eine mitochondriale Lokalisation beschrieben wurde. Eine hohe Wahrscheinlichkeit für eine mitochondriale Lokalisation von p42^{IP4} wurde durch das Programm PSORTII vorhergesagt. Diese Befunde deuteten auf eine mögliche mitochondriale Lokalisation und Funktion von p42^{IP4} hin. Daher wurde diese wichtige Fragestellung in der vorliegenden Arbeit untersucht.

Wir konnten mit verschiedenen Methoden erstmals eine mitochondriale Lokalisation von p42^{IP4} in Mitochondrien aus Rattenhirn, sowie aus N2A- und CHO-Zellen zeigen. Darüberhinaus fanden wir mittels Glutathion-S-Transferase Pull-Down-Versuchen und

Koimmunopräzipitation eine Interaktion von $p42^{IP4}$ mit den Proteinen 2',3'-cyklische Nukleotid 3'-Phosphodiesterase (CNP) und α -Tubulin.

Wir untersuchten die Verteilung von $p42^{IP4}$ und CNP in den mitochondrialen Kompartimenten durch Subfraktionierung von Mitochondrien. Die Lokalisation von $p42^{IP4}$ und CNP in der inneren Membranfraktion und in Kontaktstellen zwischen innerer und äußerer Membran deuteten auf eine funktionelle Rolle beider Proteine in Mitochondrien hin. Daher wurden im Folgenden Studien zur möglichen Beteiligung von $p42^{IP4}$ und CNP an der mitochondrialen Ca^{2+} -induzierten PTP durchgeführt. Wir etablierten eine Methode zur Isolierung von funktionell aktiven Mitochondrien aus Zellkulturen und untersuchten mitochondriale Funktionen während der Ca^{2+} -induzierten PTP. Eine simultane Messung der Atmungsrate, des Ca^{2+} -Transports und des mitochondrialen Membranpotenzials in Mitochondriensuspensionen erfolgte in einer offenen Messkammer. Dabei wurden selektive Elektroden für O_2 , Ca^{2+} und Tetraphenylphosphonium (TPP^+) eingesetzt. Letztere diente zur Membranpotentialmessung. Damit wurden die Geschwindigkeit des Ca^{2+} -Einstroms, die Ca^{2+} -Kapazität und die Verzögerungszeit für die Ca^{2+} -induzierte PTP bestimmt. Es wurden Messungen für Mitochondrien aus $p42^{IP4}$ -transfizierten und nichttransfizierten N2a-Zellen durchgeführt. Die Überexpression von $p42^{IP4}$ führte zu einer signifikanten Forcierung der Ca^{2+} -induzierten Öffnung der PTP. Phosphatidylinositol(3,4,5)trisphosphat und Inositol(1,3,4,5)tetrakisphosphat, beides spezifische Liganden für $p42^{IP4}$, beschleunigten die Öffnung der PTP in Mitochondrien aus N2a-Zellen. Erstaunlicherweise war dieser Einfluss der $p42^{IP4}$ -Liganden auf die PTP-Öffnung unabhängig von der Überexpression von $p42^{IP4}$.

In Rattenhirnmitochondrien fanden wir mittels Koimmunopräzipitation eine Proteinwechselwirkung von CNP mit Modulatoren der PTP, dem Adeninnukleotid-Transporter (ANT) und dem spannungsabhängigen Anionen-Kanal (VDAC). Darüberhinaus konnten wir zeigen, dass die Enzymaktivität von CNP bei der PTP-Öffnung reduziert war, während der CNP-Proteingehalt gleich blieb. Eine Beteiligung von CNP an der PTP-Regulation wurde in weiteren Experimenten bestätigt, bei denen Mitochondrien aus OLN93-Zellen, einer Oligodendrozyten-Zelllinie, verwendet wurden, bei denen CNP durch Transfektion mit siRNA herunterreguliert wurde. In den Mitochondrien aus diesen Zellen korrelierte die Reduktion der CNP-Expression mit einer Erniedrigung der Schwelle für eine Ca^{2+} -induzierte PTP Bildung. Des Weiteren erhöhten 2',3'-cAMP und 2',3'-cyklisches NADP, beides Substrate der CNP, die PTP Bildung in Mitochondrien aus Rattenhirn.

Zusammenfassend zeigen die hier beschriebenen Ergebnisse, dass $p42^{IP4}$ und CNP in Mitochondrien eine wichtige Funktion bei der Regulation mitochondrialer Ca^{2+} -

Transportvorgänge im Gehirn ausüben. Da die Ca^{2+} -induzierte PTP-Bildung einen wichtigen Schritt bei der Einleitung des Zelltods darstellt, könnten p42^{IP4} und CNP an Prozessen beteiligt sein, die zu neurodegenerativen Krankheiten führen.

7. References

- Aggensteiner M, Stricker R, Reiser G (1998) Identification of rat brain p42(IP4), a high-affinity inositol(1,3,4,5)tetrakisphosphate/phosphatidylinositol(3,4,5)trisphosphate binding protein. *Biochim Biophys Acta* 1387:117-128.
- Agrawal HC, Sprinkle TJ, Agrawal D (1990a) 2',3'-cyclic nucleotide-3'-phosphodiesterase in peripheral nerve myelin is phosphorylated by a phorbol ester-sensitive protein kinase. *Biochem Biophys Res Commun* 170:817-823.
- Agrawal HC, Sprinkle TJ, Agrawal D (1990b) 2',3'-cyclic nucleotide-3'-phosphodiesterase in the central nervous system is fatty-acylated by thioester linkage. *J Biol Chem* 265:11849-11853.
- Agrawal HC, Sprinkle TJ, Agrawal D (1994) In vivo phosphorylation of 2',3'-cyclic nucleotide 3'-phosphohydrolase (CNP): CNP in brain myelin is phosphorylated by forskolin- and phorbol ester-sensitive protein kinases. *Neurochem Res* 19:721-728.
- Azarashvili T, Krestinina O, Yurkov I, Evtodienko Y, Reiser G (2005) High-affinity peripheral benzodiazepine receptor ligand, PK11195, regulates protein phosphorylation in rat brain mitochondria under control of Ca(2+). *J Neurochem* 94:1054-1062.
- Azarashvili T, Grachev D, Krestinina O, Evtodienko Y, Yurkov I, Papadopoulos V, Reiser G (2007) The peripheral-type benzodiazepine receptor is involved in control of Ca²⁺-induced permeability transition pore opening in rat brain mitochondria. *Cell Calcium* 42:27-39.
- Baines CP, Kaiser RA, Sheiko T, Craigen WJ, Molkentin JD (2007) Voltage-dependent anion channels are dispensable for mitochondrial-dependent cell death. *Nat Cell Biol* 9:550-555.
- Baines CP, Song CX, Zheng YT, Wang GW, Zhang J, Wang OL, Guo Y, Bolli R, Cardwell EM, Ping P (2003) Protein kinase Cepsilon interacts with and inhibits the permeability transition pore in cardiac mitochondria. *Circ Res* 92:873-880.
- Baines CP, Kaiser RA, Purcell NH, Blair NS, Osinska H, Hambleton MA, Brunskill EW, Sayen MR, Gottlieb RA, Dorn GW, Robbins J, Molkentin JD (2005) Loss of cyclophilin D reveals a critical role for mitochondrial permeability transition in cell death. *Nature* 434:658-662.
- Baloyannis SJ (2006) Mitochondrial alterations in Alzheimer's disease. *J Alzheimers Dis* 9:119-126.
- Bambrick LL, Chandrasekaran K, Mehrabian Z, Wright C, Krueger BK, Fiskum G (2006) Cyclosporin A increases mitochondrial calcium uptake capacity in cortical astrocytes but not cerebellar granule neurons. *J Bioenerg Biomembr* 38:43-47.
- Basso E, Fante L, Fowlkes J, Petronilli V, Forte MA, Bernardi P (2005) Properties of the permeability transition pore in mitochondria devoid of Cyclophilin D. *J Biol Chem* 280:18558-18561.
- Bernardi P (1999) Mitochondrial transport of cations: channels, exchangers, and permeability transition. *Physiol Rev* 79:1127-1155.
- Berridge MJ (1993) Inositol trisphosphate and calcium signalling. *Nature* 361:315-325.

- Beutner G, Ruck A, Riede B, Brdiczka D (1998) Complexes between porin, hexokinase, mitochondrial creatine kinase and adenylate translocator display properties of the permeability transition pore. Implication for regulation of permeability transition by the kinases. *Biochim Biophys Acta* 1368:7-18.
- Bifulco M, Laezza C, Stingo S, Wolff J (2002) 2',3'-Cyclic nucleotide 3'-phosphodiesterase: a membrane-bound, microtubule-associated protein and membrane anchor for tubulin. *Proc Natl Acad Sci U S A* 99:1807-1812.
- Bijur GN, Jope RS (2003) Rapid accumulation of Akt in mitochondria following phosphatidylinositol 3-kinase activation. *J Neurochem* 87:1427-1435.
- Birnbaum G, Kotilinek L, Schlievert P, Clark HB, Trotter J, Horvath E, Gao E, Cox M, Braun PE (1996) Heat shock proteins and experimental autoimmune encephalomyelitis (EAE): I. Immunization with a peptide of the myelin protein 2',3' cyclic nucleotide 3' phosphodiesterase that is cross-reactive with a heat shock protein alters the course of EAE. *J Neurosci Res* 44:381-396.
- Bradbury JM, Thompson RJ (1984) Photoaffinity labelling of central-nervous-system myelin. Evidence for an endogenous type I cyclic AMP-dependent kinase phosphorylating the larger subunit of 2',3'-cyclic nucleotide 3'-phosphodiesterase. *Biochem J* 221:361-368.
- Bradbury JM, Campbell RS, Thompson RJ (1984) Endogenous cyclic AMP-stimulated phosphorylation of a Wolfgram protein component in rabbit central-nervous-system myelin. *Biochem J* 221:351-359.
- Braun PE, De Angelis D, Shtybel WW, Bernier L (1991) Isoprenoid modification permits 2',3'-cyclic nucleotide 3'-phosphodiesterase to bind to membranes. *J Neurosci Res* 30:540-544.
- Broekemeier KM, Dempsey ME, Pfeiffer DR (1989) Cyclosporin A is a potent inhibitor of the inner membrane permeability transition in liver mitochondria. *J Biol Chem* 264:7826-7830.
- Bronisz A, Gajkowska B, Domanska-Janik K (2002) PKC and Raf-1 inhibition-related apoptotic signalling in N2a cells. *J Neurochem* 81:1176-1184.
- Brown MR, Sullivan PG, Geddes JW (2006) Synaptic mitochondria are more susceptible to Ca²⁺ overload than nonsynaptic mitochondria. *J Biol Chem* 281:11658-11668.
- Brustovetsky N, Dubinsky JM (2000) Limitations of cyclosporin A inhibition of the permeability transition in CNS mitochondria. *J Neurosci* 20:8229-8237.
- Capano M, Crompton M (2002) Biphasic translocation of Bax to mitochondria. *Biochem J* 367:169-178.
- Carre M, Andre N, Carles G, Borghi H, Bricchese L, Briand C, Braguer D (2002) Tubulin is an inherent component of mitochondrial membranes that interacts with the voltage-dependent anion channel. *J Biol Chem* 277:33664-33669.
- Chalmers S, Nicholls DG (2003) The relationship between free and total calcium concentrations in the matrix of liver and brain mitochondria. *J Biol Chem* 278:19062-19070.
- Chanda SK, White S, Orth AP, Reisdorph R, Miraglia L, Thomas RS, DeJesus P, Mason DE, Huang Q, Vega R, Yu DH, Nelson CG, Smith BM, Terry R, Linford AS, Yu Y, Chirn GW, Song C, Labow MA, Cohen D, King FJ, Peters EC, Schultz PG, Vogt PK, Hogenesch JB, Caldwell JS

- (2003) Genome-scale functional profiling of the mammalian AP-1 signaling pathway. *Proc Natl Acad Sci U S A* 100:12153-12158.
- Chesneau V, Pierotti AR, Barre N, Creminon C, Tougard C, Cohen P (1994) Isolation and characterization of a dibasic selective metalloendopeptidase from rat testes that cleaves at the amino terminus of arginine residues. *J Biol Chem* 269:2056-2061.
- Cho SJ, Jung JS, Shin SC, Jin I, Ko BH, Kim Kwon Y, Suh-Kim H, Moon IS (2003) Nonspecific association of 2',3'-cyclic nucleotide 3'-phosphodiesterase with the rat forebrain postsynaptic density fraction. *Exp Mol Med* 35:486-493.
- Cox ME, Gao EN, Braun PE (1994) C-terminal CTII motif of 2',3'-cyclic nucleotide 3'-phosphodiesterase undergoes carboxymethylation. *J Neurosci Res* 39:513-518.
- Cozier GE, Lockyer PJ, Reynolds JS, Kupzig S, Bottomley JR, Millard TH, Banting G, Cullen PJ (2000) GAP1IP4BP contains a novel group I pleckstrin homology domain that directs constitutive plasma membrane association. *J Biol Chem* 275:28261-28268.
- Crompton M, Ellinger H, Costi A (1988) Inhibition by cyclosporin A of a Ca²⁺-dependent pore in heart mitochondria activated by inorganic phosphate and oxidative stress. *Biochem J* 255:357-360.
- Cukierman E, Huber I, Rotman M, Cassel D (1995) The ARF1 GTPase-activating protein: zinc finger motif and Golgi complex localization. *Science* 270:1999-2002.
- De Angelis DA, Braun PE (1994) Isoprenylation of brain 2',3'-cyclic nucleotide 3'-phosphodiesterase modulates cell morphology. *J Neurosci Res* 39:386-397.
- De Angelis DA, Braun PE (1996) 2',3'-Cyclic nucleotide 3'-phosphodiesterase binds to actin-based cytoskeletal elements in an isoprenylation-independent manner. *J Neurochem* 67:943-951.
- Deniaud A, Sharaf el dein O, Maillier E, Poncet D, Kroemer G, Lemaire C, Brenner C (2008) Endoplasmic reticulum stress induces calcium-dependent permeability transition, mitochondrial outer membrane permeabilization and apoptosis. *Oncogene* 27:285-299.
- Donie F, Reiser G (1991) Purification of a high-affinity inositol 1,3,4,5-tetrakisphosphate receptor from brain. *Biochem J* 275 (Pt 2):453-457.
- Douglas AJ, Fox MF, Abbott CM, Hinks LJ, Sharpe G, Povey S, Thompson RJ (1992) Structure and chromosomal localization of the human 2',3'-cyclic nucleotide 3'-phosphodiesterase gene. *Ann Hum Genet* 56:243-254.
- Dreiling CE, Schilling RJ, Reitz RC (1981) 2',3'-cyclic nucleotide 3'-phosphohydrolase in rat liver mitochondrial membranes. *Biochim Biophys Acta* 640:114-120.
- Drummond GI, Iyer NT, Keith J (1962) Hydrolysis of ribonucleoside 2',3'-cyclic phosphates by a diesterase from brain. *J Biol Chem* 237:3535-3539.
- Dubois T, Zemlickova E, Howell S, Aitken A (2003) Centaurin-alpha 1 associates in vitro and in vivo with nucleolin. *Biochem Biophys Res Commun* 301:502-508.
- Dubois T, Kerai P, Zemlickova E, Howell S, Jackson TR, Venkateswarlu K, Cullen PJ, Theibert AB, Larose L, Roach PJ, Aitken A (2001) Casein kinase I associates with members of the centaurin-alpha family of phosphatidylinositol 3,4,5-trisphosphate-binding proteins. *J Biol Chem* 276:18757-18764.

- Duszynski J, Koziel R, Brutkowski W, Szczepanowska J, Zablocki K (2006) The regulatory role of mitochondria in capacitative calcium entry. *Biochim Biophys Acta* 1757:380-387.
- Dyer CA, Benjamins JA (1988) Antibody to galactocerebroside alters organization of oligodendroglial membrane sheets in culture. *J Neurosci* 8:4307-4318.
- Dyer CA, Benjamins JA (1989) Organization of oligodendroglial membrane sheets. I: Association of myelin basic protein and 2',3'-cyclic nucleotide 3'-phosphohydrolase with cytoskeleton. *J Neurosci Res* 24:201-211.
- Dyer CA, Matthieu JM (1994) Antibodies to myelin/oligodendrocyte-specific protein and myelin/oligodendrocyte glycoprotein signal distinct changes in the organization of cultured oligodendroglial membrane sheets. *J Neurochem* 62:777-787.
- Dyer CA, Philibotte TM, Billings-Gagliardi S, Wolf MK (1995) Cytoskeleton in myelin-basic-protein-deficient shiverer oligodendrocytes. *Dev Neurosci* 17:53-62.
- Esposito C, Scrima M, Carotenuto A, Tedeschi A, Rovero P, D'Errico G, Malfitano AM, Bifulco M, D'Ursi AM (2008) Structures and micelle locations of the nonlipidated and lipidated C-terminal membrane anchor of 2',3'-cyclic nucleotide-3'-phosphodiesterase. *Biochemistry* 47:308-319.
- Ferguson KM, Kavran JM, Sankaran VG, Fournier E, Isakoff SJ, Skolnik EY, Lemmon MA (2000) Structural basis for discrimination of 3-phosphoinositides by pleckstrin homology domains. *Mol Cell* 6:373-384.
- Giacomello M, Drago I, Pizzo P, Pozzan T (2007) Mitochondrial Ca²⁺ as a key regulator of cell life and death. *Cell Death Differ* 14:1267-1274.
- Gillespie CS, Bernier L, Brophy PJ, Colman DR (1990) Biosynthesis of the myelin 2',3'-cyclic nucleotide 3'-phosphodiesterases. *J Neurochem* 54:656-661.
- Ginisty H, Sicard H, Roger B, Bouvet P (1999) Structure and functions of nucleolin. *J Cell Sci* 112 (Pt 6):761-772.
- Gottlob K, Majewski N, Kennedy S, Kandel E, Robey RB, Hay N (2001) Inhibition of early apoptotic events by Akt/PKB is dependent on the first committed step of glycolysis and mitochondrial hexokinase. *Genes Dev* 15:1406-1418.
- Gravel M, DeAngelis D, Braun PE (1994) Molecular cloning and characterization of rat brain 2',3'-cyclic nucleotide 3'-phosphodiesterase isoform 2. *J Neurosci Res* 38:243-247.
- Gravel M, Peterson J, Yong VW, Kottis V, Trapp B, Braun PE (1996) Overexpression of 2',3'-cyclic nucleotide 3'-phosphodiesterase in transgenic mice alters oligodendrocyte development and produces aberrant myelination. *Mol Cell Neurosci* 7:453-466.
- Gravel M, Robert F, Kottis V, Gallouzi IE, Pelletier J, Braun PE (2009) 2',3'-Cyclic nucleotide 3'-phosphodiesterase: a novel RNA-binding protein that inhibits protein synthesis. *J Neurosci Res* 87:1069-1079.
- Grimm S, Brdiczka D (2007) The permeability transition pore in cell death. *Apoptosis* 12:841-855.
- Haase A, Nordmann C, Sedehizade F, Borrmann C, Reiser G (2008) RanBPM, a novel interaction partner of the brain-specific protein p42(IP4)/centaurin alpha-1. *J Neurochem*.
- Hajnoczky G, Csordas G, Das S, Garcia-Perez C, Saotome M, Sinha Roy S, Yi M (2006) Mitochondrial calcium signalling and cell death: approaches for

- assessing the role of mitochondrial Ca^{2+} uptake in apoptosis. *Cell Calcium* 40:553-560.
- Halestrap AP (2004) Mitochondrial permeability: dual role for the ADP/ATP translocator? *Nature* 430:1 p following 983.
- Halestrap AP (2006) Calcium, mitochondria and reperfusion injury: a pore way to die. *Biochem Soc Trans* 34:232-237.
- Halestrap AP (2009) What is the mitochondrial permeability transition pore? *J Mol Cell Cardiol* 46:821-831.
- Halestrap AP, Davidson AM (1990) Inhibition of Ca^{2+} -induced large-amplitude swelling of liver and heart mitochondria by cyclosporin is probably caused by the inhibitor binding to mitochondrial-matrix peptidyl-prolyl cis-trans isomerase and preventing it interacting with the adenine nucleotide translocase. *Biochem J* 268:153-160.
- Halestrap AP, McStay GP, Clarke SJ (2002) The permeability transition pore complex: another view. *Biochimie* 84:153-166.
- Hammonds-Odie LP, Jackson TR, Profit AA, Blader IJ, Turck CW, Prestwich GD, Theibert AB (1996) Identification and cloning of centaurin-alpha. A novel phosphatidylinositol 3,4,5-trisphosphate-binding protein from rat brain. *J Biol Chem* 271:18859-18868.
- Hanck T, Stricker R, Sedehizade F, Reiser G (2004) Identification of gene structure and subcellular localization of human centaurin alpha 2, and p42IP4, a family of two highly homologous, Ins 1,3,4,5-P4-/PtdIns 3,4,5-P3-binding, adapter proteins. *J Neurochem* 88:326-336.
- Hanck T, Stricker R, Krishna UM, Falck JR, Chang YT, Chung SK, Reiser G (1999) Recombinant p42IP4, a brain-specific 42-kDa high-affinity Ins(1,3,4,5)P4 receptor protein, specifically interacts with lipid membranes containing Ptd-Ins(3,4,5)P3. *Eur J Biochem* 261:577-584.
- Hansson MJ, Mansson R, Mattiasson G, Ohlsson J, Karlsson J, Keep MF, Elmer E (2004) Brain-derived respiring mitochondria exhibit homogeneous, complete and cyclosporin-sensitive permeability transition. *J Neurochem* 89:715-729.
- Hayashi H, Matsuzaki O, Muramatsu S, Tsuchiya Y, Harada T, Suzuki Y, Sugano S, Matsuda A, Nishida E (2006) Centaurin-alpha1 is a phosphatidylinositol 3-kinase-dependent activator of ERK1/2 mitogen-activated protein kinases. In: *J Biol Chem*, pp 1332-1337.
- Hermosura MC, Takeuchi H, Fleig A, Riley AM, Potter BV, Hirata M, Penner R (2000) InsP4 facilitates store-operated calcium influx by inhibition of InsP3 5-phosphatase. *Nature* 408:735-740.
- Hinman JD, Chen CD, Oh SY, Hollander W, Abraham CR (2008) Age-dependent accumulation of ubiquitinated 2',3'-cyclic nucleotide 3'-phosphodiesterase in myelin lipid rafts. *Glia* 56:118-133.
- Hiraoka Y, Ohno M, Yoshida K, Okawa K, Tomimoto H, Kita T, Nishi E (2007) Enhancement of alpha-secretase cleavage of amyloid precursor protein by a metalloendopeptidase nardilysin. *J Neurochem* 102:1595-1605.
- Hofmann A, Grella M, Botos I, Filipowicz W, Wlodawer A (2002) Crystal structures of the semireduced and inhibitor-bound forms of cyclic nucleotide phosphodiesterase from *Arabidopsis thaliana*. *J Biol Chem* 277:1419-1425.
- Hofmann A, Zdanov A, Genschik P, Ruvinov S, Filipowicz W, Wlodawer A (2000) Structure and mechanism of activity of the cyclic phosphodiesterase of

- Appr>p, a product of the tRNA splicing reaction. *Embo J* 19:6207-6217.
- Horiguchi K, Hanada T, Fukui Y, Chishti AH (2006) Transport of PIP3 by GAKIN, a kinesin-3 family protein, regulates neuronal cell polarity. *J Cell Biol* 174:425-436.
- Huang CF, Chen CC, Tung L, Buu LM, Lee FJ (2002) The yeast ADP-ribosylation factor GAP, Gcs1p, is involved in maintenance of mitochondrial morphology. *J Cell Sci* 115:275-282.
- Huang YH, Grasis JA, Miller AT, Xu R, Soonthornvacharin S, Andreotti AH, Tsoukas CD, Cooke MP, Sauer K (2007) Positive regulation of Itk PH domain function by soluble IP4. *Science* 316:886-889.
- Hunter DR, Haworth RA, Southard JH (1976) Relationship between configuration, function, and permeability in calcium-treated mitochondria. *J Biol Chem* 251:5069-5077.
- Jackson TR, Kearns BG, Theibert AB (2000) Cytohesins and centaurins: mediators of PI 3-kinase-regulated Arf signaling. *Trends Biochem Sci* 25:489-495.
- Jia Y, Schurmans S, Luo HR (2008) Regulation of innate immunity by inositol 1,3,4,5-tetrakisphosphate. *Cell Cycle* 7:2803-2808.
- Jia Y, Subramanian KK, Erneux C, Pouillon V, Hattori H, Jo H, You J, Zhu D, Schurmans S, Luo HR (2007) Inositol 1,3,4,5-tetrakisphosphate negatively regulates phosphatidylinositol-3,4,5- trisphosphate signaling in neutrophils. *Immunity* 27:453-467.
- Juhaszova M, Wang S, Zorov DB, Nuss HB, Gleichmann M, Mattson MP, Sollott SJ (2008) The identity and regulation of the mitochondrial permeability transition pore: where the known meets the unknown. *Ann N Y Acad Sci* 1123:197-212.
- Kahn RA, Bruford E, Inoue H, Logsdon JM, Jr., Nie Z, Premont RT, Randazzo PA, Satake M, Theibert AB, Zapp ML, Cassel D (2008) Consensus nomenclature for the human ArfGAP domain-containing proteins. *J Cell Biol* 182:1039-1044.
- Kato M, Shirouzu M, Terada T, Yamaguchi H, Murayama K, Sakai H, Kuramitsu S, Yokoyama S (2003) Crystal structure of the 2'-5' RNA ligase from *Thermus thermophilus* HB8. *J Mol Biol* 329:903-911.
- Kim T, Pfeiffer SE (1999) Myelin glycosphingolipid/cholesterol-enriched microdomains selectively sequester the non-compact myelin proteins CNP and MOG. *J Neurocytol* 28:281-293.
- Kokoszka JE, Waymire KG, Levy SE, Sligh JE, Cai J, Jones DP, MacGregor GR, Wallace DC (2004) The ADP/ATP translocator is not essential for the mitochondrial permeability transition pore. *Nature* 427:461-465.
- Koonin EV, Gorbalenya AE (1990) Related domains in yeast tRNA ligase, bacteriophage T4 polynucleotide kinase and RNA ligase, and mammalian myelin 2',3'-cyclic nucleotide phosphohydrolase revealed by amino acid sequence comparison. *FEBS Lett* 268:231-234.
- Kozlov G, Lee J, Elias D, Gravel M, Gutierrez P, Ekiel I, Braun PE, Gehring K (2003) Structural evidence that brain cyclic nucleotide phosphodiesterase is a member of the 2H phosphodiesterase superfamily. *J Biol Chem* 278:46021-46028.
- Krauskopf A, Eriksson O, Craigen WJ, Forte MA, Bernardi P (2006) Properties of the permeability transition in VDAC1(-/-) mitochondria. *Biochim Biophys Acta* 1757:590-595.

- Kreutz MR, Bockers TM, Sabel BA, Hulser E, Stricker R, Reiser G (1997) Expression and subcellular localization of p42IP4/centaurin- α , a brain-specific, high-affinity receptor for inositol 1,3,4,5-tetrakisphosphate and phosphatidylinositol 3,4,5-trisphosphate in rat brain. *Eur J Neurosci* 9:2110-2124.
- Krieger C, Duchen MR (2002) Mitochondria, Ca²⁺ and neurodegenerative disease. *Eur J Pharmacol* 447:177-188.
- Kristal BS, Staats PN, Shestopalov AI (2000) Biochemical characterization of the mitochondrial permeability transition in isolated forebrain mitochondria. *Dev Neurosci* 22:376-383.
- Kurihara T, Monoh K, Sakimura K, Takahashi Y (1990) Alternative splicing of mouse brain 2',3'-cyclic-nucleotide 3'-phosphodiesterase mRNA. *Biochem Biophys Res Commun* 170:1074-1081.
- Kurihara T, Tohyama Y, Yamamoto J, Kanamatsu T, Watanabe R, Kitajima S (1992) Origin of brain 2',3'-cyclic-nucleotide 3'-phosphodiesterase doublet. *Neurosci Lett* 138:49-52.
- Laezza C, Wolff J, Bifulco M (1997) Identification of a 48-kDa prenylated protein that associates with microtubules as 2',3'-cyclic nucleotide 3'-phosphodiesterase in FRTL-5 cells. *FEBS Lett* 413:260-264.
- Lakshmana MK, Yoon IS, Chen E, Bianchi E, Koo EH, Kang DE (2009) Novel role of RanBP9 in BACE1 processing of amyloid precursor protein and amyloid beta peptide generation. *J Biol Chem* 284:11863-11872.
- Lappe-Siefke C, Goebbels S, Gravel M, Nicksch E, Lee J, Braun PE, Griffiths IR, Nave KA (2003) Disruption of Cnp1 uncouples oligodendroglial functions in axonal support and myelination. *Nat Genet* 33:366-374.
- Lawlor MA, Alessi DR (2001) PKB/Akt: a key mediator of cell proliferation, survival and insulin responses? *J Cell Sci* 114:2903-2910.
- Lawrence J, Mundell SJ, Yun H, Kelly E, Venkateswarlu K (2005) Centaurin- α 1, an ADP-ribosylation factor 6 GTPase activating protein, inhibits beta 2-adrenoceptor internalization. *Mol Pharmacol* 67:1822-1828.
- Lee J, Gravel M, Gao E, O'Neill RC, Braun PE (2001) Identification of essential residues in 2',3'-cyclic nucleotide 3'-phosphodiesterase. Chemical modification and site-directed mutagenesis to investigate the role of cysteine and histidine residues in enzymatic activity. *J Biol Chem* 276:14804-14813.
- Lee J, Gravel M, Zhang R, Thibault P, Braun PE (2005) Process outgrowth in oligodendrocytes is mediated by CNP, a novel microtubule assembly myelin protein. *J Cell Biol* 170:661-673.
- Lee J, O'Neill RC, Park MW, Gravel M, Braun PE (2006) Mitochondrial localization of CNP2 is regulated by phosphorylation of the N-terminal targeting signal by PKC: implications of a mitochondrial function for CNP2 in glial and non-glial cells. *Mol Cell Neurosci* 31:446-462.
- Leissring MA, Farris W, Wu X, Christodoulou DC, Haigis MC, Guarente L, Selkoe DJ (2004) Alternative translation initiation generates a novel isoform of insulin-degrading enzyme targeted to mitochondria. *Biochem J* 383:439-446.
- Lemmon MA, Ferguson KM (2000) Signal-dependent membrane targeting by pleckstrin homology (PH) domains. *Biochem J* 350 Pt 1:1-18.
- Leung AW, Halestrap AP (2008) Recent progress in elucidating the molecular mechanism of the mitochondrial permeability transition pore. *Biochim Biophys Acta* 1777:946-952.

- Leung AW, Varanyuwatana P, Halestrap AP (2008) The mitochondrial phosphate carrier interacts with cyclophilin D and may play a key role in the permeability transition. *J Biol Chem* 283:26312-26323.
- Levy M, Faas GC, Saggau P, Craigen WJ, Sweatt JD (2003) Mitochondrial regulation of synaptic plasticity in the hippocampus. *J Biol Chem* 278:17727-17734.
- Loewenstein Y, Sompolinsky H (2003) Temporal integration by calcium dynamics in a model neuron. *Nat Neurosci* 6:961-967.
- Lopez JR, Lyckman A, Oddo S, Laferla FM, Querfurth HW, Shtifman A (2008) Increased intraneuronal resting $[Ca^{2+}]$ in adult Alzheimer's disease mice. *J Neurochem* 105:262-271.
- Luckhoff A, Clapham DE (1992) Inositol 1,3,4,5-tetrakisphosphate activates an endothelial Ca^{2+} -permeable channel. *Nature* 355:356-358.
- Maatta JA, Kaldman MS, Sakoda S, Salmi AA, Hinkkanen AE (1998) Encephalitogenicity of myelin-associated oligodendrocytic basic protein and 2',3'-cyclic nucleotide 3'-phosphodiesterase for BALB/c and SJL mice. *Immunology* 95:383-388.
- Majewski N, Nogueira V, Bhaskar P, Coy PE, Skeen JE, Gottlob K, Chandel NS, Thompson CB, Robey RB, Hay N (2004) Hexokinase-mitochondria interaction mediated by Akt is required to inhibit apoptosis in the presence or absence of Bax and Bak. *Mol Cell* 16:819-830.
- Marzo I, Brenner C, Zamzami N, Susin SA, Beutner G, Brdiczka D, Remy R, Xie ZH, Reed JC, Kroemer G (1998a) The permeability transition pore complex: a target for apoptosis regulation by caspases and bcl-2-related proteins. *J Exp Med* 187:1261-1271.
- Marzo I, Brenner C, Zamzami N, Jurgensmeier JM, Susin SA, Vieira HL, Prevost MC, Xie Z, Matsuyama S, Reed JC, Kroemer G (1998b) Bax and adenine nucleotide translocator cooperate in the mitochondrial control of apoptosis. *Science* 281:2027-2031.
- Mayrleitner M, Schafer R, Fleischer S (1995) IP₃ receptor purified from liver plasma membrane is an (1,4,5)IP₃ activated and (1,3,4,5)IP₄ inhibited calcium permeable ion channel. *Cell Calcium* 17:141-153.
- McFerran B, Burgoyne R (1997) 2',3'-Cyclic nucleotide 3'-phosphodiesterase is associated with mitochondria in diverse adrenal cell types. *J Cell Sci* 110 (Pt 23):2979-2985.
- Menager C, Arimura N, Fukata Y, Kaibuchi K (2004) PIP₃ is involved in neuronal polarization and axon formation. *J Neurochem* 89:109-118.
- Miller AT, Chamberlain PP, Cooke MP (2008) Beyond IP₃: roles for higher order inositol phosphates in immune cell signaling. *Cell Cycle* 7:463-467.
- Miller AT, Sandberg M, Huang YH, Young M, Sutton S, Sauer K, Cooke MP (2007) Production of Ins(1,3,4,5)P₄ mediated by the kinase Itpkb inhibits store-operated calcium channels and regulates B cell selection and activation. *Nat Immunol* 8:514-521.
- Mironov SL, Ivannikov MV, Johansson M (2005) $[Ca^{2+}]_i$ signaling between mitochondria and endoplasmic reticulum in neurons is regulated by microtubules. From mitochondrial permeability transition pore to Ca^{2+} -induced Ca^{2+} release. *J Biol Chem* 280:715-721.
- Monoh K, Kurihara T, Takahashi Y, Ichikawa T, Kumanishi T, Hayashi S, Minoshima S, Shimizu N (1993) Structure, expression and chromosomal localization of the gene encoding human 2',3'-cyclic-nucleotide 3'-phosphodiesterase. *Gene* 129:297-301.

- Moore CD, Thacker EE, Larimore J, Gaston D, Underwood A, Kearns B, Patterson SI, Jackson T, Chapleau C, Pozzo-Miller L, Theibert A (2007) The neuronal Arf GAP centaurin alpha1 modulates dendritic differentiation. *J Cell Sci* 120:2683-2693.
- Morris-Downes MM, McCormack K, Baker D, Sivaprasad D, Natkunarajah J, Amor S (2002) Encephalitogenic and immunogenic potential of myelin-associated glycoprotein (MAG), oligodendrocyte-specific glycoprotein (OSP) and 2',3'-cyclic nucleotide 3'-phosphodiesterase (CNPase) in ABH and SJL mice. *J Neuroimmunol* 122:20-33.
- Muraro PA, Kalbus M, Afshar G, McFarland HF, Martin R (2002) T cell response to 2',3'-cyclic nucleotide 3'-phosphodiesterase (CNPase) in multiple sclerosis patients. *J Neuroimmunol* 130:233-242.
- Nakagawa T, Shimizu S, Watanabe T, Yamaguchi O, Otsu K, Yamagata H, Inohara H, Kubo T, Tsujimoto Y (2005) Cyclophilin D-dependent mitochondrial permeability transition regulates some necrotic but not apoptotic cell death. *Nature* 434:652-658.
- Nakai K, Kanehisa M (1992) A knowledge base for predicting protein localization sites in eukaryotic cells. *Genomics* 14:897-911.
- Neupert W (1997) Protein import into mitochondria. *Annu Rev Biochem* 66:863-917.
- O'Neill RC, Braun PE (2000) Selective synthesis of 2',3'-cyclic nucleotide 3'-phosphodiesterase isoform 2 and identification of specifically phosphorylated serine residues. *J Neurochem* 74:540-546.
- O'Neill RC, Minuk J, Cox ME, Braun PE, Gravel M (1997) CNP2 mRNA directs synthesis of both CNP1 and CNP2 polypeptides. *J Neurosci Res* 50:248-257.
- Pastorino JG, Shulga N, Hoek JB (2002) Mitochondrial binding of hexokinase II inhibits Bax-induced cytochrome c release and apoptosis. *J Biol Chem* 277:7610-7618.
- Peirce TR, Bray NJ, Williams NM, Norton N, Moskvina V, Preece A, Haroutunian V, Buxbaum JD, Owen MJ, O'Donovan MC (2006) Convergent evidence for 2',3'-cyclic nucleotide 3'-phosphodiesterase as a possible susceptibility gene for schizophrenia. *Arch Gen Psychiatry* 63:18-24.
- Pizzo P, Pozzan T (2007) Mitochondria-endoplasmic reticulum choreography: structure and signaling dynamics. *Trends Cell Biol* 17:511-517.
- Poon PP, Wang X, Rotman M, Huber I, Cukierman E, Cassel D, Singer RA, Johnston GC (1996) *Saccharomyces cerevisiae* Gcs1 is an ADP-ribosylation factor GTPase-activating protein. *Proc Natl Acad Sci U S A* 93:10074-10077.
- Prestwich GD (2004) Phosphoinositide signaling; from affinity probes to pharmaceutical targets. *Chem Biol* 11:619-637.
- Prinos P, Slack C, Lasko DD (1995) 5'phosphorylation of DNA in mammalian cells: identification of a polymin P-precipitable polynucleotide kinase. *J Cell Biochem* 58:115-131.
- Rasband MN, Tayler J, Kaga Y, Yang Y, Lappe-Siefke C, Nave KA, Bansal R (2005) CNP is required for maintenance of axon-glia interactions at nodes of Ranvier in the CNS. *Glia* 50:86-90.
- Reinikainen KJ, Pitkanen A, Riekkinen PJ (1989) 2',3'-cyclic nucleotide-3'-phosphodiesterase activity as an index of myelin in the post-mortem brains of patients with Alzheimer's disease. *Neurosci Lett* 106:229-232.

- Reiser G, Bernstein HG (2002) Neurons and plaques of Alzheimer's disease patients highly express the neuronal membrane docking protein p42IP4/centaurin alpha. *Neuroreport* 13:2417-2419.
- Reiser G, Bernstein HG (2004) Altered expression of protein p42IP4/centaurin-alpha 1 in Alzheimer's disease brains and possible interaction of p42IP4 with nucleolin. *Neuroreport* 15:147-148.
- Reiser G, Kunzelmann U, Steinhilber G, Binmoller FJ (1994) Generation of a monoclonal antibody against the myelin protein CNP (2',3'-cyclic nucleotide 3'-phosphodiesterase) suitable for biochemical and for immunohistochemical investigations of CNP. *Neurochem Res* 19:1479-1485.
- Reiser G, Striggow F, Hackmann C, Schwegler H, Yilmazer-Hanke DM (2004) Short-term down-regulation of the brain-specific, PtdIns(3,4,5)P3/Ins(1,3,4,5)P4-binding, adapter protein, p42IP4/centaurin-alpha 1 in rat brain after acoustic and electric stimulation. *Neurochem Int* 45:89-93.
- Reiser G, Schafer R, Donie F, Hulser E, Nehls-Sahabandu M, Mayr GW (1991) A high-affinity inositol 1,3,4,5-tetrakisphosphate receptor protein from brain is specifically labelled by a newly synthesized photoaffinity analogue, N-(4-azidosalicyl)aminoethanol(1)-1-phospho-D-myoinositol 3,4,5-trisphosphate. *Biochem J* 280 (Pt 2):533-539.
- Reyland ME (2009) Protein kinase C isoforms: Multi-functional regulators of cell life and death. *Front Biosci* 14:2386-2399.
- Rice JE, Lindsay JG (1997) Subcellular fractionation of mitochondria. In: *Subcellular fractionation: a practical approach* (Graham JM, Rickwood D, eds), pp 107-142. Oxford: IRL Press.
- Richter-Landsberg C, Heinrich M (1996) OLN-93: a new permanent oligodendroglia cell line derived from primary rat brain glial cultures. *J Neurosci Res* 45:161-173.
- Rodic N, Oka M, Hamazaki T, Murawski MR, Jorgensen M, Maatouk DM, Resnick JL, Li E, Terada N (2005) DNA methylation is required for silencing of ant4, an adenine nucleotide translocase selectively expressed in mouse embryonic stem cells and germ cells. *Stem Cells* 23:1314-1323.
- Rosener M, Muraro PA, Riethmuller A, Kalbus M, Sappeler G, Thompson RJ, Lichtenfels R, Sommer N, McFarland HF, Martin R (1997) 2',3'-cyclic nucleotide 3'-phosphodiesterase: a novel candidate autoantigen in demyelinating diseases. *J Neuroimmunol* 75:28-34.
- Salzer JL (2003) Polarized domains of myelinated axons. *Neuron* 40:297-318.
- Schinzel AC, Takeuchi O, Huang Z, Fisher JK, Zhou Z, Rubens J, Hetz C, Danial NN, Moskowitz MA, Korsmeyer SJ (2005) Cyclophilin D is a component of mitochondrial permeability transition and mediates neuronal cell death after focal cerebral ischemia. *Proc Natl Acad Sci U S A* 102:12005-12010.
- Sedehizade F, von Klot C, Hanck T, Reiser G (2005) p42(IP4)/centaurin alpha1, a brain-specific PtdIns(3,4,5)P3/Ins(1,3,4,5)P4-binding protein: membrane trafficking induced by epidermal growth factor is inhibited by stimulation of phospholipase C-coupled thrombin receptor. *Neurochem Res* 30:1319-1330.
- Sedehizade F, Hanck T, Stricker R, Horstmayer A, Bernstein HG, Reiser G (2002) Cellular expression and subcellular localization of the human

- Ins(1,3,4,5)P(4)-binding protein, p42(IP4), in human brain and in neuronal cells. *Brain Res Mol Brain Res* 99:1-11.
- Sharer JD, Shern JF, Van Valkenburgh H, Wallace DC, Kahn RA (2002) ARL2 and BART enter mitochondria and bind the adenine nucleotide transporter. *Mol Biol Cell* 13:71-83.
- Shepherd PR, Withers DJ, Siddle K (1998) Phosphoinositide 3-kinase: the key switch mechanism in insulin signalling. *Biochem J* 333 (Pt 3):471-490.
- Sims NR (1990) Rapid isolation of metabolically active mitochondria from rat brain and subregions using Percoll density gradient centrifugation. *J Neurochem* 55:698-707.
- Sinensky M (2000) Recent advances in the study of prenylated proteins. *Biochim Biophys Acta* 1484:93-106.
- Smaili SS, Hsu YT, Youle RJ, Russell JT (2000) Mitochondria in Ca²⁺ signaling and apoptosis. *J Bioenerg Biomembr* 32:35-46.
- Sogin DC (1976) 2',3'-Cyclic NADP as a substrate for 2',3'-cyclic nucleotide 3'-phosphohydrolase. *J Neurochem* 27:1333-1337.
- Sprinkle TJ (1989) 2',3'-cyclic nucleotide 3'-phosphodiesterase, an oligodendrocyte-Schwann cell and myelin-associated enzyme of the nervous system. *Crit Rev Neurobiol* 4:235-301.
- Stephens LR, Jackson TR, Hawkins PT (1993) Agonist-stimulated synthesis of phosphatidylinositol(3,4,5)-trisphosphate: a new intracellular signalling system? *Biochim Biophys Acta* 1179:27-75.
- Stricker R, Lottspeich F, Reiser G (1994) The myelin protein CNP (2',3'-cyclic nucleotide 3'-phosphodiesterase): immunoaffinity purification of CNP from pig and rat brain using a monoclonal antibody and phosphorylation of CNP by cyclic nucleotide-dependent protein kinases. *Biol Chem Hoppe Seyler* 375:205-209.
- Stricker R, Adelt S, Vogel G, Reiser G (1999) Translocation between membranes and cytosol of p42IP₄, a specific inositol 1,3,4,5-tetrakisphosphate/phosphatidylinositol 3,4, 5-trisphosphate-receptor protein from brain, is induced by inositol 1,3,4,5-tetrakisphosphate and regulated by a membrane-associated 5-phosphatase. *Eur J Biochem* 265:815-824.
- Stricker R, Vandekerckhove J, Krishna MU, Falck JR, Hanck T, Reiser G (2003) Oligomerization controls in tissue-specific manner ligand binding of native, affinity-purified p42(IP₄)/centaurin alpha1 and cytohesins-proteins with high affinity for the messengers D-inositol 1,3,4,5-tetrakisphosphate/phosphatidylinositol 3,4,5-trisphosphate. *Biochim Biophys Acta* 1651:102-115.
- Stricker R, Chow KM, Walther D, Hanck T, Hersh LB, Reiser G (2006) Interaction of the brain-specific protein p42IP₄/centaurin-alpha1 with the peptidase nardilysin is regulated by the cognate ligands of p42IP₄, PtdIns(3,4,5)P₃ and Ins(1,3,4,5)P₄, with stereospecificity. *J Neurochem* 98:343-354.
- Stricker R, Hulser E, Fischer J, Jarchau T, Walter U, Lottspeich F, Reiser G (1997) cDNA cloning of porcine p42IP₄, a membrane-associated and cytosolic 42 kDa inositol(1,3,4,5)tetrakisphosphate receptor from pig brain with similarly high affinity for phosphatidylinositol (3,4,5)P₃. *FEBS Lett* 405:229-236.

- Sullivan PG, Rabchevsky AG, Waldmeier PC, Springer JE (2005) Mitochondrial permeability transition in CNS trauma: cause or effect of neuronal cell death? *J Neurosci Res* 79:231-239.
- Sultana R, Boyd-Kimball D, Cai J, Pierce WM, Klein JB, Merchant M, Butterfield DA (2007) Proteomics analysis of the Alzheimer's disease hippocampal proteome. *J Alzheimers Dis* 11:153-164.
- Szabadkai G, Bianchi K, Varnai P, De Stefani D, Wieckowski MR, Cavagna D, Nagy AI, Balla T, Rizzuto R (2006) Chaperone-mediated coupling of endoplasmic reticulum and mitochondrial Ca²⁺ channels. *J Cell Biol* 175:901-911.
- Szabo I, Zoratti M (1993) The mitochondrial permeability transition pore may comprise VDAC molecules. I. Binary structure and voltage dependence of the pore. *FEBS Lett* 330:201-205.
- Szinyei C, Behnisch T, Reiser G, Reymann KG (1999) Inositol 1,3,4,5-tetrakisphosphate enhances long-term potentiation by regulating Ca²⁺ entry in rat hippocampus. *J Physiol* 516 (Pt 3):855-868.
- Tanaka K, Horiguchi K, Yoshida T, Takeda M, Fujisawa H, Takeuchi K, Umeda M, Kato S, Ihara S, Nagata S, Fukui Y (1999) Evidence that a phosphatidylinositol 3,4,5-trisphosphate-binding protein can function in nucleus. *J Biol Chem* 274:3919-3922.
- Tanaka K, Imajoh-Ohmi S, Sawada T, Shirai R, Hashimoto Y, Iwasaki S, Kaibuchi K, Kanaho Y, Shirai T, Terada Y, Kimura K, Nagata S, Fukui Y (1997) A target of phosphatidylinositol 3,4,5-trisphosphate with a zinc finger motif similar to that of the ADP-ribosylation-factor GTPase-activating protein and two pleckstrin homology domains. *Eur J Biochem* 245:512-519.
- Tang F, Qu M, Wang L, Ruan Y, Lu T, Zhang H, Liu Z, Yue W, Zhang D (2007) Case-control association study of the 2',3'-cyclic nucleotide 3'-phosphodiesterase (CNP) gene and schizophrenia in the Han Chinese population. *Neurosci Lett* 416:113-116.
- Thacker E, Kearns B, Chapman C, Hammond J, Howell A, Theibert A (2004) The arf6 GAP centaurin alpha-1 is a neuronal actin-binding protein which also functions via GAP-independent activity to regulate the actin cytoskeleton. *Eur J Cell Biol* 83:541-554.
- Toker A, Cantley LC (1997) Signalling through the lipid products of phosphoinositide-3-OH kinase. *Nature* 387:673-676.
- Tsubokawa H, Oguro K, Robinson HP, Masuzawa T, Kawai N (1996) Intracellular inositol 1,3,4,5-tetrakisphosphate enhances the calcium current in hippocampal CA1 neurones of the gerbil after ischaemia. *J Physiol* 497 (Pt 1):67-78.
- Vanhaesebroeck B, Leever SJ, Ahmadi K, Timms J, Katso R, Driscoll PC, Woscholski R, Parker PJ, Waterfield MD (2001) Synthesis and function of 3-phosphorylated inositol lipids. *Annu Rev Biochem* 70:535-602.
- Vartanian T, Szuchet S, Dawson G (1992) Oligodendrocyte-substratum adhesion activates the synthesis of specific lipid species involved in cell signaling. *J Neurosci Res* 32:69-78.
- Vartanian T, Sprinkle TJ, Dawson G, Szuchet S (1988) Oligodendrocyte substratum adhesion modulates expression of adenylate cyclase-linked receptors. *Proc Natl Acad Sci U S A* 85:939-943.

- Venkateswarlu K (2005) Centaurin-alpha1 and KIF13B kinesin motor protein interaction in ARF6 signalling. *Biochem Soc Trans* 33:1279-1281.
- Venkateswarlu K, Brandom KG, Lawrence JL (2004) Centaurin-alpha1 is an in vivo phosphatidylinositol 3,4,5-trisphosphate-dependent GTPase-activating protein for ARF6 that is involved in actin cytoskeleton organization. *J Biol Chem* 279:6205-6208.
- Venkateswarlu K, Hanada T, Chishti AH (2005) Centaurin-alpha1 interacts directly with kinesin motor protein KIF13B. *J Cell Sci* 118:2471-2484.
- Venkateswarlu K, Oatey PB, Tavare JM, Jackson TR, Cullen PJ (1999) Identification of centaurin-alpha1 as a potential in vivo phosphatidylinositol 3,4,5-trisphosphate-binding protein that is functionally homologous to the yeast ADP-ribosylation factor (ARF) GTPase-activating protein, Gcs1. *Biochem J* 340 (Pt 2):359-363.
- Vlkolinsky R, Cairns N, Fountoulakis M, Lubec G (2001) Decreased brain levels of 2',3'-cyclic nucleotide-3'-phosphodiesterase in Down syndrome and Alzheimer's disease. *Neurobiol Aging* 22:547-553.
- Vogel US, Thompson RJ (1988) Molecular structure, localization, and possible functions of the myelin-associated enzyme 2',3'-cyclic nucleotide 3'-phosphodiesterase. *J Neurochem* 50:1667-1677.
- Voineskos AN, de Luca V, Bulgin NL, van Adrichem Q, Shaikh S, Lang DJ, Honer WG, Kennedy JL (2008) A family-based association study of the myelin-associated glycoprotein and 2',3'-cyclic nucleotide 3'-phosphodiesterase genes with schizophrenia. *Psychiatr Genet* 18:143-146.
- von Heijne G, Steppuhn J, Herrmann RG (1989) Domain structure of mitochondrial and chloroplast targeting peptides. *Eur J Biochem* 180:535-545.
- Vyssokikh M, Zorova L, Zorov D, Heimlich G, Jurgensmeier J, Schreiner D, Brdiczka D (2004) The intra-mitochondrial cytochrome c distribution varies correlated to the formation of a complex between VDAC and the adenine nucleotide translocase: this affects Bax-dependent cytochrome c release. *Biochim Biophys Acta* 1644:27-36.
- Vyssokikh MY, Zorova L, Zorov D, Heimlich G, Jurgensmeier JJ, Brdiczka D (2002) Bax releases cytochrome c preferentially from a complex between porin and adenine nucleotide translocator. Hexokinase activity suppresses this effect. *Mol Biol Rep* 29:93-96.
- Walsh MJ, Murray JM (1998) Dual implication of 2',3'-cyclic nucleotide 3'-phosphodiesterase as major autoantigen and C3 complement-binding protein in the pathogenesis of multiple sclerosis. *J Clin Invest* 101:1923-1931.
- Walter J, Schindzielorz A, Hartung B, Haass C (2000) Phosphorylation of the beta-amyloid precursor protein at the cell surface by ectocasein kinases 1 and 2. *J Biol Chem* 275:23523-23529.
- Wu CY, Lu J, Cao Q, Guo CH, Gao Q, Ling EA (2006) Expression of 2',3'-cyclic nucleotide 3'-phosphodiesterase in the amoeboid microglial cells in the developing rat brain. *Neuroscience* 142:333-341.
- Yin X, Peterson J, Gravel M, Braun PE, Trapp BD (1997) CNP overexpression induces aberrant oligodendrocyte membranes and inhibits MBP accumulation and myelin compaction. *J Neurosci Res* 50:238-247.
- Zemlickova E, Dubois T, Kerai P, Clokie S, Cronshaw AD, Wakefield RI, Johannes FJ, Aitken A (2003) Centaurin-alpha(1) associates with and is

- phosphorylated by isoforms of protein kinase C. *Biochem Biophys Res Commun* 307:459-465.
- Zhang B, Cao Q, Guo A, Chu H, Chan YG, Buschdorf JP, Low BC, Ling EA, Liang F (2005) Juxtalin: an oligodendroglial protein that promotes cellular arborization and 2',3'-cyclic nucleotide-3'-phosphodiesterase trafficking. *Proc Natl Acad Sci U S A* 102:11527-11532.
- Zhu DM, Tekle E, Huang CY, Chock PB (2000) Inositol tetrakisphosphate as a frequency regulator in calcium oscillations in HeLa cells. *J Biol Chem* 275:6063-6066.
- Zoratti M, Szabo I, De Marchi U (2005) Mitochondrial permeability transitions: how many doors to the house? *Biochim Biophys Acta* 1706:40-52.

8. Abbreviations

2',3'-cAMP, 2',3'cyclic AMP;
2',3'-cGMP, 2',3'cyclic GMP;
2',3'-cNADP, 2',3'cyclic NADP;
Ab, antibody;
AD, Alzheimer's disease;
ADAP, a Dual PH domain ARF GAP;
ANT, adenine nucleotide transporter;
ARF GAP, ARF GTPase activating protein;
ARF, ADP ribosylation factor;
ATP, adenosine 5-triphosphate;
BSA, bovine serum albumin;
CHO, Chinese hamster ovary cells;
CK I, casein kinase I;
CNP, 2', 3'-cyclic nucleotide 3'-phosphodiesterase;
COXIV, cytochrome oxidase subunit IV;
CsA, cyclosporin A;
CyP-D, cyclophilin D;
Cyt c, cytochrome c;
DMEM, Dulbecco's Modified Eagle's Medium;
DNA, deoxyribonucleic acid;
EDTA, ethylene diamine tetraacetic acid;
EGF, epidermal growth factor;
EGTA, ethylene glycol tetraacetic acid;
ER, endoplasmic reticulum;
FCS, fetal calf serum;
G418, Geneticin sulphate;
GST, glutathione S-transferase;
HEK293, human embryonic kidney cell line;
IM/IMM, inner mitochondrial membrane;
IMS, intermembrane space;
IP₃, inositol (1,4,5) trisphosphate;
IP₄, inositol(1,3,4,5)tetrakisphosphate;

KIF, kinesin;
MT, microtubules;
Mx, matrix;
N2a, mouse neuroblastoma cells;
OLN-93, oligodendrocyte cell line;
OM/OMM outer mitochondrial membrane;
PAGE, polyacrylamide gel electrophoresis;
PBR, peripheral benzodiazepine receptor;
PBS, phosphate-buffered saline;
PCR, polymerase chain reaction;
pEGFP-C2, enhanced green fluorescent protein expression vector;
PH, pleckstrin homology;
PI 3-K, phosphoinositide 3-kinase or phosphatidylinositol 3-kinase;
PiC, mitochondrial phosphate carrier;
PIP₂, phosphatidylinositol(4,5)bisphosphate;
PIP₃ BP, phosphatidylinositoltrisphosphate binding protein;
PIP₃, phosphatidylinositol(3,4,5)trisphosphate;
PKC, protein kinase C;
PTP, permeability transition pore;
RanBPM, Ran binding protein in microtubule-organizing centre;
RBM, rat brain mitochondria;
ROS, reactive oxygen species;
SDS, sodium dodecyl sulphate;
siRNA, small interfering RNA;
SOD2, Mn-superoxide dismutase;
STS, staurosporin;
TPP⁺, tetraphenylphosphonium;
VDAC, voltage-dependent anion channel;
 $\Delta\psi_m$, mitochondrial membrane potential.

9. Appendix

Curriculum vitae

Name: Anastasia V. Galvita

Birthday: May 11, 1973

Place of Birth: Novosibirsk, Russia

Nationality: Russian

Education and Experience

1995

Novosibirsk State University, Novosibirsk, Russia

Master of Science in chemistry

Master thesis: “Cloning of *Staphylococcus aureus* α -toxin gene. Synthesis of Ni-chelate sorbent for affinity purification of the recombinant α -toxin form

1995-2002

Institute of Bioorganic Chemistry, Russian Academy of Science, Siberian Branch, Novosibirsk, Russia.

Research project:

Study of dynamic of DNase activity induction in serum of animals.

Study of catalytic diversity of DNA hydrolyzing IgG antibodies

2003-present

Institute for Neurobiochemistry, Medical Faculty, Otto-von-Guericke University, Magdeburg, Germany.

PhD-project :

“Mitochondrial localization of p42^{IP4} (Centaurin- α 1) and interaction with 2', 3'-cyclic nucleotide 3'-phosphodiesterase (CNP) and their involvement in regulation of mitochondrial Ca²⁺.”

24. 11. 2009, Magdeburg

Anastasia Galvita

Publications and presentations

1. **Anastasia Galvita**, Dmitry Grachev, Tamara Azarashvili, Yulia Baburina, Olga Krestinina, Rolf Stricker, and Georg Reiser. The brain-specific protein, p42^{IP4} (ADAP1) is localized in mitochondria and involved in regulation of mitochondrial Ca²⁺. *J Neurochem.* 2009 Jun;109(6):1701-13.
2. Tamara Azarashvili, Olga Krestinina, **Anastasia Galvita**, Dmitry Grachev, Yulia Baburina, Rolf Stricker, Yuri Evtodienko, and Georg Reiser. Ca²⁺-dependent permeability transition regulation in rat brain mitochondria by 2',3'-cyclic nucleotides and 2',3'-cyclic nucleotide 3'-phosphodiesterase. *Am J Physiol Cell Physiol.* 2009 Jun;296(6):C1428-39.
3. Buneva VN, Kudryavtseva AN, **Gal'vita AV**, Dubrovskaya VV, Khokhlova OV, Kalinina IA, Galenok VA, Nevinsky GA. Dynamics of antibody nuclease activity in blood of women during pregnancy and lactation. *Biochemistry (Mosc).* 2003 Aug; 68(8):890-900.
4. Andrievskaya OA, Buneva VN, Baranovskii AG, **Gal'vita AV**, Benzo ES, Naumov VA, Nevinsky GA. Catalytic diversity of polyclonal RNA-hydrolyzing IgG antibodies from the sera of patients with systemic lupus erythematosus. *Immunol Lett.* 2002 May 1; 81(3):191-8.
5. Breusov AA, **Gal'vita AV**, Benzo ES, Baranovskii AG, Prints AV, Naumov VA, Buneva VN, Nevinsky GA. Comparison of the Level of DNA-Hydrolyzing Polyclonal IgG Antibodies in Sera of Patients with Hashimoto's Thyroiditis and Nontoxic Nodal Goiter. *Russ J Immunol.* 2001 Apr; 6(1):17-28.
6. Kovalenko GA, **Gal'vita AV**. Dynamic of DNase activity induction in serum of normal animals after heterogeneous DNA injection and in hereditary pathology, *Vopr Virusol.* 2001 Mar-Apr; 46(2):29-32. Russian.
7. Kovalenko GA, **Gal'vita AV**. Time course of serum nuclease activity in mice infected with plasmodium malariae. *Bull Exp Biol Med.* 2000 Sep; 130(9):877-8.
8. Nevinsky GA, Kanyshkova TG, Semenov DV, Vlassov AV, **Gal'vita AV**, Buneva VN. Secretory immunoglobulin A from healthy human mothers' milk catalyzes nucleic acid hydrolysis. *Appl Biochem Biotechnol.* 2000 Jan-Mar;83(1-3):115-29; discussion 129-30, 145-53.

Conferences and symposiums

1. **Galvita A.**, Grachev D., Baburina Y, Krestinina O., Azarashvili T., Stricker R., Reiser G. The neuron-specific protein, p42^{IP4} (Centaurin- α 1) is localized in mitochondria, interacts with 2',3'-cyclic nucleotide 3'-phosphodiesterase and is involved in regulation and control of mitochondrial Ca²⁺. Proceedings of the 12th Joint Meeting "Signal Transduction- Receptors, Mediators and Genes", Weimar, Germany, Oct 29-31, 2008. Poster session (PB6), p.107.
2. **Galvita A.**, Azarashvili T., Krestinina O., Grachev D., Evtodienko Y., Stricker R., Reiser G. In brain mitochondria, calcium and cell death-associated permeability transition are controlled by possibly associated proteins, 2',3'-CNPase, Centaurin-alpha1 and peripheral benzodiazepine receptor, and their substrates/ligands. Proceedings of the 12th Joint Meeting "Signal Transduction- Receptors, Mediators and Genes", Weimar, Germany, Oct 29-31, 2008. Workshop E5.
3. **Anastasia Galvita**, Dmitry Grachev, Yulia Baburina, Olga Krestinina, Tamara Azarashvili, Rolf Stricker, and Georg Reiser. Mitochondrial localization and interaction of Centaurin- α 1 (p42^{IP4}) and CNP (2',3'-cyclic nucleotide 3'-phosphodiesterase) and their involvement in regulation of mitochondrial Ca²⁺ and control of permeability transition. Proceedings of National Conference: Molecular pathways in health and disease of the nervous system, Homburg/Saar, Germany, Sept 11-13, 2008. Poster session (P 8), p.14.
4. **Galvita A.**, Baburina Y, Grachev D., Krestinina O., Azarashvili T., Stricker R., Reiser G. Novel subcellular localization of two brain-specific proteins, p42^{IP4} (Centaurin- α 1) and CNP (2',3'-cyclic nucleotide 3'-phosphodiesterase) in mitochondria. Proceedings of the 5th International Symposium on Neuroprotection and Neurorepair: Cerebral Ischemia and Stroke, Magdeburg, Germany, May 17-20, 2008. Poster session (P 33), p.18
5. **Galvita A.**, Azarashvili T., Stricker R., Schild L., Krestinina O., Grachev D., Baburina Y., Reiser G. Brain IP₄ and PtdInsP₃-binding protein, p42^{IP4}, is involved in the regulation of Ca²⁺ transport in mitochondria. Proceedings of the International Conference "Neurodegenerative Diseases: Molecular Mechanisms in a Functional Genomics Framework" MDC, Berlin, Germany, September 6-9, 2006. Poster session (P 20), p.61
6. Baranovskii A.G., Gorbunov D.A., Matyushin V.G., **Gal'vita A.V.**, Benzo E.S., Ershova N.A., Kudryavtseva A.N. Possible induction pathways of natural catalytic antibodies. Proceedings of the International Conference "RNA as Therapeutic and Genomics Target", Novosibirsk, August 30-September 2, 2001, NIBC Poster Session (19), P. 115.

7. **Gal'vita A.V.**, Kanyshkova T.G., Isaeva N.V., Polosukhina D.I., Nevinsky G.A. Effect of DNA-hydrolyzing antibodies on cell division and immunoresponse of experimental mice. Proceedings of the Second International Conference on Bioinformatics of Genome Regulation and Structure, BGRS'2000, Novosibirsk, August 7-11, 2000, 3, 92-94.
8. Nevinsky G., Baranovskii A., Matushin V., **Galvita A.**, Vlassov A., Ershova N., Buneva V. Variability of Substrate Specificity of Antibodies from the Blood of Patients with Different Autoimmune and Viral Diseases in Hydrolysis of DNA and RNA. Proceedings of 18th International Congress of Biochemistry and Molecular Biology, Birmingham, UK, 16-20 July, 2000, 245 (P 858).